

**VOLTAMMETRIC, SPECTROSCOPIC AND COMPUTATIONAL
STUDY OF THREE BIOLOGICALLY ACTIVE ORGANIC
COMPOUNDS**



Islamabad

Master of Philosophy

In

Physical Chemistry

By

ASAD ULLAH

DEPARTMENT OF CHEMISTRY

Quaid-i-Azam University

Islamabad

2011-2012

DECLARATION

*This is to certify that this dissertation submitted by **Asad ullah** is accepted in its present form by the Department of Chemistry, Quaid-i-Azam University, Islamabad, Pakistan, as satisfying the dissertation requirements for the degree of **Master of Philosophy in Physical Chemistry**.*

Supervisor:

Dr. Afzal Shah

Assistant Professor

Department of Chemistry

Quaid-i-Azam, University

Islamabad.

Head of Section:

Prof. Dr. Muhammad Siddiq

Department of Chemistry

Quaid-i-Azam University

Islamabad.

External Examiner:

Chairman:

Prof. Dr. Amin Badshah

Department of Chemistry

Quaid-i-Azam University

Islamabad.



بِسْمِ اللَّهِ الرَّحْمَنِ الرَّحِيمِ

And Allah has brought you out from the wombs of your mothers, while you know nothing. And He gave you hearing, sight and hearts that you might give thanks (to Allah)

[16:78]



Dedicated to

My “PARENTS”

*A parent's love is whole no
matter how many times
divided.*

Robert Brault

ACKNOWLEDGEMENT

*Praise and gratitude to Almighty **Allah**, the omnipotent, the omniscient who showered upon me His blessing throughout the thick and thin of my life and who blessed me courage, power, good health, company and support of good teachers and friends to materialize my research. All respect for His Last **Prophet Hazrat Muhammad (peace be upon him)**, who gave my conscience the essence of belief in Allah.*

*Words are wane in expressing my veneration for my supervisor **Dr. Afzal Shah** whose valuable guidance and encouragement remained with me throughout my research and emboldened me to remove the predicaments which I faced during this laborious work. His fortitude, cooperation and support in carrying out this project always created in me the sense of patronization and humbleness.*

*I would like to express my sincere appreciation to chairman department of chemistry **Prof. Dr. Amin badshah** for the provision of lab facilities and compounds for my research work. I heartily acknowledge head of the section **Prof. Dr. M Siddiq** for his kind behavior. I acknowledge **Dr. Rumana Qureshi**, for her open heart permission to use her lab for UV-visible study of our compounds.*

*Apart from these personalities, I am also overwhelmingly thankful to all my teachers. Very special thanks to my lab fellows especially to **Shamsa Mumir**, for their help and cooperation throughout my research work. I would like to pay thanks to my friends **zafar Ali**, **Inayat Ali** and **Habib ullah** for their help and cooperation.*

*In the last I would like to presents special thanks to my **parents** especially to my father whose constant encouragements,, good wishes, financial support and non stopping prayers enabled me to complete this task. They are a valuable asset of mine really I wish them a long life and good health. I feel a deep sense of obligations to my younger brothers **Dr. M. Rasool khan** and **Hafiz. M. kamil** whose special interest and continues prayers throughout my life and especially during this project is the moral fiber of my success.*

Asad ullah

ABSTRACT

In the present work, an endeavor has been made to study the redox mechanism of three biologically active organic compounds namely 1-methoxyphenazine (MPZ), 2-benzoyl-7-methoxy-2,3-dihydroisoquinoline-4(1H)-one (IQN) and 1-hydroxy-2-(hydroxymethyl)anthracene-9,10-dione (HAQ) in a wide pH using three different voltammetric techniques (cyclic, differential pulse and square wave voltammetry), UV-Visible spectroscopy and computational study.

Phenazines, isoquinolines and anthraquinones are known to have strong potency of antibacterial, antifungal, hypertension, antiparasitic and anti cancer activities. Therefore, the detailed electrochemistry of three novel derivatives of these classes was carried out in different pH media with the objective to understand the mechanism of their redox behavior. These mechanistic pathways are expected to present a key in considering the hidden routes by which such compounds exert its biochemical action.

In the present work, voltammetry was performed for the three mentioned compounds in buffered ethanolic aqueous media. Cyclic voltammetry was used to determine diffusion coefficient and heterogeneous electron transfer rate constant from scan rate and concentration effect respectively. The involvement of protons in redox mechanism was confirmed from a shift in peak potential as a function of medium pH. Differential pulse voltammetry was used to verify the exact number of electrons involved in the redox process. Similarly the nature of the redox process was decided from the results of square wave voltammetry. The redox mechanism proposed on the basis of CV, DPV and SWV investigations was supported by theoretical calculations. Furthermore, a detailed UV-Visible spectroscopy was performed in a wide pH range to investigate the effect of medium on the absorption response of these compounds. Pka values were also determined from spectroscopic experiments. IQN and HAQ exhibited pH dependent reduction and oxidation while MPZ underwent pH dependent reduction and pH independent oxidation.

LIST OF SCHEMES

Scheme	Title	Page
1	Proposed reduction mechanism of MPZ.....	70
2	Proposed oxidation mechanism of MPZ.....	70
3	Proposed reduction mechanism of IQN.....	71
4	Proposed oxidation mechanism of IQN.....	72
5	Proposed reduction mechanism of HAQ.....	73
6	Proposed oxidation mechanism of HAQ.....	73

LIST OF TABLES

Table	Title	Page
3.1	Abbreviations, IUPAC names, structures and molar masses of the studied compounds.	36
3.2	Composition of supporting electrolytes having 0.1 M ionic strength.....	37
4.1	E_{HOMO} and E_{LUMO} values of compounds obtained through DFT.....	84

LIST OF FIGURES

Figure	Title	Page
2.1	Mechanism showing transfer of electrons at an electrode surface.	16
2.2	Variation of potential with time in cyclic voltammetry	18
2.3	Cyclic voltammogram of 1 mM K Fe(CN) ₆ recorded in 0.1 M acetate buffer (pH4.5) at a potential scan rate of 100 mV s ⁻¹	19
2.4	Cyclic voltammogram of irreversible redox process.	22
2.5	Typical cyclic voltammogram for a quasi-reversible process.	23
2.6	plot of E_p vs $\log v$ indicating critical scan rate.	25
2.7	(A) differential pulse voltammetry (B) DPV of 0.3mM 1-methoxyphenazine at pH 7 and 5 mV/S.	27
2.8	(A) square wave voltammetry. (B) SW voltamogram of 1-methophenazine at pH8 and 100mV/s.	27
2.9	Probable transitions in electronic spectroscopy.	29
4.1	CVs recorded in 0.3mM solution of 1-methoxyphenazine at pH 3 and 100mV/s scan rate.	41
4.2.	CVs of 0.3 mM solution of MPZ recorded in pH 3.0-12.8 at 100 mV/s scan rate.	42
4.3	(A) CVs of 0.3 mM solution of 1-methoxyphenazine recorded in different pH media at 100 mV/s scan rate (B) Peak potential <i>versus</i> pH plots of both peaks of 1-methoxyphenazine (using CV data of Fig. 4.3A).	43
4.4	CVs of 0.5 mM solution of MPZ at different scan rates using glassy carbon electrode at pH 3.0 (A) and pH7.0 (B).	43
4.5	I_{pc} vs squar root of scan rate at pH 3.0 and pH 7.0.	44
4.6	Plot of $\log I_{pc}$ vs $\log v$ for the CV data of 0.5 mM solution at pH3 and pH7.	44
4.7	CVs of 1-methoxyphenazine recorded in different concentrations using glassy carbon electrode at 100 mV/s and pH pH7.1.	45
4.8	Current intensity of cathodic (A) and (B) anodic peaks (obtained in pH7 at 100 mV/s scan rate) <i>versus</i> concentration of 1- methoxyphenazine	45

4.9	(A) CVs of 0.4 mM solution of IQN recorded in medium of pH 7.0 at 100 mV/s scan rate (B) CVs of IQN recorded in in 0.1M acetate buffer of pH 4.0 at 100 mV/s scan rate.	46
4.10	(A) CVs showing first reduction peak of IQN recorded in different pH media at 100 mV/s scan rate using 0.4 mM solution (B) plot of peak potential vs pH.	47
4.11	(A) CVs obtained at a GCE in N ₂ saturated solution of 0.4 mM IQN in buffer of pH 5 at different scan rates. (B) Plot of $I_{pc}/\mu A$ vs $v^{1/2}$ of 1st and 2nd reduction peaks.	48
4.12	plot of $\log I_{pc}$ (μA) vs. $\log V$ (V) at pH5.	48
4.13	(A) CVs recorded in pH 5.0 at 100 mV/s scan rate sing different concentrations of IQN (B) Plot of $I_{pc1}(\mu A)$ vs concentration ($\mu M/cm^3$) using peak current data of 4.13A.	50
4.14	(A) CVs of 0.4mM solution of IQN recorded in a wide pH range at100 mV/s scan rate (B) E_p vs pH plot for the oxidation peak of IQN.	51
4.15	A. CVs of IQN recorded in 0.4mM solution at different scan rates at pH8. (B) Plot of I_{pa} vs $v^{1/2}$ using data obtained from Fig. 4.15A.	51
4.16	(A) CVs recorded in different concentration at pH8 and 100mV/s scan rate (B) Plot of I_{pa} vs concentration using data obtained from Fig. 4.16A.	52
4.17	CVs of 0.2 mM solution of HAQ recorded with GCE in N ₂ saturated solution of pH4 at 100mV/s scan rate.	53
4.18	A. pH effect on the CVs of 0.2 mM HAQ obtained at100mV/s scan rate (B) Plot of E_p vs pH of both anodic and cathodic peaks using data of Fig. 4.18A.	54
4.19	CVs obtained with GCE in 0.2 mM HAQ at pH 5 and pH7.1 at different scan rates	55
4.20	plot of I_{pc} vs $V^{1/2}$ of cathodic peaks. at pH5 and pH7.	55
4.21	plot of $\log I_{pc}(A)$ vs $\log V(Vs^{-1})$ of cathodic peak of 0.2mM HAQ at pH5 and pH7.1.	56
4.22	(A) CVs of 0.2 mM HAQ obtained on GCE at different pH and 100 mV/s scan rate (B) Plot of E_{pa} vs pH.	57
4.23	(A) CVs of 0.2 mM HAQ obtained with GCE in pH 5 at different scan rates (B) Plot of I_{pa} vs $v^{1/2}$.	58

4.24	Plot of $\log I_{pa}$ vs $\log \nu$ at pH 5.	58
4.25	A. CVs of different concentration of HAQ in pH 5 (B) Plot of I_{pa} (μA) vs concentration ($\mu\text{M}/\text{cm}^{-3}$).	59
4.26	(A) DPVs of 0.3 mM 1-methoxyphenazines in different media (B) Plot of E_p vs pH prom using data obtained from DPV results of Fig. 4.26A.	60
4.27	(A) DPVs of 0.4 mM IQN in different media. (B) Plots of E_p vs pH for both reduction peaks.	61
4.28	(A) Representation DPVs of the oxidation of 0.4 mM IQN in supporting electrolytes of different pH (B) Plot of E_p vs pH using data of Fig. 4.28A.	62
4.29	(A) Representation of DPVs of 0.2 mM HAQ in various pH media (B) Plot of E_p vs pH of HAQ data obtained from Fig. 4.30A.	63
4.30	(A) DPVs representing oxidation of 0.2 mM HAQ in different media (B) Plot of E_{pa} of HAQ vs pH	64
4.31	SWVs of 0.3mM solution of 1- methoxyphenazine in different media at scan rate of 100 mV/s.	65
4.32	Square wave voltamogram of 0.3 mM solution of 1-methoxyphenazine at pH 7.1 showing forward, backward and net currents at scan rate of 100mV/s.	65
4.33	Square wave voltammograms of 0.3 mM 1-methoxyphenazine at pH 7.1 without polishing the surface of glassy carbon electrode.	66
4.34	(A) Representation of SWVs obtained in different pH conditions (B) Square wave voltammogram of IQN showing forward and backward components of the total current at pH 4.	67
4.35	(A) SWV of 0.4 mM IQN showing the nature of oxidation at pH 7.1 (B) SWVs representing IQN oxidation in different media.	67
4.36	(A) SWVs of 0.2 mM MAQ representation its reduction in different media (B) SWV of 0.2 mM HAQ at pH 7.1 showing forward and backward Components of the total current.	68
4.37	SWV of 0.2 mM solution of HAQ showing irreversible oxidation in pH 7.1	69
4.38	UV-visible spectra of 16 μM 1-methoxyphenazne in different media of pH range from 1.2 to 12.8.	74

4.39	3-D view UV-visible spectra of 16 μ M 1-methoxyphenazne showing absorbance in different media of pH range from 1.2 to 12.8.	75
4.40	Plot of absorbance 1-methoxyphenazine vs pH at 261 nm for pKa determination.	76
4.41	UV-visible spectra of 20 μ M IQN in different media of pH range from 1.2 to 12.8.	77
4.42	Plot of absorbance of IQN <i>versus</i> pH at 285 nm for pKa determination.	78
4.43	UV-visible spectra of 15 μ M HAQ solution in the pH range of 1.2 to 12.	79
4.44	Plot of absorbance of HAQ <i>versus</i> pH at 280 nm for pKa determination.	80
4.45	Mullikan Charge distribution on each atom of PM3 optimized MPZ structure .using 631G basis set of ab initio method through gaussian 03 software.	81
4.46	Mullikan Charge distribution on each atom of PM3 optimized IQN using 631G basis set of ab initio method through Gaussian 03 software.	82
4.47	Mullikan Charge distribution on each atom of PM3 optimized HAQ using 631G basis set of ab initio method through gaussian 03 software.	83
4.48	Pictorial representation of HOMO (A) and LUMO (B) of MPZ, IQN and HAQ.	85

CONTENTS

Acknowledgements.	V
Abstract	VI
List of schemes	VII
List of tables	VII
List of figures.	VIII
Contents.	XII
Chapter 1: Introduction.	01-13
INTRODUCTION.....	1
1.1 Phenazines Producers.....	2
1.1.1 Pseudomonades.....	2
1.1.2 Streptomycetes.....	3
1.2 Mode of action.....	3
1.2.1 Polynucleotide interaction.....	4
1.2.2 Topoisomerase Inhibition	4
1.2.3 Radical Scavenging.....	5
1.2.4 Charge Transfer.....	6
1.3 Isoquinoline.....	6
1.4 Anthraquinone.....	8
References.....	10
Chapter 2.....	14-33
THEORITICAL BACKGROUND OF EXPERIMENTAL TECHNEQUES.....	14
2.1 Cyclic Voltammetry.....	17
2.1.1 Single electron transfer process.....	20
2.1.2 Multi-electron transfer process.....	23
2.1.3 Methods used for the Determination of k_{sh} from cyclic voltammetry.....	24
2.2 Pulse Voltammetric techniques.....	26
2.2.1 Differential pulse voltammetry.....	26
2.2.2 Square wave voltammetry.....	27
2.3 UV-visible spectroscopy.....	28
2.3.1 Types of electronic transitions.....	28

2.3.2	Principle of absorption spectroscopy; the beer Lambert law.....	29
2.3.3	Chromophore.....	30
2.3.4	Auxochromes.....	30
2.4	Computational study.....	30
	References.....	32
Chapter 3		34-39
EXPERIMENTAL		34
3.1.	INSTRUMENTATION	34
3.1.1	Instruments used for voltammetric measurements.....	34
3.1.2	Instruments Used For Buffer Preparation.....	35
3.1.3	Instrument used for UV-Visible spectroscopic measurements.....	35
3.2	CHEMICALS	35
3.2.1	Compounds under investigation.....	35
3.2.2	Solvents and supporting electrolytes.....	35
3.3	PROCEDURES	38
3.3.1	Voltammetric Experiments.....	38
3.3.2	UV-Visible Spectrophotometric Measurements.....	38
3.3.3	Computational Measurements.....	38
	References.....	39
Chapter 4		40-89
RESULTS AND DISCUSSION		40
4.1	REDOX MECHANISM USING MODERN VOLTAMMETRIC.....	40
	METHODES	
4.2	Cyclic voltammetry of electroactive compounds.....	41-59
4.3	Differential pulse voltammetry of electro active compounds.....	59-64
4.4	Square wave voltammetry of electro active compounds	64-69
4.5	Proposed Reduction / oxidation Mechanism of electrode reactions.....	69-73
4.6	Electronic absorbtion spectroscopy.....	74-80
4.7	Computational Study.....	80-85
4.8	Conclusion.....	86
4.9	References.....	88

Phenazine ($C_{12}H_8N_2$ or $C_6H_4N_2C_6H_4$) also known as azophenylene, dibenzo-p-diazine, dibenzopyrazine or acridizine are nitrogen containing heterocyclic compounds which have been of great interest to pharmaceutical and clinical research groups for the last 50 years [1]. Phenazine molecule is a dibenzo annulated pyrazine having two nitrogens separated by two carbons in a highly conjugated system and is cited for its antibiotic, antitumor, and antiparasitic activities [2]. However, phenazines show a large variation in physical and chemical properties due to difference in nature or position of the functional group on the main structural ring. Approximately more than 100 structural derivatives of phenazine have been identified in nature and over 6000 compounds synthesized that contain phenazine as the basic unit [3]. Many phenazine derivatives are bestowed with antibacterial activity. 1-Hydroxyphenazine is known to possess antifungal potential against many microorganisms such as *Candida Albicans* and *Aspergillusfumigatus*, the risk factor of pulmonary candidiasis [4]. It has a parent role in the synthesis of many important dyestuffs including eurhodines, toluylenered, indulines and safranines [5]. Phenazine dyes exhibit temperature and light stability. Such dyes and their mixtures have recently reported to possess greater efficiency in solar cells [6,7]. Moreover, phenazine dyes are used for coloring wood and textiles. The lipophilic phenazine dye has been employed in biological systems as an expedient stain for bright-field microscopy [8]. They have also found applications as cell markers in microbiology. Rock record of phenazines provides an incentive to study their evolutionary importance in many grounds. It has served as a model system for many studies due to its structural simplicity. Phenazine dyes are known to form 1:1 charge-transfer (CT) or electron-donor-acceptor (EDA) complex with TX-100 [9]. Literature survey reveals their role in biochemical sensors and biosensors. Successful analysis of trace amounts of parathion in fruit samples by safranine biosensor serves as a practical proof of their high sensitivity and selectivity as sensors. Owing to their unique redox and chromatic properties they are now being practiced as redox mediators and are helpful in increasing sensitivity and

detection limit when used as electrocatalysts [10]. Some phenazine derivatives such as phenazine-1-carboxylic acid works as electron shuttle to transfer electrons under alkaline conditions between organic matter and microbial fuel cells [11]. Natural products like phenazines have been studied to prove pivotal in promoting the microbial mineral reduction in the environment. [12]. Various *Pseudomonas* can produce phenazine-1-carboxylic acid which can increase soil environment survival and posses biological control activity against certain strains [13,14]. 1-Methoxy-5-methyl phenazinium methyl sulfate has been considered valuable in the field of biochemistry and medical technology where it serves as an electron mediator for various electron transfer systems [15].

Phenazine 5,10-dioxide derivatives have been studied for their cytotoxicities *in vitro* on V79 cells under hypoxic and aerobic conditions via DNA experiments and QSAR studies [16]. Phenazine based chromophores have been evaluated to posses photo induced DNA cleavage abilities. The extended, aromatic ring systems of these compounds are expected to intercalate between adjoining base pairs in the DNA double-helix. Some electron carrier phenazine derivatives such as methosulphate and 1-methoxy-phenazine methosulphate enhance the formazan production [17].

1.1 Phenazines Producers

Phenazines which are secondary metabolite are produced mainly by streptomycetes, pseudomonas and some other genera of bacteria of soil and marine habitats. The biological importance of this class of compounds is due to their antitumor, antiparasitic, antibiotic and antimalarial activities.

1.1.1 Pseudomonades

Pseudomonas is known as the first producer of phenazine and is considered as the main source of phenazine pigments. For example chlorophine green and pyocyanin blue obtained from pseudomonas were discovered in 19th century and similarly purple iodinin was obtained from pseudomonas aureofaciens in 1938 [18]. Almost all of the phenazines that are produced by bacteria of pseudomonas genus are simple hydroxyl and carboxyl substituted structures [19-23].

1.1.2. Streptomycetes

Gram positive bacteria streptomycetes also produce phenazine. Umezawa isolated antibiotic griseolutivein from streptomycetes and was the first phenazine that was obtained from streptomycetes [22]. Recently streptomycetes species (e.g. griseolutein, luteogriseus, antibioticus and prunicolor) are considered the main source of some simple and complex phenazines.

1.2. Mode of action

Naturally phenazines are produced by cells that have stopped cell division and show slow metabolism. They play no function in cell growth, i.e. as energy source and no storing ability of any type. A general underlying principle of phenazines production is that it controls the excess accumulation of the primary products by excretion and synthesis of some innocuous products at the late stage of the cell growth. This inactiveness of phenazines in metabolism has drawn the attention of the scientists to unfold their physiological role in the cell. It has been noticed that phenazines producing organisms can survive longer in their natural habitat than those which produce no phenazine. This shows that due antibiotic activities it protects the phenazines producing organisms against other microbial and microorganisms competitors and hence provides more stable living facilities for the host organisms [25,26]. For instance the production of phenazines-1-carboxylic acid in pseudomonas fluorescent is required to secure the survival of the host in the rhizospheres and control a bacterial wheat root disease [27, 28].

Instead of the fact that phenazines have a vital role in the prevention of a number of diseases but their detailed study showed that some phenazines also possess the bacterial virulence factors to the host organism, i.e providing help for the development of the disease. Paeruginosa which is producing 1-hydroxyphenazines and pyocyanin sometime attack on the patient of cystic fibrosis and cause the blue green discoloration of the mucus. This is because phenazines disturb the ciliary moments of the epithelial cells through a decrease in ATP and cAMP and thus excite mucus secretion in the epithelial cells by changing the calcium concentration in the cytosole by inhibition of cell membrane Ca^{+} ATPase, and to cause death in leukocytes. These functions of the virulence factors leads to prolonged inflammation of the disease [25,26,29–31]. In the

current era the main focus on synthetic phenazines is to further improve their known antitumor, antibiotic, antiparasitic and antimalarial activities.

1.2.1. Polynucleotide interaction

Several attempts have been made to study the interactions of phenazines with DNA and RNA. The results of all these experiments show that phenazines have planar and aromatic structures having similarities with known intercalators such as chromomycin, acridines and daunomycin. Hollstein et al [32] in 1971 studied the interaction of several polynucleotides with pyocyanin iodinin and myxin produced by pseudomonas. A change in the UV/visible spectrum of phenazine in the absence and presence of calf thyme DNA expose the interaction if any. The binding ability to double stranded DNA and single stranded RNA is different. The binding constant of all the studied phenazines came out in 10^4 --- 10^6 M^{-1} range which seems comparable to classical intercalators; ethidium bromide and actinomycines. Myxin interact strongly with GC region which is attributed to the electrostatic attraction between polar region in the GC base pairs in DNA. But some phenazines show no binding specificity. Pyocynin, iodinin and myxin all inhibit DNA and RNA synthesis either by binding to RNA polymerase via blocking the template or binding to ribonucluside 5-triphosphate. Among these three phenazines, iodinin has the strongest inhibitory effect.

1.2.2. Topoisomerase Inhibition

Enzymes topoisomerase I and II is believed to be the main cause of topological changes in the DNA strands during the cell division comprising uncoiling, supercoiling, catenation, decatenation etc. Cancer infected cells showing high rate of cell division contain sufficient concentration of topoisomerases and are used as target in cancer treatment. A number of drugs (e.g. etoposide and doxorubicin) have been used for topoisomerase II inhibition. Whereas, topoisomerase I inhibitors such as camptothecin has shown better results for the treatment of colon cancer [33]. Phenazine and its derivatives have shown the topoisomerase inhibition properties. Synthetic phenazines are mostly used in this regard but no naturally occurring phenazines have been reported to have topoisomerase inhibition properties.

Phenazines-1-carboxamide derivatives have proved to function best for topoisomerase I and II inhibitions in more than one receptor and more than one steps in cell life cycle and thus exhibiting multidrug resistance [34,35].

1.2.3. Radical Scavenging

Free radicals are believed the primary sources of the procession and developments of a number of serious human diseases. An irreversible damage is caused by free radical delivered by oxygen in natural cells in some diseases such as Parkinson's and atherosclerosis, dementia, cerebral traumas and strokes. It was also reported that these free radicals have a role in asthma, cells aging, carcinogenesis, rheumatoid arthritis, inflammation and renal failure. Vitamins C and E and some other naturally occurring antioxidants have an important physiological role. But due to insufficient amount they are unable to control these diseases induced by free radicals. So to control such diseases and natural damages sufficient amount of synthetic antioxidants and radical scavengers are needed.

Lipids on peroxidation produce free radicals and cause disintegration of cell organelles membrane and cells. The radical scavenging property of phenazines was authenticated by measuring their capability to stop lipid peroxidation in liver microsomes. L glutamate is released during the brain ischemia and oxygen radicals are produced due to this over stimulation of L glutamate through cell cascades. Finally the natural cells death occurs. Shin et al has reported that some phenazines including benthocyanine, phenostatin and aestivophoenins have the ability to effectively control these brain injuries [36,37].

Interestingly we can explain the antibiotic activities of phenazines by opposite function called generation of free radicals [38]. Pyocyanin presents a best example by accepting one electron and shows high stability in the radical form. It was believed in the earlier literature that this anion radical undergo redox cycling causing the increased production of H₂O₂ and toxic super oxides. Thus increasing the degenerating capacity of the cellular superoxide dismutase and accumulation of the radicals in cell eventually results in the cell death [20,25,27,37]. Baron et al concluded from the results of their experiment that there is no correlation between the dismutase activity and resistance towards pyocyanin.

Instead pyocynin radical is further stabilized in the physiological media by divalent metal cation like Mg^{2+} .

1.2.4. Charge Transfer

Some phenazines possess a unique property of charge transfers due to large electron rich chromospheres. It has been documented in the early literature that 2-hydroxyphenazine and its reduced form 5, 10 dihydro-2-hydroxyphenazine can behave as artificial electron carrier in cytoplasmic membrane in *Achaea* for the enzyme system specifically in the metabolic path way for the production of methane in methanogenic *Achaea* [39]. In methanogenic path way the main intermediate is the co enzyme methyl –S-CoM which in the presence of methyl-CoM reductase reductively demethylated to methane. Methanophenazine was identified to play the role of electron carrier in the methanogenic archaea. As most of the electron transfer processes are membrane bound thus the structure of methanophenazine allows it for anchoring into the membrane mediating transport of electron in membrane bound enzymes [40,41].

Owing to their extensive importance some phenazines have been studied electrochemically. Their study on platinum electrode in various aprotic media has shown that phenazines undergo reduction processes. They reduce via two one electron steps in neutral media and single two electron processes in acidic media [42]. Redox behavior of phenazine was also studied using hanging mercury drop electrode via cyclic voltammetry and polarography [43]. Adsorption of various phenazines on zirconium phosphate has been studied electrochemically [44].

1.3. Isoquinoline

Isoquinolines are heterocyclic nitrogen containing organic compounds widely spread in nature represent the structural isomer of quinoline in which benzene is fused with a pyridine ring. A number of isoquinoline derivatives have been identified that possess remarkable biological activity. Andreas et al [45] investigated the inhibitory properties of some isoquinolines against the gastric acid secretion i.e they used tetrahydroimidazo[2,1-a]isoquinoline with significant results for the treatment of peptic disease that is caused by the hypersecretion of acid in stomach. Literature survey also

shows the cytotoxicity of isoquinolines against cancer cells. Won et al [46] reported indeno[1,2-c] isoquinoline to have strong potency against tumor cells. They further investigated that the cytotoxicity of these derivatives of isoquinolines is owing to their ability of inhibiting topoisomerase I. Berberine a medicinally important isoquinoline derivative has shown strong potency against some intestinal pathogens that cause acute diarrhea such as shigella dysenteriae and salmonella paratyphi. [47] and also prevent the adherence of E coli to the host cells without producing any harm in the intestinal layer [48]. Isoquinoline also find its use in biology and environmental monitoring activities owing to its role as sensor. i.e. bis(isoquinoline N-oxide) has been identified as fluorosensor with significant sensitivity towards Li^{+1} Ca^{+2} and Mg^{+2} [49].

The role of isoquinoline is not only limited to medicines but it has also shown significantly important role in agricultural as well. Isothan q-15 (2-dodecylisoquinolinium bromide) is used as pesticides [50] and similarly insecticidal activities of these compounds have been reported [50]. Some quaternary isoquinolinium salts differing in side alkyl chain are members of cationic surfactants having quaternary nitrogen in their structures and some of them are used as disinfectants or micellar catalyst which is counted as its largest industrial application [51]. For brightness purpose of metal surface few isoquinoline derivatives have been reported as additive in metal plating [50]. Isoquinolinium quaternary salts are industrially used as demulsifiers in petroleum industry and also as flocculating agents [52-55]. Similarly isoquinoline methobisulphate is playing an activating role in photographic improvement [50]. Other unique and special uses of some other isoquinoline derivatives are their use as organic semiconductors [56,57] and as catalyst in the ring opening or polymerization reaction of epoxide [58]. Owing to their wide range applications in various fields some isoquinolines are studied electrochemically. Komorsky et al [59] have investigated the electro-reduction of berberine through polarography and square wave voltammetry in different pH media and their results have shown its completely irreversible nature and pH dependent behavior.

1.4. Anthraquinone

Anthraquinones, also recognized as anthracenediones or dioxoanthracenes, represent an important class of aromatic organic compounds. A number of isomers are possible and each one of these can be considered as a quinone derivative. However, the term anthraquinone is invariably used for one specific isomer, 9,10-anthraquinone.

Many anthraquinone derivatives have been studied to investigate their role against cancer. The results show that some members of this class have strong potency against leukemia and tumor [60]. Glycosidic derivatives of anthraquinones are used as laxatives and for the treatment of skin diseases caused by fungus [61]. Owing to their structural importance many anthraquinone derivatives have shown its excellent antioxidant properties [62]. Some anthraquinones are more efficient in the treatment of malaria because of their use against other quinine resistant plasmodium species in human body [63]. Antibacterial properties of some anthraquinone has also been reported; for example, 9-methoxydihydrodeoxybostrycin and 10-deoxybostrycin exhibit strong potency against bacillus cereus than ciprofloxacin [64]. Younos et al., have documented some anthraquinone derivatives as analgesic and hypotensive [65]. Some anthraquinones have been used as bird repellents for crops protection [66]. They are also used as precursor for the synthesis of some dyes. However, some of its derivatives are used as natural pigments [67]. Chaoyan Li *et al* have introduced the use of anthraquinone dyes as photo sensitizer in photosensitized dye solar cell with some excellent results [68]. Literature survey has also revealed that some anthraquinone derivatives are used for the production of gas in satellite balloons. Similarly the industrial applications of this class are further enhanced by its use in paper making industries as digestive additives [69]. Another important industrial application of anthraquinones is their role in the production of H₂O₂. Alkylated derivatives including 2-ethyl-9,10-anthraquinone are used for this purpose rather than simple anthraquinones [70].

Due to the broad range biological, agricultural and industrial importance of phenazines, isoquinolines and anthraquinones a systematic study including redox mechanism, the effect of pH, substituents, scan rate and concentration is still missing. To bridge this gap detailed electrochemistry of three novel derivatives selecting one from each class was carried out via more sensitive techniques such as cyclic voltammetry, differential pulse

voltammetry and square wave voltammetry. An attempt has been made to understand the factors controlling their metabolic state and dynamics. Computational study of the compounds theoretically validated the electrochemical results. Moreover, electronic absorption spectroscopy was performed in a wide pH range to investigate the effect of medium on the absorption response of these compounds towards UV-visible radiations. These investigations are expected to provide valuable insights about the unknown mechanistic pathways by which such compounds exert their biochemical actions

References

- [1] Laursen, J.B.; Nielsen, J. *Am.chem.sci.Rew.* **2004**, 104, 1663.
- [2] WulfBlankenfeldt, Kuzin, A.P.; Skarina, T.; Korniyenko, Y.; Tong, Y.; Bayer, P.; Janning, P.; Thomashow, L.S.; Mavrodi, D.V. *PNAS*, **2004**, 101, .16431.
- [3] Mavrodi, D.V.; Blankenfeldt, W.; Thomashow, L.S.; Mentel, M. *Annual review of Phytopathology.* **2006**, 44, 417.
- [4] Saosong, K.; Wongphathanakul, W.; Poasiri, C. *KKU Sci. J.* **2009**, 37, 163-172.
- [5] Nitin, C.; Sunayana, S.S.; Sharma, M.K.; Chaturvedi, R.K. *Int. J. Res. Chem. Environ.* **2011**, 1, 66.
- [6] Jana, A.K. *J. Photochem. Photobiol. A.* **2000**, 132, 1.
- [7] Jana, A.K.; Bhowmik, B.B. *J. Photochem. Photobiol. A.* **1999**, 122, 53.
- [8] Dubrovsky, J.G.; Guttenberger, M.; Saralegui, A.; Mendivil, S.N.; Voigt, B.; Baluska, F.; Menzel, D. *Ann. Bot.* **2006**, 97, 1127.
- [9] Jana, A.K.; Rajavenii, S. *Spectrochim. Acta, Part A.* **2004**, 60, 2093.
- [10] Pauliukaite, R.; Ghica, M.E.; Barsan, M.M.; Brett, C.M.A. *Anal. Lett.* **2010**, 43, 1588.
- [11] Zhang, T.; Zhang, L.; Su, W.; Gao, P.; Li, D.; He, X.; Zhang, Y. *Bioresours. Technol.* **2011**, 102, 7099.
- [12] Hernandez, M.E.; Kappler, A.; Newman, D.K. *Appl. Environ. Microbiol.* **2004**, 70, 921.
- [13] Turner, J.M.; Messenger, A.J. *Adv Microb Physiol.* **1986**, 27, 211.
- [14] Surrey, A.R. *Org. Synth. Coll.* **1995**, 3, 753.
- [15] Hisada, R.; Yagi, T. *J Biochem.* **1977**, 82, 1469.
- [16] Cerecetto, H.; González, M.; Lavaggi, M.L.; Aravena, M.A.; Rigol, C.; Olea-Azar, C.; Azqueta, A.; de Cerain, L.D.; Monge, A.; Bruno, A.M. *Med Chem.* **2006**, 2, 511.
- [17] Stellmach, J. *J. Histo chem.* **1984**, 80, 137.
- [18] Turner, J.M.; Messenger, A.J. *Adv. Microb. Physiol.* **1986**, 27, 211.
- [19] Budzikiewicz, H. *FEMS. Microbiol. Rev.* **1993**, 104, 209.
- [20] Leisinger, T.; Margraff, R. *Microbiol Rev.* **1979**, 43, 422.

- [21] McDonald, M.; Mavrodi, D. V.; Thomashow, L. S.; Floss, H. G. *J. Am. Chem. Soc.* **2001**, *123*, 9459.
- [22] Hollstein, U.; McCamey, D. A. *J. Org. Chem.* **1973**, *38*, 3415.
- [23] Delaney, S. M.; Mavrodi, D. V.; Bonsall, R. F.; Thomashow, L.S. *J. Bacteriol.* **2001**, *183*, 318.
- [24] Umezawa, H.; Hayano, S.; Maeda, K.; Ogata, Y.; Okami, Y. *J. Antibiot.* **1951**, *4*, 34.
- [25] Kerr, J. R. *Infect. Dis. Rev.* **2000**, *2*, 184.
- [26] Kitahara, M.; Nakamura, H.; Matsuda, Y.; Hamada, M.; Naganawa, H.; Maeda, K.; Umezawa, H.; Iitaka, Y. *J. Antibiot.* **1982**, *35*, 1412.
- [27] Hollstein, U.; Butler, P. L. *Biochemistry* **1972**, *11*, 1345.
- [28] Thomashow, L. S.; Weller, D. M. *J. Bacteriol.* **1988**, *170*, 3499.
- [29] Parsons, J. F.; Calabrese, K.; Eisenstein, E.; Ladner, J. E. *Biochemistry* **2003**, *42*, 5684.
- [30] Mavrodi, D. V.; Bonsall, R. F.; Delaney, S. M.; Soule, M. J.; Phillips, G.; Thomashow, L. S. *J. Bacteriol.* **2001**, *183*, 6454.
- [31] Mavrodi, D. V.; Ksenzenko, V. N.; Bonsall, R. F.; Cook, R. J.; Boronin, A. M.; Thomashow, L. S. *J. Bacteriol.* **1998**, *180*, 2541.
- [32] Hollstein, U.; Van Gemert, R. J. *J. Biochemistry* **1971**, *10*, 497.
- [33] Vicker, N.; Burgess, L.; Chuckowree, I. S.; Dodd, R.; Folkes, A.J.; Hardick, D.; Hancox, T. C.; Miller, W.; Milton, J.; Sohal, S.; Wang, S.; Wren, S. P.; Charlton, P. A.; Dangerfield, W.; Liddle, C.; Mistry, P.; Stewart, A.; Denny, W. A. *J. Med. Chem.* **2002**, *45*, 721.
- [34] Stewart, A. J.; Mistry, P.; Dangerfield, W.; Bottle, D.; Baker, M.; Kofler, B.; Okiji, S.; Baguley, B. C.; Denny, W. A.; Carlton, P. A. *Anti-Cancer Drugs* **2001**, *12*, 359.
- [35] Hassan, H. M.; Fridovich, I. *J. Bacteriol.* **1980**, *141*, 156.
- [36] Shin-ya, K.; Furihata, K.; Teshima, Y.; Hayakawa, Y.; Seto, H. *J. Org. Chem.* **1993**, *58*, 4170.

- [37] Kim, W.-G.; Ryoo, I.-J.; Yun, B.-S.; Shin-Ya, K.; Seto, H.; Yoo, I.-D. *J. Antibiot.* **1999**, *52*, 758.
- [38] Muller, M. *Biochim. Biophys. Acta.* **1995**, *1272*, 185.
- [39] Abken, H.J.; Tietze, M.; Brodersen, J.; Bauer, S.; Beifuss, U.; Deppenheimer, U. *J. Bacteriol.* **1998**, *180*, 2027.
- [40] Beifuss, U.; Tietze, M.; Bauer, S.; Deppenheimer, U. *Angew. Chem. Int. Ed.* **2000**, *39*, 2470.
- [41] Beifuss, U.; Tietze, M. *Tetrahedron Lett.* **2000**, *41*, 9759.
- [42] D.T.Sawyer, D.T.; Komai, R.Y. *Anal. Chem.* **1972**, *44*, 715.
- [43] Kern, W.; Kublik, Z. *Anal.Chem.Acta.* **1958**, *18*, 104.
- [44] Kabuta, L.T.; Gorton, L. *Electroanal.* **1999**, *11*, 719.
- [45] Palmer, A.M.; Grobbel, B.; Brehm, C.; Zimmermann, P.J.; Buhr, W.; Feth, M.P.; Holst, H.C.; Simon, W.A. *Bio & med chem.* **2007**, *15*, 7647.
- [46] Cho, W.J.; Le, Q.L.; Van, H.T.M.; Lee, K.Y.; Kang, B.K.; Lee, E.S.; Lee, S.K.; Won, Y.K. *Bioorg Med Chem Lett.* **2007**, *17*, 3531.
- [47] Sack, R.B.; J. L. Froehlich, J.L. *Infect. Immun.* **1982**, *35*, 471.
- [48] Sun, D.; Courtney, S.H.; Beachey, E.H. *Antimicrob. Agents. Chemother.* **1988**, *32*, 1370.
- [49] Collado, D.; Inestrosa, E.P.; Suau, R.; Desvergne, J.P.; H.B. Laurent, H.B. *org lett.* **2002**, *4*, 855.
- [50] Geunter Grethe, *the chemistry of heterocyclic compounds*, **2009**, John Wiley & son.
- [51] Stodulka, J.M.J.; soutkup, O.; Mus, K.; Cabal, K.; Kuca, W. *Mil. Med. Sci. Lett.* **2012**, *81*, 76.
- [52] Degroote, M.; Keiser, B.; *Bio & med chem.* **1974**, *39*,1531.
- [53] Degroote, M.; Keiser, B. *chem. Abstr* **1950**, *44*, 4665.
- [54] Dunaevskaya, L.A.; balakin, V.M.; kokoshko, Z.Y.; skrylev, I.D.; khim, Z.P. *through chem. Abstre.* **1971**, *74*, 6596.
- [55] Dunaevskaya, L.A.; Balakin, V.M.; kokoshko, Z.Y.; skrylev, I.D.; khim, Z.P.; 1971, 47, *through chem. Abstr*, **1974**, *81*, 6892.

- [56] Surpateanu, G.; Stefan, V.; Rusinschi, E.; Zegravescue, I. *Dyes and Pigments*. **1997**, 74, 2698.
- [57] Surpateanu, G.; Stefan, V.; Rusinschi, E.; Zegravescue, I. *Med Res Rev*. **1975**, 82, 4872.
- [58] Moberly, C.W. *Int.J.Electchem.SCI*. **1965**, 63, 1898.
- [59] Lovric, K.S. *Electroanal*. **2000**, 12, 599.
- [60] Huang, Q.; Lu, G.; Shen, H.M.; Chung, M.C. *Med Res Rev*. **2007**, 27, 609.
- [61] Singh, D.N.; Verma, N.; Raghuwanshi, S.; Shukla, P.K.; Kulshreshtha, D.K. *Bio & Med. Chem. Letter*. **2006**, 16, 4512.
- [62] Yen, G.C.; Duh, P.D.; Chuang, D.Y. *Food Chem*. **2000**, 74, 437.
- [63] Hou, Y.; Cao, S.; Brodie, P.J.; Callmander, M.W.; Ratovoson, F.; Rakotobe, E.A.; Rasamison, V.E.; Ratsimbason, M.; Alumasa, J.N.; Roepe, P.D.; Kingston, D.G. *Bioorg Med Chem*. **2009**, 17, 2871.
- [64] Yang, K.L.; Wei, M.Y.; Shao, C.L.; Fu, X.M.; Guo, Z.Y.; Xu, R.F.; Zheng, C.J. She, Z.G.; Lin, Y.C.; Wang, C.Y. *J Nat Prod*. **2012**, 75, 935.
- [65] Younos, C.; Rolland, A.; Fleurentin, J.; Lanhers, M.; Misslin, R.; Mortier, F. *Planta Med*. **1990**, 56, 430.
- [66] Werner, S.J.; Linz, G.M.; Carlson, J.C, Pettit, S.E.; Tupper, S.K.; Santer, M. *M. App. Ani Beh. Sci*. **2011**, 129, 162.
- [67] Nagia, F.A.; EL-Mohamedy, R.S.R. *Dyes and Pigments*. **2007**, 75, 550.
- [68] Chaoyan, L.; Xichuan, Y.; Ruikui, C.; Jingxi, P.; Haining, T.; Hongjun, Z.; Xiuna, W.; Anders, H, Licheng, S. *Solar Energy Materials & Solar Cells*. **2007**, 91, 1863.
- [69] Sara, G.G.; Moreira, M.T.; Artal, G.; Maldonado, L.; Feijoo, G. *Journal of Cleaner Production*. **2010**, 18, 137.
- [70] Shang, H.; Zhou, H.; Zhu, Z.; Zhang, W. J. *In. & Eng. Chem*. **2012**, 18, 1851.

The chemical phenomena that linked with the charge separation form the basis of electrochemistry. Mostly charge transfer resulting by this charge separation shows its homogeneous transfer in solution while on surface of electrode it transfers heterogeneously. For the complete electrical neutrality more than one charge transfer half reaction can take place in opposite directions. The electrodes are connected by an external link and ionic species in the solution transfer the charge between electrodes.

Negative value of the total sum of the free energies of the two electrodes leads to the production of electrical energy while an energy must be provided to the electrode for electrolysis when the sum of the free energies of the electrodes are positive [1]. Heterogeneous charge transfer has been recommended for electrode reactions which undergoes in that part of the solution where there is a distinction in charge distribution from the bulk phase. This region is normally named as the interfacial region and strongly affects the electrode reactions. Normally the capacitance of an electrode shows its ability to separate the charge while resistance attributes to the hurdle of charge transfer.

In an electrochemical reaction electrode can behave like a source (for reduction) or a sink (for oxidation) for charge transferred to or from electrochemically active species in the solution.



O and *R* represent the oxidized and reduced form of a species.

For the transfer of electrons a matching in the orbital energies must be necessary where exchange takes place in the acceptor and donor. The highest filled orbital in the electrode represents this level. Fermi energy level for metals but for a soluble species this corresponds to the orbital of the valence electron to be gained or knock out. So

- In reduction the transferable electrons must have least amount of energy from the electrode prior to the transfer of electron and gives a sufficient negative value.
- for oxidation the lowest unoccupied orbitals have the highest amount of energy to accept electron from the species.

The limit and direction of the electrochemical reaction can be controlled externally by the provision of suitable potential. All the electrode processes are considered as half reactions and are designated as reduction reaction by convention. Every one has its own standard potential E^0 in comparison to standard hydrogen electrode, at unit activity for all species.

The relationship between the potential, E , for the half reaction at equilibrium and the standard electrode potential is given by Nernst equation

$$E = E^{\circ} - \frac{RT}{nF} \sum \nu_i \ln a_i \quad (2.1)$$

ν_i represents the stoichiometric numbers. Nernst equation can be applied for an electrode reaction when the oxidized and reduced species are in equilibrium. The electrode process can be considered as reversible when it follows the criteria assigned for thermodynamic reversibility. The rate of redox reaction depends on the concentration of the species in the solution while mass transport affects the availability of the species at the interface. When the kinetics of the electrode reaction is much faster than the transport, then such a situation represents the most favorable condition for reversible reaction.

$$k \gg k_d$$

The above condition represents the criterion for reversible reaction where k is the kinetic rate constant and k_d is the mass transfer coefficient. In comparison the reaction is considered to be irreversible when the electrode reaction cannot proceed in the reverse direction. For such condition

$$k \ll k_d$$

The electrode reaction characterized by partial behaviors of reversible and irreversible reactions is recommended as quasi-reversible reaction [2]. Three methods have been reported for mass transport, diffusion, migration and convection. Mass transport arising from the concentration gradient developed at the electrode surface represents diffusion of the species, while in convection a mechanical mean support the movement of the species toward the electrode and migration occurs because of opposite charges with respect to electrodes [3]. All of these three processes can participate at a time. But for the

electroanalytical purpose we are only interested in the diffusion controlled process. So for the study of electrode reactions best and reproducible experimental conditions should be adopted to overcome the contribution of the unnecessary factors. In other words it means to block the migration effect. The mass transport of the species by migration can be blocked by the addition of inert electrolyte having concentration 100---1000 times greater than the concentration of analyzing species, while the suitable concentration for an electroactive species is 5 mM or less [1]. So under these conditions the solution is left to show mass transport through diffusion and convection. If there is an externally controlled convection it is thought to occur at the diffusion layer thickness and transport is only by diffusion closer to the surface. The mechanism consists of various steps shown in the Fig. 2.1.

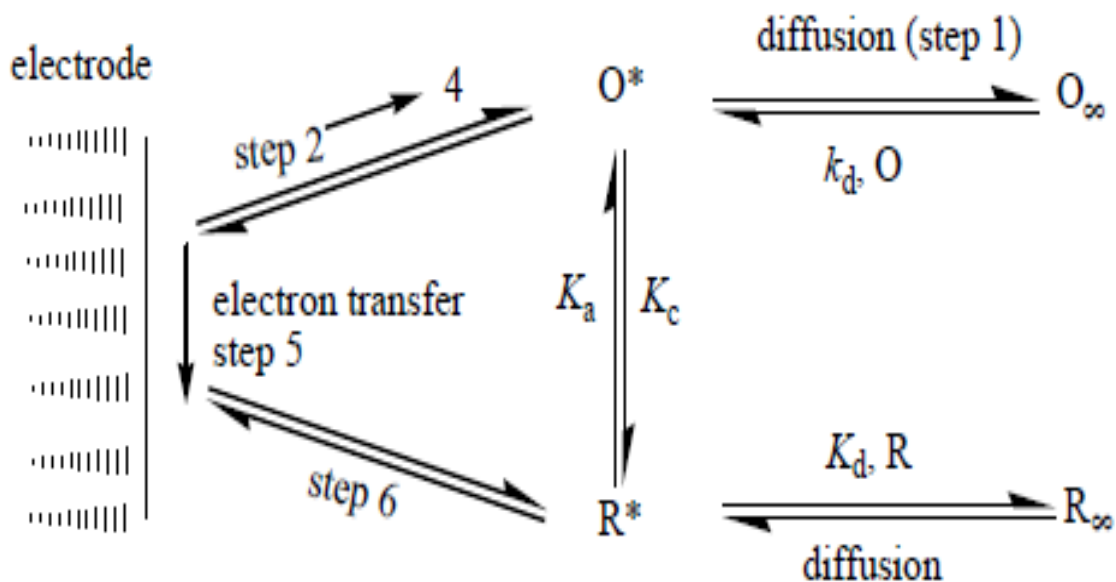


Figure 2.1. Mechanism showing transfer of electrons at an electrode surface.

Step 1: diffusion of the electroactive species to the reaction site.

Step 2: reorganization of the ionic environment (10^{-8} s)

Step 3: rearrangement of the solvent dipoles to corresponding ions (10^{-11} s)

Step 4: adjustment in the distances involving the ligands and central ion

Step 5: transfer of electron (10^{-16} s)

Step 6: relaxation in the reverse condition.

Among these steps diffusion of electroactive species is considered as the rate determining step.

The kinetics of the electrode reactions can be best explained in terms of anodic and cathodic rate constants, k_a and k_c , which are given by the Butler-Volmer equations:

$$K_a = k^0 \exp[\alpha_a nF (E - E^0) / RT] \quad (2.2)$$

$$K_c = k^0 \exp[\alpha_c nF (E - E^0) / RT] \quad (2.3)$$

Where k_c and k_a represents the cathodic and anodic charge transfer co-efficients, n number of electrons, F Faraday constant and E^0 shows formal potential of the system in case when concentration is used for activities.

In order to study the exact nature and mechanism of a redox reaction occurring in electrochemical system, voltammetric methods are used. Both kinetic and thermodynamic parameters can be evaluated from the detailed analysis of voltammogram. The rate of an electrochemical reaction occurring in the interfacial region between the solution and electrode can be recorded as peak current and helps in suggesting mechanism of the reaction.

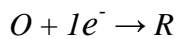
The present work has been accomplished with the use of three voltammetric techniques; cyclic voltammetry (CV), square wave voltammetry (SWV) and differential pulse voltammetry (DPV). UV-Vis spectrophotometric technique was also employed.

2.1 CYCLIC VOLTAMMETRY

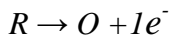
Cyclic voltammetry is the most widely used electroanalytical technique providing qualitative information about the nature of electrochemical reactions. More precisely it offers the site for the redox potential of an electroactive species and gives useful information about the role of media on redox process. The basic principle of cyclic voltammetry is the application of a triangular (Fig. 2.2) potential waveform which scans linearly the potential of a stationary working electrode. During the potential sweep, current is measured by potentiostate as a response of the applied potential. The result of CV scan appears in the form of a voltammogram which is the plot of current vs potential. The cyclic voltammogram can be affected by a large number of physical and chemical

parameters. The expected I - E response for a single cycle of redox couple is shown in Fig. 2.3.

By assuming a general reaction, in the forward scan reduction of the species occurs as



The product of the reduction process is reoxidized in the reverse scan indicated by anodic current.



The CV has the ability of rapidly producing a new species in the forward scan and then probing its fate on the reverse scan. This shows a very classical feature of the technique [4].

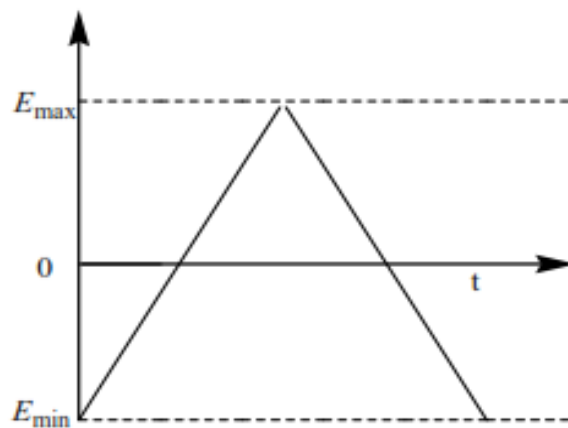


Fig. 2.2. Variation of potential with time in cyclic voltammetry

A salient feature of cyclic voltammogram is the appearance of a peak, specified by its potential E attributable to a reaction involving the transfer of electron/s. In cyclic voltammetry the reversible process is characterized by the oxidation or reduction of the reduced or oxidized products by reversing the scan direction.

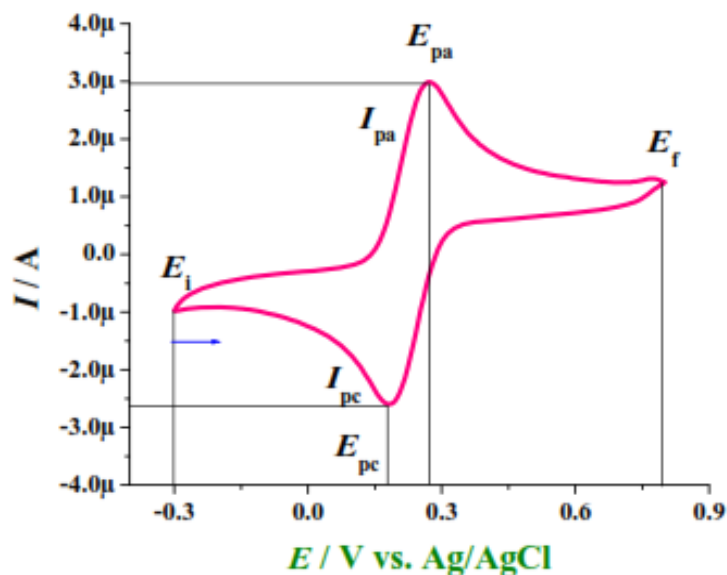


Fig. 2.3. Cyclic voltammogram of 1 mM K Fe(CN)_6 recorded in 0.1 M acetate buffer (pH 4.5) at a potential scan rate of 100 mV s^{-1} .

Peak potentials (E_{pa} and E_{pc}) and peak currents (I_{pa} and I_{pc}) are the important parameters that completely describe a cyclic voltammogram. Peak potential qualitatively identifies the potential at which redox reaction occurs whereas the magnitude of the peak current quantitatively measures the rate of redox reaction.

The species in a redox couple undergoing rapid exchange of electrons with electrode are named as reversible couple and from cyclic voltammogram such a couple is determined by measuring the potential difference between the two peaks.

$$\Delta E_p = E_{pa} - E_{pc} \approx 0.058/n \text{ at } 298 \text{ K} \quad (2.4)$$

This equation holds good for an electrochemical reversible process in which n indicates the number of electrons transferred, E_{pc} and E_{pa} are the potentials of cathodic and anodic signals. Furthermore, scan rate has no effect on the peak separation value of $0.058/n$ in case of a reversible couple but switching potential and cycle numbers has a slight effect. In reversible couple both peak potentials are separated by a midway potential termed as its formal reduction potential.

$$E^0 = \frac{E_{pa} + E_{pc}}{2} \quad (2.5)$$

The above equation can be applied for an electron transfer reversible reaction having $\alpha = 0.5$. The sluggish electron exchange between the working electrode and redox species cause the irreversibility of the electrochemical reaction. Such a process is characterized by separation of peak potential greater than $0.058V/n$ and shows some dependency on the scan rate.

Adsorption of species on the surface of electrode strongly affects the shape of cyclic voltammograms. As the species have no tendency to diffuse away from the surface of electrode. More precisely when the adsorb species are oxidized or reduced its fast kinetics result in symmetrical voltammogram having immediate oxidation as well as reduction peaks potential [5].

Cyclic voltammetry is considered as the most resourceful technique for the analysis of electrically active species, because of the stipulation of mathematical study of electrode reactions [6-10] CV can also be used as an electroanalytical tool in biochemistry and macromolecular chemistry [11]. In Voltammetric study the redox reaction may involve one or more than one electrons depending upon the nature of the species. In the following section a brief detail of such conditions is given.

2.1.1. Single electron transfer process

The accurate nature of an electrochemical reaction whether it is reversible, irreversible or quasi- reversible can be justified from the values of a number of parameters such as E_p , peak potential, $E_{p/2}$ half peak potential, $W_{1/2}$ half peak width, ΔE peak separation, I_p peak currents of the anodic and cathodic peak, $E_{1/2}$ half wave potential etc. Single electron transfer can take place via three different modes.

(i) reversible process, (ii) Irreversible process and (iii) Quasi-reversible process.

(i) Reversible processes

In reversible process the species being oxidized or reduced in the forward scan is reduced or oxidized in the reverse scan producing a reversible wave. The current values of both anodic and cathodic peaks are matching to each other and their ratio is unity. A rapid electron exchange occurs between the species and electrode in a reversible redox couple. Due to the difference in concentration of electroactive species on the electrode surface and

in bulk of the solution the mass transport will occur through diffusion. To obtain the time dependent concentration distribution we can apply Fick's law as

$$\frac{\partial C_{i(x,t)}}{\partial t} = D_i \frac{\partial^2 C_{i(x,t)}}{\partial x^2} \quad (2.6)$$

C and D stand for concentration and diffusion respectively of the electroactive species.

The peak current for a reversible process is given by Randles sevcik equation [7-8]

$$I_p = (2.69 \times 10^5) n^{3/2} ACD^{1/2} \nu^{1/2} \quad (2.7)$$

This equation shows that peak current is directly related to the concentration of the analyte and to the square root of scan rate and such increase in peak current with scan rate is an indication of electrode reaction controlled by diffusion mass transport. n is the number of electrons, A is area of electrode (cm²), I_p is peak current (A) and D is the diffusion coefficient (cm²/s).

Criteria for reversible reactions

The electrochemical reaction will be considered as reversible if it fulfills the following criteria:

- Peak potential is related to half peak potential as

$$E_{pc} = E_{1/2} - (1.109 \pm 0.002) RT/nF \quad (2.8)$$

$$E_{pa} = E_{1/2} + (1.109 \pm 0.002) RT/nF \quad (2.9)$$

- The ratio of peak currents for a reversible process is usually equal to unity
- Separation between two peak potential is given by

$$\Delta E = E_{pa} - E_{pc} \approx 0.059 / n \text{ V} \quad (2.10)$$

Thus for a fast single electron reversible couple ΔE has the value of 59 mV. Eq (2.10) is also used to determine the number of electrons in the electrode reactions. Scan rate has no effect on ΔE but sometime a slight increase in peak separation is possible due to the limited solution resistance between reference and working electrode.

- Peak potential is independent of scan rate. In broad peaks where E_p is doubtful, for convenience we can use $E_{p/2}$ instead of E_p and is related to the half wave potential $E_{1/2}$ by

$$E_{p/2} = E_{1/2} \pm 28/n \text{ (mV) at 298K} \quad (2.11)$$

Where, + sign is used for reduction process.

Criteria for irreversible processes

Electrochemical reaction that involves the dead slow transfer of electrons is categorized as irreversible process and characterized by the appearance of individual peaks widely separated from each other i.e. $\Delta E > 59/n$ mV. There is no reversible peak in complete irreversible process [12].

Randles equation for peak current is given by

$$I_p = (2.99 \times 10^5) \alpha^{1/2} n^{3/2} A C D^{1/2} \nu^{1/2} \quad (2.12)$$

Again peak current is proportional to the bulk concentration. α is the transfer coefficient.

For an irreversible process

Remarkable shift in peak potential occurs with scan rate.

Peak width is related to number of electrons as

$$|E_p - E_{p/2}| = 1.857RT/\alpha nF \quad (2.13)$$

Reinmuth equation is used for calculation of k_{sh}

$$I_p = C * k_{sh} / nFA \quad (2.14)$$

for irreversible process standard heterogeneous electron transfer rate constant has the value less than 10^{-5} cm/s as well as with very low value of α . A typical cyclic voltammogram of an irreversible process is shown in Fig. 2.4.

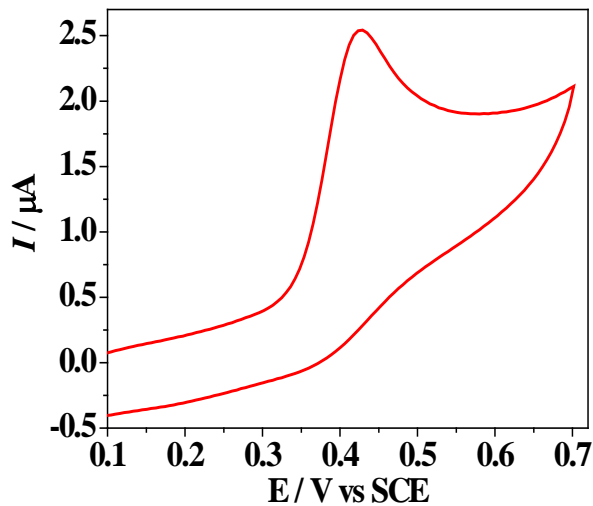


Figure 2.4. Cyclic voltammogram of irreversible redox process.

Quasi- reversible process:

Quasi-reversible processes are intermediate between reversible and irreversible processes. A peak comparatively of less current appears in the reverse scan. Cyclic voltammogram of a quasi-reversible process is more drawn out as compared to a reversible system and shows large peak separation. For a quasi-reversible process

- $E_p - E_{p/2}$ value range from 60 mV to 100 mV.
- Small shift in peak potential with scan rate.
- ΔE exceeds 60 mV and increase with scan rate.

In quasi-reversible process current depends both on mass transport and charge transfer. k_{sh} has value in the range of 10^{-1} to 10^{-5} cm/s [13]. Fig. 2.5 shows a typical cyclic voltammogram of quasi-reversible system.

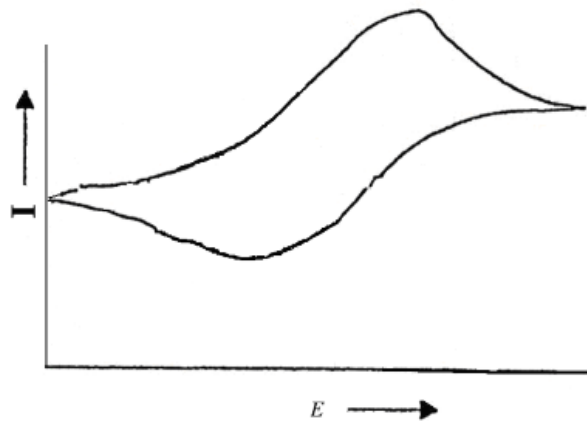


Fig.2.5. Typical cyclic voltammogram of a quasi-reversible process.

2.1.2. Multi-electron transfer process

In multi-electron transfer process usually the transfer of electrons occur in more than one steps following EE mechanism. However, the transfer of electrons in each step is characterized by its separate kinetics [14-15]. When the energy required for the transfer of second electron is not matching the first one, then two steps electron transfer take place and for each electron a separate wave appears. Furthermore, when the energy for the second electron is slightly different from the first electron then the two peaks fuse together and results in a broad peak.





These two equations represent a two step reversible process.

Most of the quinines in aprotic media have shown two step electron transfers [16-24]. Similarly electron transfer is also accompanied by H^+ transfer in some cases especially in biological systems [25]. These processes are then categorized as EC or CE mechanism depending upon the situation whether proton or electron transfer occurs first. Generally protic acidic medium prefers CE mechanism for reduction process while in basic protic media EC mechanism holds good for reduction process [26]. A reverse can be considered for the oxidation. Depending upon the systems several other types of mechanisms have been reported, including, EECC, ECEC and CEC.

2.1.3 Methods used for the determination of k_{sh} from cyclic voltammetry

Like other kinetic parameters cyclic voltammetry is also used for the determination of heterogenous rate constant, k_{sh} . Depending on nature of the process different methods are used to evaluate k_{sh} from the data obtained from CV. These methods include

(i) Nicholson's method

This method is used for quasi-reversible processes and was introduced by Nicholson for the first time. He derived an equation that relates peak separation to a dimensionless parameter Ψ through k_{sh} . This equation is given as

$$\Psi = \gamma^{\alpha/2} k_{sh} / (\pi \alpha D_0)^{1/2} \quad (2.17)$$

Where $\alpha = nFv/RT$ and $\gamma = D_0/D_r$

Ψ is different for different value of α and is obtained from Nicholson table. We can apply this method where peak separation of voltammogram is in the range of 57 to 250 mV.

(ii) Kochi's method

Kochi and his co-worker Klinger made another attempt for the determination of heterogeneous rate constant by the following equation

$$k_{sh} = 2.18[D_0 \alpha n F v / RT]^2 \exp[-\alpha^2 n F / RT (E_{pa} - E_{pc})] \quad (2.18)$$

So k_{sh} can be calculated from peak potential difference if other parameters are known. This equation is restricted to those processes where sweep rates are enough to establish

irreversibility. Kochi used Nicholson (2.19) and Shain (2.20) equations as the basis for this expression.

$$E_{pc} = E_0 - RT/\alpha nF [0.780 + \ln(\alpha D_0 n F \nu / RT)^{1/2} - \ln k_{sh}] \quad (2.19)$$

$$E_{pa} = E_0 - RT/\beta nF [0.780 + \ln(\beta D_0 n F \nu / RT)^{1/2} - \ln k_{sh}] \quad (2.20)$$

ν is the scan rate and $\beta = 1 - \alpha$

(iii) Gileadi's method

Gileadi developed a very classical method for the determination of k_{sh} in cases where anodic peak is not present on the basis of critical scan rate [27]. When k_{sh} for a reversible process is analyzed E_p values are affected and the nature of the process approaches to irreversibility. By plotting E_p values *versus* log of scan rate a straight line is achieved at lower scan rate and at higher scan rate an ascending curve is obtained. Critical scan rate is the point where these two curves intersect each other (Fig. 2.6) after the determination of ν_c heterogeneous rate constant can be calculated by the following equation

$$k_{sh} = -0.48\alpha + 0.52 + \log[nF\alpha\nu_c D_0 / 2.303RT]^{1/2} \quad [2.21]$$

ν_c is the critical scan rate

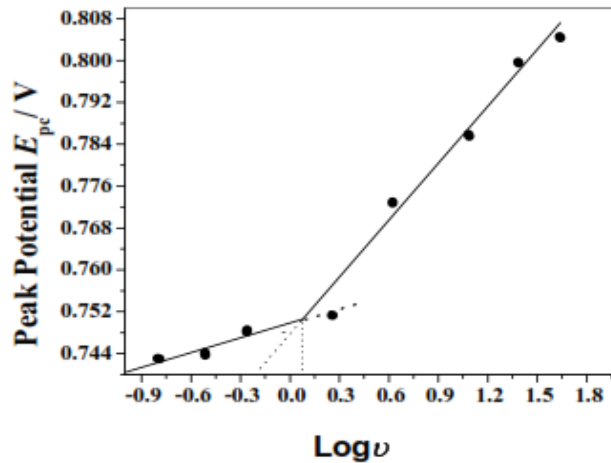


Fig. 2.6. Plot of E_p vs $\log \nu$ indicating critical scan rate.

Redox processes are sometime accompanied by chemical reactions and affect the cyclic voltammogram shape, because these decrease the accessible surface concentration of the active species. These changes in shape of voltammograms arising from a chemical

antagonism are very helpful in proposing reaction pathways and it also provides trustworthy information for reactive intermediates [28].

2.2. Pulse voltammetric techniques

The differences in rate of decrease in faradic and charging current form the basis of all pulse techniques. The rate of charging current decay is very fast but faradic current decay slowly as a function of time. These techniques were developed by Barker and Jenkin with the objective to study the redox behavior of compounds with very low concentrations. The basis of these techniques consists of applying potential in the form of pulses to working electrode. After the application of potential step, the decrease in faradic current is much slow while a rapid decay in charging current takes place. At the end of pulse when current is sampled the contribution of charging current is mostly negligible. The significantly important pulse techniques that we have used in our present work are described below.

2.2.1. Differential pulse voltammetry

This voltammetric technique has more sensitivity as compared to cyclic voltammetric technique for compound analysis. Pulses of fixed magnitude which are superimposed on a linear ramp are applied to the stationary electrode. The details are summarized in Fig. 2.7. The resulting current is measured just before the application and at the end of pulse application. A plot of differential current ($I_b - I_f$) vs potential is automatically recorded in the instrument called differential pulse voltamogram. Like the CV peak current is a function of the analyte concentration. The potential is related to the half wave potential as

$$E_p = E_{1/2} - \Delta E/2 \quad (2.22a)$$

DPV can detect upto 10^{-8} M concentration. It has also the ability to improve the resolution between two peaks. The most important use of DPV is that to find out the exact number of electrons involved in redox reaction through the following equation.

$$W_{1/2} = 90.4/n \quad (2.22b)$$

In DPV the potential is applied in 5 mV/s scan rate having pulse magnitude in the range 25-50 mV.

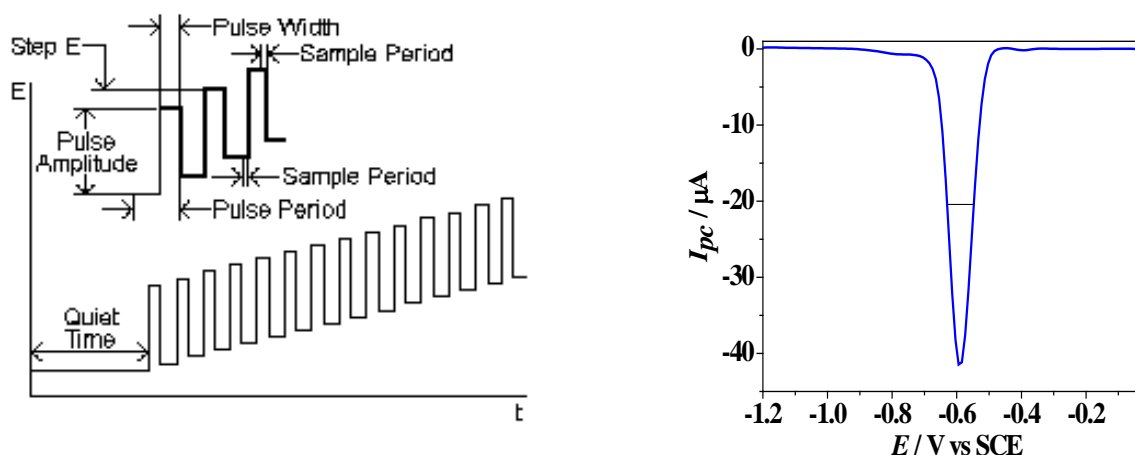


Fig. 2.7. (A) differential pulse voltammetry (B) DPV of 0.3mM 1-methoxyphenazine at pH 7 and 5 mV/S.

2.2.2. Square wave voltammetry

SWV is a fast voltammetric technique and is characterized as the large amplitude pulse technique consisting of square waves superimposed on staircase base potential. Like DPV current in this technique is again sampled twice, at the end of forward pulse and at the late time of reverse pulse. Fig. 2.8 depicts the details of SWV. The product can undergo reaction in the reverse pulse. A square wave voltammogram is obtained by plotting the difference between the two currents *versus* base staircase potential.

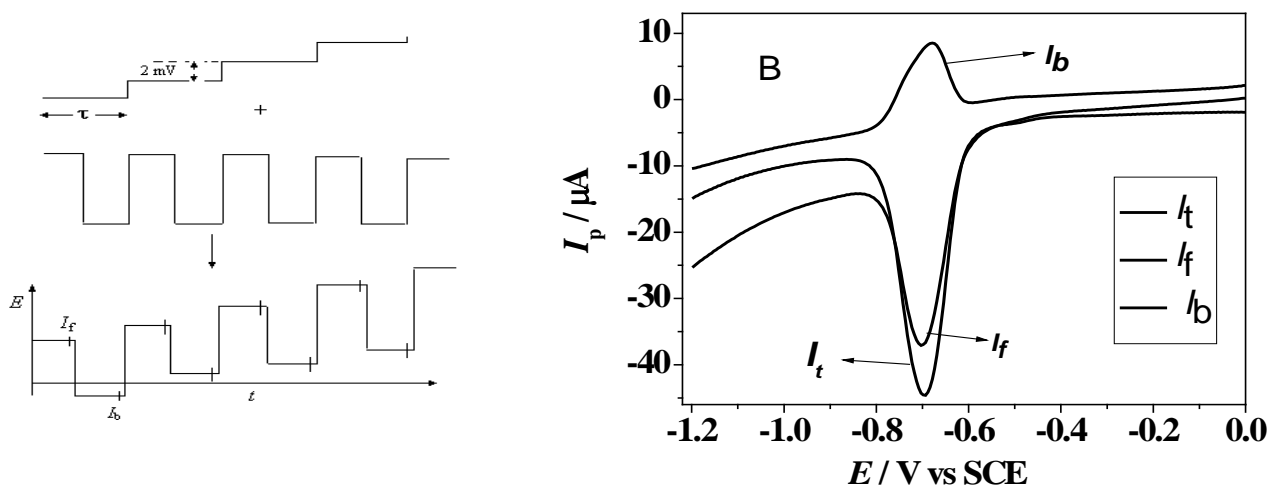


Fig.2.8. (A) square wave voltammetry. (B) SW voltammogram of 1-methoxyphenazine at pH 8 and 100mV/s.

By comparing DPV and SWV sensitivity it was observed that SWV is about 3.3 or 4 times more sensitive as compared to DPV. Moreover, it has a secondary benefit of high speed as well as to determine the exact nature of redox process by plotting the forward and backward components of the total current. Effective scan rate for SQW is given by $f\Delta E$, where ΔE is the potential step and f is frequency. If $\Delta E = 10$ mV, $f = 50$ Hz then 0.5 V/s will be the effective scan rate.

2.3. UV-visible spectroscopy

Organic compounds are mostly transparent in UV-visible region (200-800 nm). Absorption spectroscopy in this region is very important to characterize a compound and to determine pKa value of biologically active compounds. Similarly it can be used to complement the results obtained through other techniques.

2.3.1. Types of electronic transitions

The absorption of UV-visible radiations by a molecule is associated with the excitation of electrons from ground state to higher energy state. Generally this transition occurs from the highest occupied molecular orbital to lowest unoccupied orbitals. The energy gap between these two types of orbitals dictates the wavelength to be selected for absorption. When UV-visible radiation of particular wavelength is absorbed by a molecule only one photon is absorbed and it is assumed that only one electron is promoted to the higher energy level and leaving the other electrons unaffected.

Due to the absorption of UV-visible radiations 4 types of transitions shown in Fig. 2.9 are possible $\sigma \rightarrow \sigma^*$, $\pi \rightarrow \pi^*$, $n \rightarrow \sigma^*$ and $n \rightarrow \pi^*$.

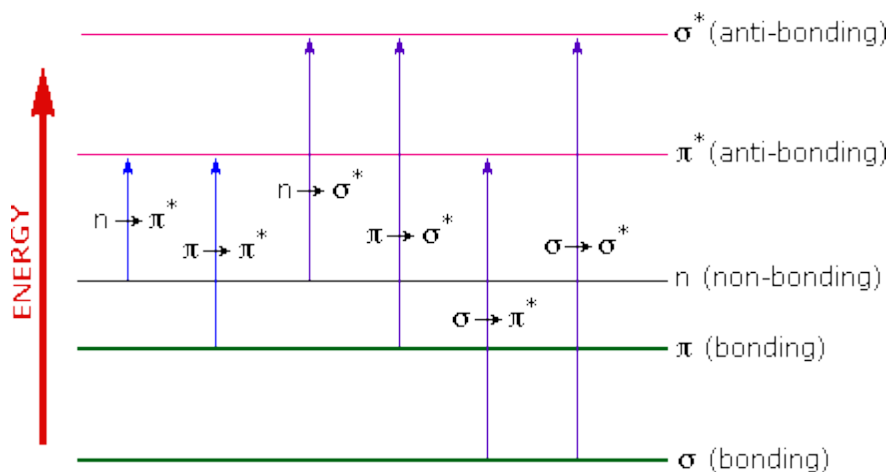


Fig. 2.9. Probable transitions in electronic absorption spectroscopy.

The $\sigma \rightarrow \sigma^*$ transition occurs only in saturated organic compounds where there is only strongly bonded sigma electrons. Such transitions normally occur at lower wavelengths due to high energy gap between the two energy levels. $\pi \rightarrow \pi^*$ transitions normally occur in unsaturated compounds having double or triple bonds and saturated compounds having a hetero atom shows $n \rightarrow \sigma^*$ transitions. Similarly compounds having double or triple bonds with a hetero atom exhibits $n \rightarrow \pi^*$.

All the transitions as mentioned above are not possible because there are certain selection rules that must be obeyed by a particular transition to occur. The electronic transitions that do not obey these selection rules are categorized as forbidden transition. $n \rightarrow \pi^*$ transition is an example of forbidden transition. But sometime experimentally it is observable with a very low intensity.

2.3.2. Principle of absorption spectroscopy; the Beer Lambert law

The extent to which a compound absorbs UV-visible radiations depends on the number of absorbing molecule in the sample. However, the nature of compound also affects the extent of absorption. These two conditions were formulated by Beer and Lambert in the form of a law known as Beer Lambert law.

$$A = \log (I_0/I) = \epsilon cl \quad (2.23)$$

Where A represents absorbance, I_0 is the intensity of incident light, I is the intensity of light of emitted from the cell, c is the concentration of the compound, l is the length and ϵ is the molar absorptivity. Generally values of molar absorptivity appear in the range of 20 to 10^6 . Value of ϵ higher than 10^4 is considered as the higher intensity absorption. While

those having ϵ less than 10^3 are considered as low intensity absorption. ϵ value in the of 0-1000 shows forbidden transition [29].

2.3.3. Chromophore

Any structural feature in a molecule responsible for the absorption of radiations in the UV-visible region is termed as chromophore. Both energy and intensity of absorption change with change in chromophores. The carbonyl group in acetone is chromophore.

2.3.4. Auxochrome

The wavelength of maximum absorption not only depends on the nature of chromophore present in molecule but also on the environment of the chromophore. There are certain groups i.e. OH, NH₂, -SH and halogens that do not absorb in the UV-visible region but when attached to chromophore they cause a shift in the λ_{max} . Such groups are known as auxochromes. For example the replacement of H of carbonyl by OH or Cl. Substitution results in one of the following four conditions:

Bathochromic effect: shift in wavelength to longer wavelength as a result of substitution is called red shift or bathochromic shift.

Hypsochromic shift: a shift toward shorter wavelength is called hypsochromic effect.

Hyperchromic effect: an increase in intensity of absorbance is called hyperchromic effect.

Hypochromic effect: decrease in intensity of absorbance is known as hypochromic effect

2.4. Computational study

Computational chemistry is the sub branch of theoretical chemistry. It is based on mathematical description of chemistry problems using computer. Thus it is the computer based study of chemistry problems. Computational study deals mainly with the significance of the output of theoretical chemistry incorporated in computer for the structural and various other properties of the molecules. The properties of a molecule that can be analyzed theoretically through computer study include dipole moment, charge distribution on each atom within molecule, spectroscopic data, energy of HOMO and LUMO, and some other electronic properties. For the detailed study of a compound a number of computational methods are used depending on the nature of study, e.g. ab initio, semi-empirical and empirical methods.

In collaboration with experimental results computational study can provide an explanatory insight in understating the nature of chemical reaction. Similarly it also forms the basis for a number of experimental results [30]. It can also work for the prediction of new compounds to be synthesized by exposing various types of interactions between the molecules. Following are the various areas where computational chemistry can support or reject the experimental results.

To predict the structure of molecules using simulation methods.

To obtain and store data for a chemical species.

Computational study is efficiently used to provide a link between the structure of compounds and their investigated chemical properties.

The possibility for the synthesis of new compound can be studied before starting the reaction.

The interaction of a drug with other molecule by designing some specific models shows the role of computational chemistry in pharmaceutical industries.

Computational methods are mainly categorized into three sub branches including

- Ab initio.
- Semi-empirical methods
- Molecular mechanics.

In Ab initio method only the theoretical concepts and equations are used showing high accuracy. Hartree-Fock method is the most basic of ab initio which is based on the molecular orbital theory and these calculations neglect the electron electron repulsion. Increasing the value of basis set Hartree-Fock limit can be obtained. The methods which start with Hartree-Fock and later on correction for electron electron repulsion are known as post Hartree-Fock methods. This method is more applicable to smaller molecules because of large computational time [31]. Empirical and semi empirical methods are also applicable to heavier molecules where the use of ab initio calculations is limited. These methods use both theoretical approximations and experimental data. Classical physics principles form the basis of molecular mechanics computational technique and thus there is no use of quantum mechanical calculations.

References

- [1] Brett, C.M.A.; Brett, A.M.O. *Electrochemistry Principles, Methods and Applications*, **1993**, Oxford University Press.
- [2] Denis, H.; Evan, J. *phys.chem.* **1972**, 76, oxford.
- [3] Conway, B.E. *theory and principles of electrode process*, **1965**, Ronald, new York.
- [4] Kissinger, P.T.; Heineman, W.R. *Laboratory Techniques in Electroanalytical Chemistry*, **1996**, Marcel Dekker, Inc.
- [5] Brett, C.M.A.; Brett, A.M.O. *Electroanalysis*, **1998**, Oxford University Press.
- [6] Chaires, J.B.; Dattagupta, N.; Crothers, D.M. *Biochemistry*. **1982**, 21, 3933.
- [7] Randles, J.E.B. *Trans. Faraday, Soc.* **1948**, 44, 327.
- [8] Sevcik, A. *Collec. Czech. Chem. Common.* **1948**, 13, 349.
- [9] Bott, A.W. *Curr. Seps.* **1994**, 13, 49.
- [10] Bard, A.J.; Faulkner, L.R.; *Electrochemical Methods, Fundamentals and Applications*, **1980**, John Wiley, New York.
- [11] Klinger, R.J.; Kochi, J.K. *J. Phy. Chem.* **1981**, 85, 12.
- [12] Nicholson, R.S. *Anal. Chem.* **1965**, 37, 135.
- [13] Adrian, W.B. *curr, sep.* **1997**, 16, 61.
- [14] Eugen, T.S. *Curr. Sep.* **2004**, 21, 11.
- [15] Josealdo, T.; Luciana, R.F.; Fabiane, C.A.; Dayse, C.A.; carlos, L.Z.; alaida, B. de O; Marilia, O.f.G. *J. Braz. Chem. soc.* **1998**, 9, 163.
- [16] Wenbin, Z.; Scott, M.R.; Ian, J.B. *J. phys. chem.* **2010**, 114, 2738.
- [17] May, Q.; Daniel, S.; Mark, F. W.; Diane, K.S. *J. Am. Chem .soc.* **2007**, 129, 12847.
- [18] Susan, M.A.B.H.; Begum, M.; Takeoka, Watanabe, Y. M. *J. electroanal Chem.* **2000**, 481, 192.
- [19] Gomez, M.; Gonzalez,; Gonzalez, I. *J. electroanal Chem.* **2005**, 578, 193.
- [20] Felipe, J.G. *electroanal.* 1998, 10638.
- [21] Celine, C.; Frederic, K.; Allen, J.B. *Langmuir* **2002**, 18, 8134.

- [22] Reza, O.; Jahanbakhsh, R.; Manoochehr, E.; *Iran. J. chem & chem. Eng.* **2001**, 2, 75.
- [23] Golabo, S.M.; Davarkhah, R.; Nematollah, D.; *Scientia iranica*, **1997**, 4, 112.
- [24] Costentin, C.; *chem. Rev.* **2008**, 108, 2145.
- [25] Guin, P.S.; Das, S.; Mandal, P.C. *int .j. Electrochem*, **2010**, 2011, 1.
- [26] Ucar, M.; Solak, A.L. *Turk J. chem.* **2002**, 26, 509.
- [27] Maboob, M.; Athar. Y.k.; Romania, Q.; Naila, A.; Waheeda, B. *Collect. Czech. Chem. Commun.* **1992**, 57, 1410.
- [28] Wang, J. *Analytical Electrochemistry*, **1994**, VCH Publishers, New York.
- [29] Pavia, D. L.; Lampman, G.M.; Kriz, G.S.; Vyvyan, J.R. *introduction to spectroscopy*, 4th Eds, **2008**, 381.
- [30] Smith, S.J.; Sutcliffe, B.T. *Rev .comput. chem.* **1997**, 70, 271.
- [31] Levine, I. N. *Quantum chemistry*, **1991** , Englewood Cliffs, New jersey: Prentice Hall. 455.

The details of various instruments and reagents that were used are given as below

3.1. Instrumentation

3.1.1. Instruments used for electrochemical investigations

All the voltammetric measurements were performed using μ Autolab running with GPES 4.9 software, Eco-Chemie, The Netherlands. The details of the cell and electrodes used are given below:

3.1.1. (a) Electrochemical cell

It is a double walled cylindrical cell with cell top (Model K64 PARC), adjustable plastic cap with substitutable bottom. At the top of cell cap five 14/20 standard taper ports are present into which electrodes (working electrode, auxiliary electrode and reference electrode) and inert gas inlet etc could be inserted. A thermostat of LAUDA Model K-4R is also connected to the cell through a side opening for the maintenance of a specific temperature during the measurement. A volume of 10 mL of the electrochemical cell was used for voltammetric study.

3.1.1. (b) Electrode system

Three-electrode system was used for all voltammetric experiments;

(i) Working electrode

Glassy carbon electrode with active surface area of 0.071 cm^2 was used as working electrode.

(ii) Reference electrode

Saturated calomel electrode (SCE), (fisher scientific company) was used as a reference electrode. This electrode consists of a glass tube containing a layer of mercury at the bottom with a paste of Hg and Hg_2Cl_2 over it and is surrounded by saturated KCl, behaving as an electrolyte. Electric connection with mercury of calomel electrode is

made via a platinum wire fused to a copper wire. This electrode is denoted as Hg/Hg₂Cl₂/KCl.

(iii) Counter or auxiliary electrode

Platinum electrode with geometric area greater than the working electrode connected to a copper wire for external connection at one end through mercury in a pyrex glass tube was used as an auxiliary electrode.

3.1.2. Instruments used for buffers preparation.

3.1.2.1. pH meter

INOLAB pH meter with Model no pH 720 was used for all pH measurements.

3.1.2.2. Balance

An electrical balance (SHIMADZU AUW220D) was used for mass determination.

3.1.3. Instrument used for UV-Visible spectroscopic measurements:

UV-Visible spectrophotometer (UV-1601 Shimadzu spectrophotometer) with measurement wavelength range of 200-1100 nm was used for UV-Visible spectroscopic experiments.

3.2. Chemicals

3.2.1. Compounds under investigation

The three studied compounds were a donation from Prof. Dr. Amin Badshah. The names, structures and abbreviations of these electroactive compounds are given in Table 3.1.

3.2.2. Solvents and supporting electrolytes

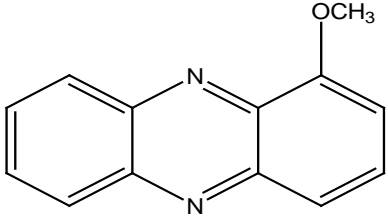
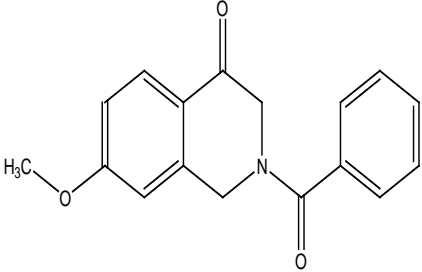
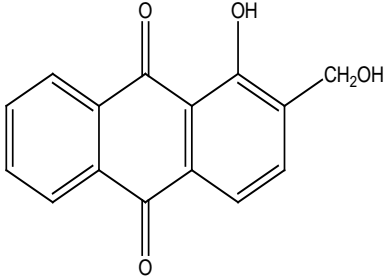
The voltammetric and spectroscopic measurements of the electroactive compounds were performed in solution form using different solvents and supporting electrolytes.

(a) Solvents

Voltammetric measurements were performed in solution consisting of solvent and supporting electrolyte in addition to electroactive compound. The selection of a solvent was considered an important step in electrochemical measurements and the selection was made according to analyte solubility and redox activity. Similarly some specific properties like electrical conductance, electrochemical behavior and chemical reactivity of a solvent can also dictate its recommendation for electrochemical study. Solvent

should not react with the analyte and it should not undergo electrochemical reactions in the potential window of the working electrode. In the present work a mixture of water and ethanol was used as solvents to reduce the solubility problem. For this purpose doubly distilled water and analytical grade ethanol were used.

Table 3.1. Abbreviations, IUPAC names, structures and molar masses of the studied compounds.

S.N o.	Abbreviations	IUPAC Names	Structures	Molar masses
1	MPZ	1-methoxyphenazine		210.1 g/mol
2	IQN	2-benzoyl-7-methoxy-2,3-dihydroisoquinolin-4(1H)-one		281.1 g/mol
3	HAQ	1-hydroxy-2-(hydroxymethyl)anthracene-9,10-dione.		254.1 g/mol

(b) Supporting electrolytes

Supporting electrolytes were prepared in the range of pH 1 to 13 using analytical grade reagents. These supporting electrolytes were used for two main purposes; 1st to maintain pH of the medium and secondly to reduce the contribution of migration current. The migration current is effectively reduced by the addition of inert supporting electrolytes in large excess normally 100 times greater than the concentration of electro active species [1]. Thus conditions can be adjusted to study current due to diffusion of electroactive specie rather than its migration [2]. The ions of supporting electrolytes do not interfere with the redox properties of the electroactive analyte because these ions oxidize or reduce at potentials out of the potential window of the working electrode. Composition of various supporting electrolytes having 0.1 M ionic strength are given in Table 3.2.

Table 3.2. composition of supporting electrolytes having 0.1 M ionic strength.

pH	Composition
1.1	HCl + KCl
2.0	HCl + KCl
3.0	HCl + KCl
4.0	HAcO + NaAcO
5.02	HAcO + NaAcO
6.0	NaH ₂ PO ₄ + Na ₂ HPO ₄
7.1	NaH ₂ PO ₄ + Na ₂ HPO ₄
8.0	NaH ₂ PO ₄ + Na ₂ HPO ₄
9.4	NaHCO ₃ + NaOH
10.02	NaHCO ₃ + NaOH
11.0	KCl + NaOH
12.8	KCl + NaOH

3.3. Procedures

3.3.1. Voltammetric experiments

Glassy carbon electrode as working electrode was used to polish with alumina powder through a pad for each assay and then washed with deionized water and dipping in the solvent for 2 minutes. After cleaning the surface of the electrode, a background current response was recorded in supporting electrolyte. Electrode surface was judged by recording successive scans in supporting electrolyte via cyclic voltammetry in the working potential range [3-5].

The appearance of smooth baseline ensured the cleaned surface of the electrode. All the electrochemical experiments were conducted at ambient temperature. A constant flux of nitrogen gas was supplied to the solutions of the studied compounds for 8-10 minutes to ensure the complete removal of oxygen. Normal cyclic voltammograms were recorded at 100 mV/s scan rate. But for scan rate effect a range of 10-500 mV/s was also used. SWV and DPV were performed with 100 and 5 mV/s scan rate respectively. Effect of scan rate, scan number and concentration was studied through CV while for medium effect all three techniques, CV, SWV and DPV were carried out.

3.3.2. UV-Visible spectrophotometric measurements

The electronic absorption spectroscopy was carried out to investigate the response of these compounds to UV-Visible radiations in different media. pKa value of each compound was evaluated by plotting absorbance versus pH [6-8]. For spectroscopic measurements solutions were normally prepared by mixing calculated amount of supporting electrolytes of different pH with analyte solution. All the absorption spectra were recorded keeping same composition of solvent system in both reference and sample cell to overcome the interference of solvent system on the compound peaks.

3.3.3. Computational studies

Computational studies were performed for charge distribution on each atom and energy calculations of HOMO and LUMO of the studied compounds.. Using semi-empirical PM3 method the geometry of all these structures was optimized followed by charge distribution and energy calculation using RHF/3-21G and RHF/6-31G basis set in Ab-initio. GAUSSIAN 03W software was used for all these calculations. P-4 computer was used for these computations.

References

- [1] Zainal, Z.; Lee, C.Y.; Hussein, M.Z.; Kassim, A.; Yusof, N.A. *J. Photochem.* **2005**, 172, 316.
- [2] Wang, J. *Analytical Electrochemistry*, **1994**, VCH Publishers, New York.
- [3] Shah, A.; Zaheer, M.; Qureshi, R.; Akhter, Z.; Nazar, M.F. *Spectrochimica Acta* **2010**, 75, 1082.
- [4] Shah, A.; Diculescu, V.C.; Qureshi, R.; Brett, A.M.O. *Bioelectrochemistry*. **2010** 79, 173.
- [5] Shah, A.; Diculescu, V.C.; Muhammad, N.; Qureshi, R.; Ali, S.; Brett, A.M.O. *Electroanalysis*. **2010**, 22, 121.
- [6] Savko, M.; Kascakova, S.; Mojes, P.; Jancura, D.; Miskovvsky, P.U. *J. Mol. Struct. Theochem.* **2007**, 803, 79.
- [7] Castro, M.; Giordana, O.S.; Balaco, S.E. *J. Mol. Struct. Theochem.* **2003**, 626, 167.
- [8] El-Mossalamy, E.H.; Al-Thabati, S.S.; Al-Nowaise, F.M.; Al-Sulami, Q.A. *Commun. Fac. Sci. Univ. Ank. Series B*, **2005**, 51, 21.

RESULTS AND DISCUSSION

The redox mechanistic pathways of three biologically important compounds were proposed on the basis of the results obtained from three voltammetric methods with the objectives of providing valuable insights about the action mechanism of such compounds in cellular milieu. Several important physical parameters were evaluated from voltammetric signatures. The pH effect, providing a key role in pKa determination was examined. For supporting the voltammetric results electronic absorption spectroscopy was also carried out. Moreover, computational studies were performed to bridge the theoretical concepts and experimental results of the studied compounds.

4.1. REDOX MECHANISM USING MODERN VOLTAMMETRIC METHODES.

The electrochemical response of three biologically active organic compounds namely 1-methoxyphenazine, 2-benzoyl-7-methoxy-2,3-dihydroisoquinoline-4(1H)one, and 1-hydroxy-2-(hydroxymethyl)anthracene-9,10-dione was investigated in a wide pH range by three sensitive electrochemical methods. For the evaluation of electrochemical and kinetic parameters the effect of scan rate, concentration, pH and number of scans on the voltammetric response of the analytes were examined. The nature of the electrochemical reaction (reversible, irreversible, quasi-reversible, fast, slow, EE EC etc) was judged from the variation in peak potential and peak current. The adsorption behavior of the reduced or oxidized products was ensured from the decrease in peak current by recording successive scans without cleaning the surface of electrode [1]. The voltammetric studies in different pH media pinpoints the fact that the electrochemical redox reactions involve only electrons or couple with a proton transfer [2]. Similarly square wave voltammetry (SWV) is carried out for the verification of the nature of redox process as it is superior over cyclic voltammetry (CV) in sensitivity and ability to record both forward and reverse current components in the same scan. Finally the number of electrons involved in

oxidation or reduction process was determined from differential pulse voltammetry (DPV).

4.2. Cyclic voltammetry of electroactive compounds

In order to propose the redox mechanism of the selected biologically active compounds initial experiments were carried out using cyclic voltammetry. The nature of the redox process such as reversibility, irreversibility and quasi-reversibility was ensured from anodic and cathodic peak potential difference of CV experiments. The data obtained from CV results were also used for the determination of kinetic parameters like heterogeneous electron transfer rate constant and diffusion co-efficient.

4.2.1. Cyclic voltammetry of-1-methoxyphenazine (MPZ)

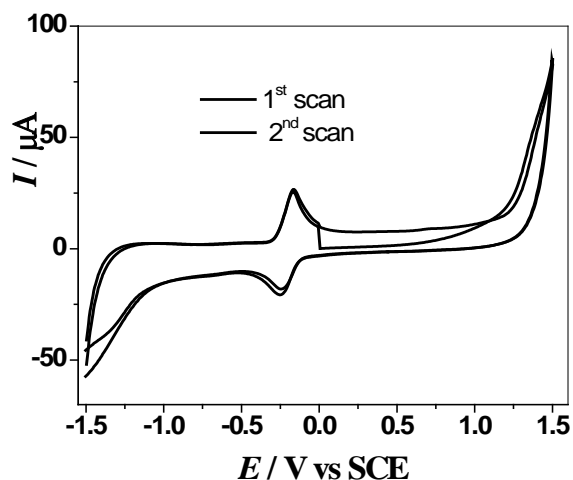


Fig.4.1. CVs of 0.3 mM solution of MPZ recorded in pH 3.0 at 100 mV/s scan rate.

Fig.4.1. presents a characteristic cyclic voltammogram of 1-methoxyphenazine in medium buffered at pH 3.0 having nitrogen saturated environment. Throughout the voltammetric measurements a constant flux of N_2 was kept over the analyte surface with the aim of avoiding the interruption of atmospheric oxygen with the analyte. MPZ was observed to undergo reduction as indicated by the appearance of a cathodic peak at $E = -0.239$ V. On the reversal of scan anodic signal was observed that indicated oxidation of the reduced product of MPZ. The absence of signal/s in the positive domain (starting from 0 V) indicated the stability of the analyte to oxidation in strongly acidic

environment. However, in slightly acidic, neutral and alkaline media an anodic peak indicating the oxidation of the analyte was also appeared (Fig. 4.2).

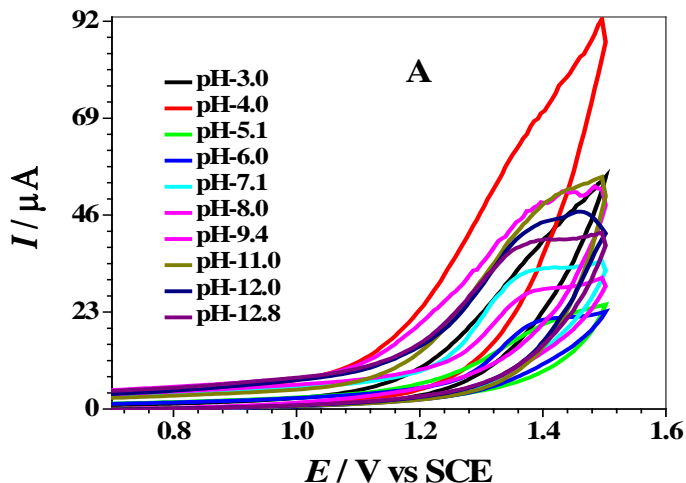


Fig.4.2. CVs of 0.3 mM solution of MPZ recorded in pH 3.0-12.8 at 100 mV/s scan rate.

The CVs shown in Fig.4.3A demonstrates the consequence of pH on the redox behavior of 1-methoxyphenazine. It can be viewed that redox signals shift towards more negative potentials with the escalation in pH. This shift is justifying the difficulty in reduction process owing to lesser number of protons in the basic environment. These voltammogram represent pH dependent redox process of 1-methoxy phenazine up to pH 11.2 after which it becomes pH independent. So pH 11.2 represents pKa of MPZ at which it undergoes chemical protonation deprotonation reactions. Literature study shows that organic compounds whose potentials are pH reliant undergo protonation deprotonation reactions [3]. This shift in potential when plotted verses pH (see Fig. 4.3B) for both cathodic and its corresponding anodic peak gave slope value close to 59 mV confirming the involvement of equal number of protons in addition to electrons in the reduction and its corresponding oxidation steps [4] according to following equations:

$$E_{pc} = -0.056 \text{ pH} + 0.078 \quad (\text{cathodic peak}) \quad (4.1)$$

$$E_{pa} = -0.059 \text{ pH} + 1.160 \quad (\text{anodic peak}) \quad (4.2)$$

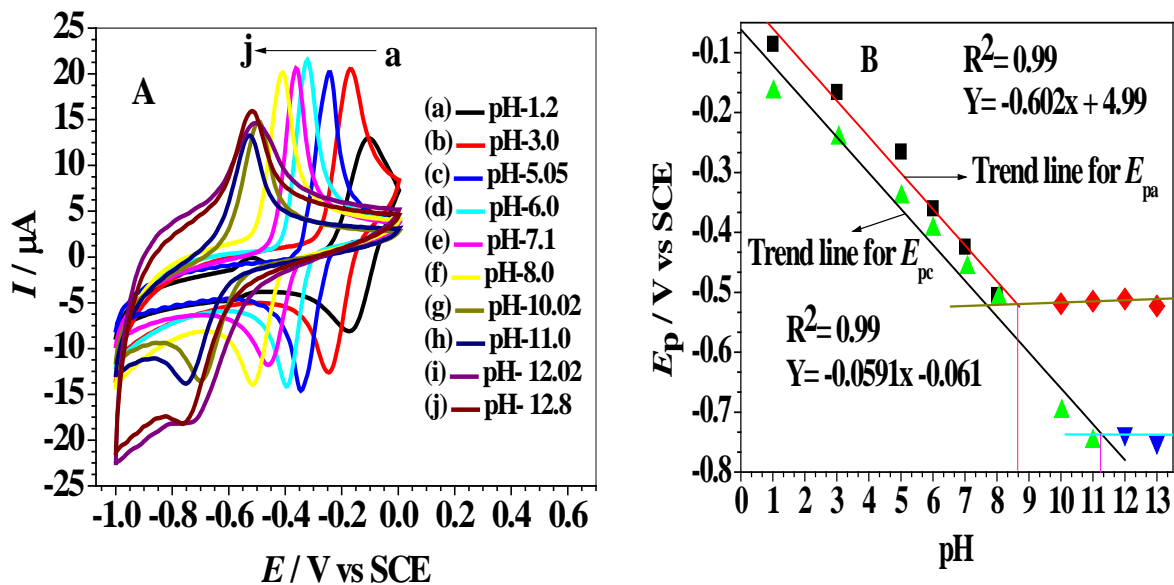


Fig.4.3. (A) CVs of 0.3 mM solution of 1-methoxyphenazine recorded in different pH media at 100 mV/s scan rate (B) Peak potential *versus* pH plots of both peaks of 1-methoxyphenazine (using CV data of Fig. 4.3A).

In order to determine the diffusion co-efficient of MPZ, CVs were recorded in nitrogen saturated 0.5 mM solution at different scan rate in media buffered at pH 3.0 and pH7.1. (Fig.4.4)

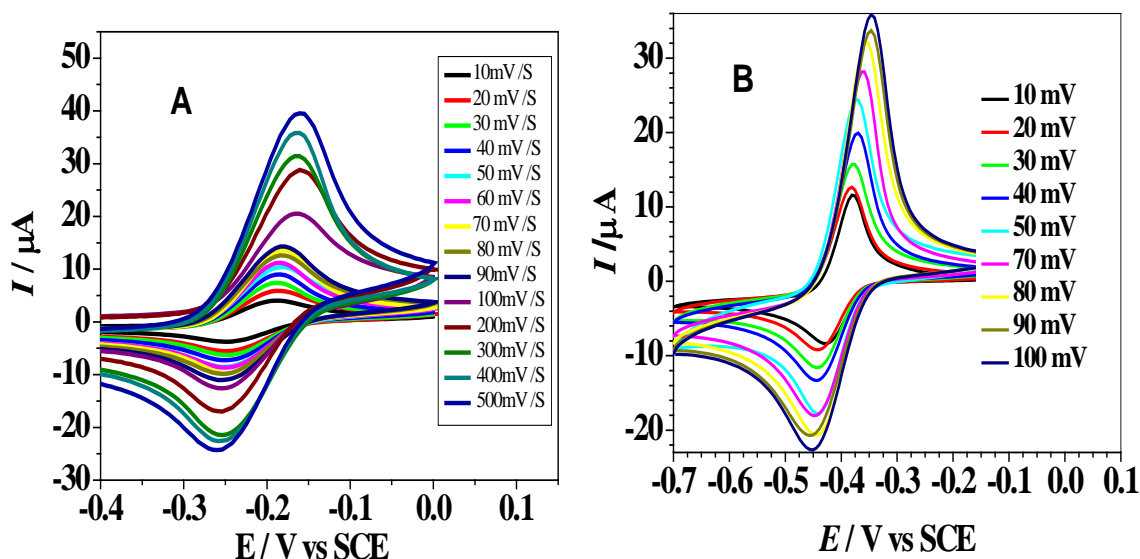


Fig.4.4. CVs of 0.5 mM solution of MPZ at different scan rates using glassy carbon electrode at pH 3.0 (A) and pH7.0 (B).

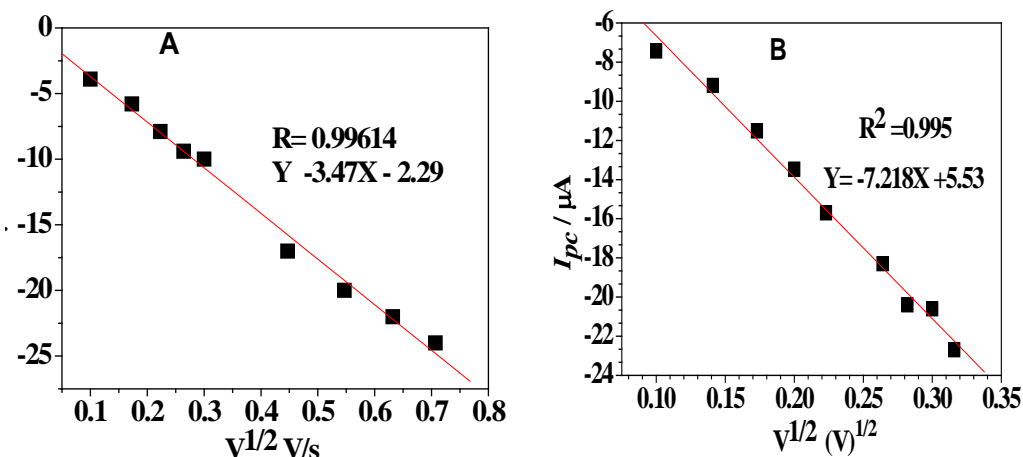


Fig.4.5. I_{pc} vs squar root of scan rate at pH 3.0 and pH 7.0.

Slight shift in potential with the increasing scan rate observed for 1-methoxyphenazine indicated quasi-reversible redox nature of MPZ. Cathodic to anodic current ratio of less than one also supported the quasi-reversibility. Moreover, increasing scan rate was accompanied with the rise in peak current from 10-100 mV/s. Disparity of peak current with scan rate is a significant diagnostic criterion for understanding the redox behavior of compounds. Peak current when plotted vs $v^{1/2}$ (Fig. 4.5) showed the reduction of 1-methoxyphenazine to be a diffusion controlled process. Diffusion coefficients with values $1.324 \times 10^{-5} \text{ cm}^2 \text{ s}^{-1}$ and $2.39 \times 10^{-5} \text{ cm}^2 \text{ s}^{-1}$ were determined via Randles-Sevcik equation from CV data recorded in pH 3.0 and 7.0 respectively.

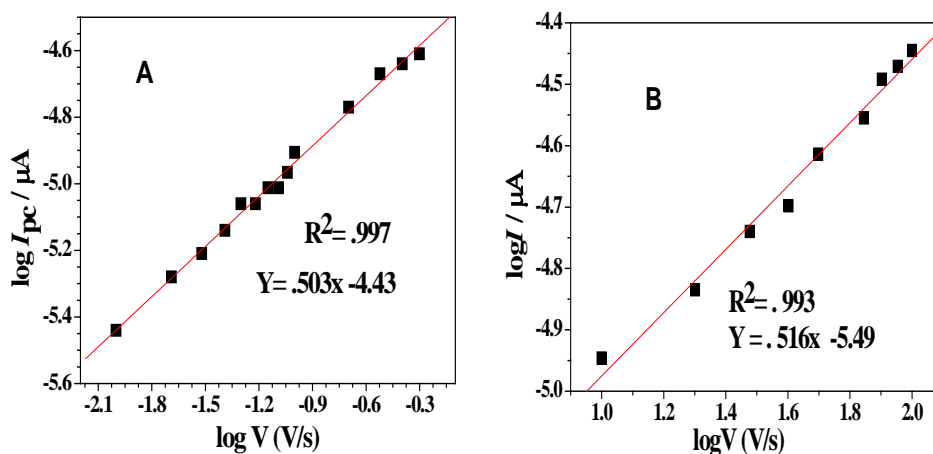


Fig. 4.6. Plot of $\log I_{pc}$ vs $\log v$ for the CV data of 0.5 mM solution at pH3 and pH7.

Linearity of the plots between $\log I_p$ vs $\log \nu$ with slope values of 0.503 (Fig. 4.6A) and 0.516 (Fig. 4.6B) at pH 3 and pH 7 very close to the theoretical value of 0.5 offered another evidence for the redox process of 1-methoxyphenazine to be diffusion limited [5].

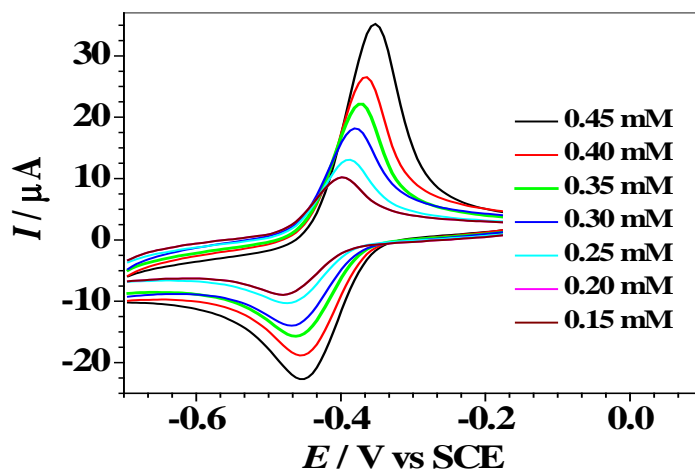


Fig. 4.7. CVs of different concentrations of 1-methoxyphenazine obtained in pH 7 at 100 mV/s.

Peak current of this compound varied linearly with the increasing concentration as shown in Fig. 4.7. This relationship is exploited using Nicholson expression for the evaluation of an important kinetic parameter i.e. heterogeneous electron transfer rate constant. Its estimated values of 1.043×10^{-2} cm/s and 1.397×10^{-2} cm/s from cathodic and anodic peak currents (Fig. 4.8) also support quasi-reversibility of its redox couple [6,7].

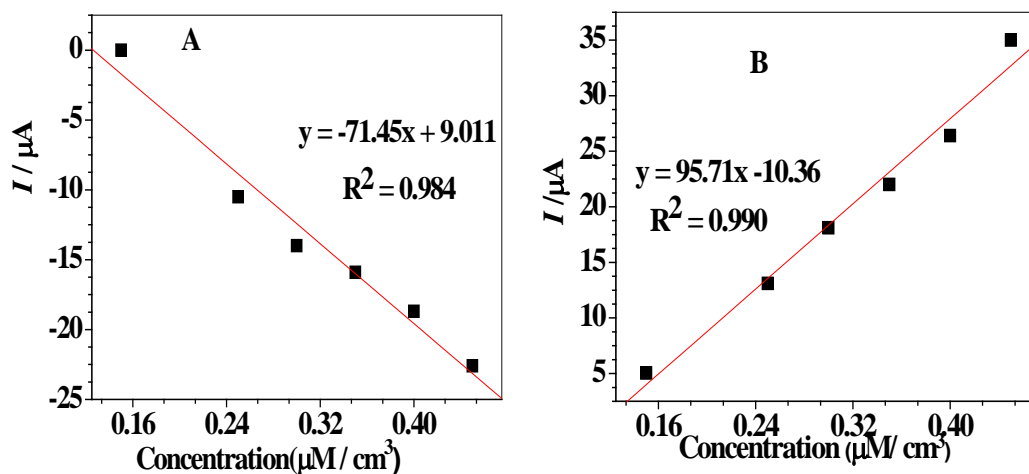


Fig.4.8. Current intensity of cathodic (A) and (B) anodic peaks (obtained in pH7 at 100 mV/s scan rate) versus concentration of 1- methoxyphenazine.

4.2.2. Cyclic voltammetry of 2-benzoyl-7-methoxy-2,3-dihydroisoquinolin-4(1H)one

Cyclic voltammetric experiments of 2-benzoyl-7-methoxy-2,3-dihydroisoquinolin-4(1H)-one abbreviated as IQN were carried out at a clean GCE between the potential limits +1.5 and -1.5 V in neutral conditions (pH 7.0) using 50 % aqueous ethanol (50% ethanol and 50 % water). During the voltammetric experiments the solution was purged through a constant flux of nitrogen for 8 to 10 minutes to confirm the removal of oxygen. Moreover, the same flux of nitrogen gas was kept over the solution surface to ensure the inert atmosphere in the cell. On starting from 0 in the positive direction one oxidation signal was observed at +0.908 V showing that IQN can oxidize under these conditions. Similarly on the reverse scan prominent peaks were observed on the cathodic part of the voltamogram at -0.528 and -1.247 V respectively which indicate that IQN reduces on the GCE. The extent of adsorption on the surface of electrode was confirmed from the successive second scan without cleaning the surface of electrode which shows that the peak current decrease for all the peaks in the second scan attributing to the adsorption of redox products on the surface of electrode. As cyclic voltammograms showed that IQN undergoes both oxidation and reduction on GCE (Fig. 4.9A) and both process are independent of each other. Therefore, for the detailed study further experiments were carried out separately.

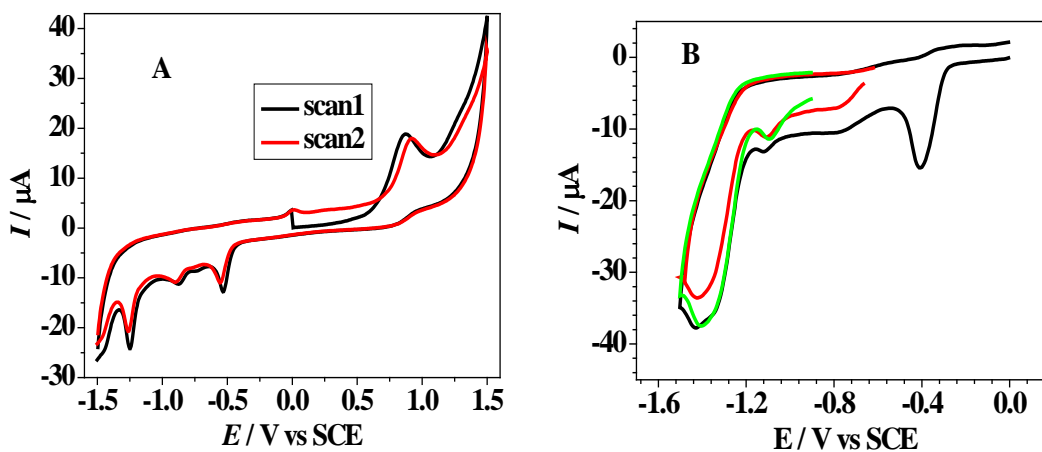


Fig. 4.9. (A) CVs of 0.4 mM solution of IQN recorded in medium of pH 7.0 at 100 mV/s scan rate (B) CVs of IQN recorded in in 0.1M acetate buffer of pH 4.0 at 100 mV/s scan rate.

4.2.2.1. Electro-reduction

All the CVs of the reduction region were obtained between the potential limits 0 and -1.5 V at 100 mV/s scan rate using 0.4 mM IQN solution. However, for the clipping experiments narrow potential windows were used to confirm the correlation between these peaks. The clipping experiments showed that all the reduction peaks are independent of each other (see Fig. 4.9B).

To investigate the effect of medium further cyclic voltammetric studies of IQN were conducted in different electrolytes with different pH ranging from 1.2 to 12.8. The results showed that the reduction of IQN is strongly dependent on pH of the medium. Starting from the acidic medium pH 1.2 upto pH 8 all the reduction peaks were observed. However, a constant shift in peak potential towards more negative potential were observed for both the reduction peaks with increasing pH (shown in Fig. 4.10). This shift in peak potential towards more negative values indicates that the reduction become more and more difficult at less acidic and neutral medium attributing to the less availability of H^+ [8]. All the reduction peaks disappeared at pH higher than 8 (Fig. 4.10A). DPV results showed that the average half width of the 1st reduction peak was 49 mV at all the studied pH. By plotting E_p vs pH the slope value came out to be 53 mV/pH (see Fig. 4.10B) closer to the theoretical value of 59 mV indicating that same number of electrons and protons involvement in this reduction process. Similarly the slope value of E_{pc} vs pH of the second reduction peak was 52 mV/pH near to the theoretical value of 59 mV which shows that addition of electrons is coupled by same number of protons [4,9].

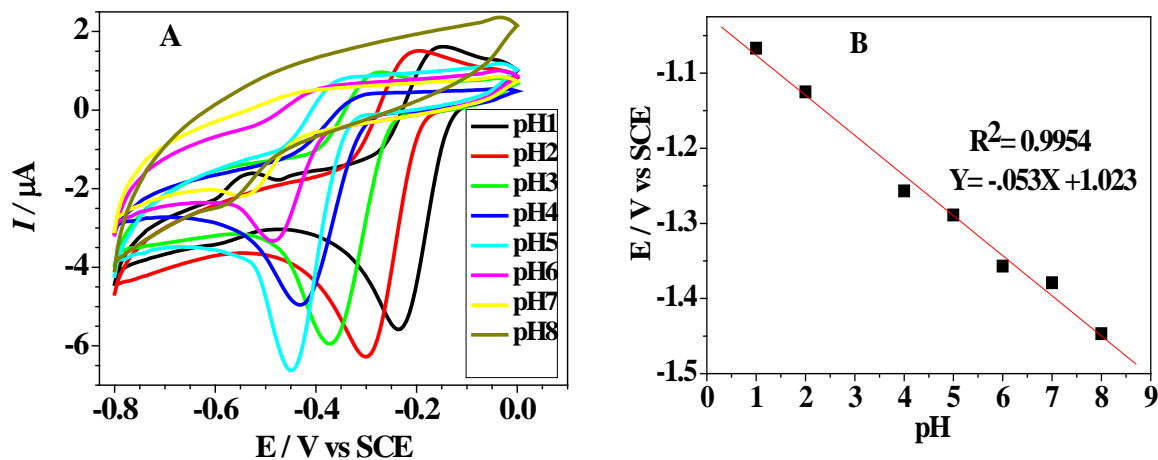


Fig. 4.10. (A) CVs showing first reduction peak of IQN recorded in different pH media at 100 mV/s scan rate using 0.4 mM solution (B) plot of peak potential vs pH.

CVs were also obtained for 0.4 mM IQN solution in 0.1M acetate buffer having pH 5.05 at different scan rates (Fig. 4.11A). A slight shift in E_{pc1} to more negative potential was observed with increase in scan rate indicating that the reduction process to be of quasi-reversible nature under these conditions. The Fig. 4.11A also shows that the I_{pc} is very low at lower scan rate.

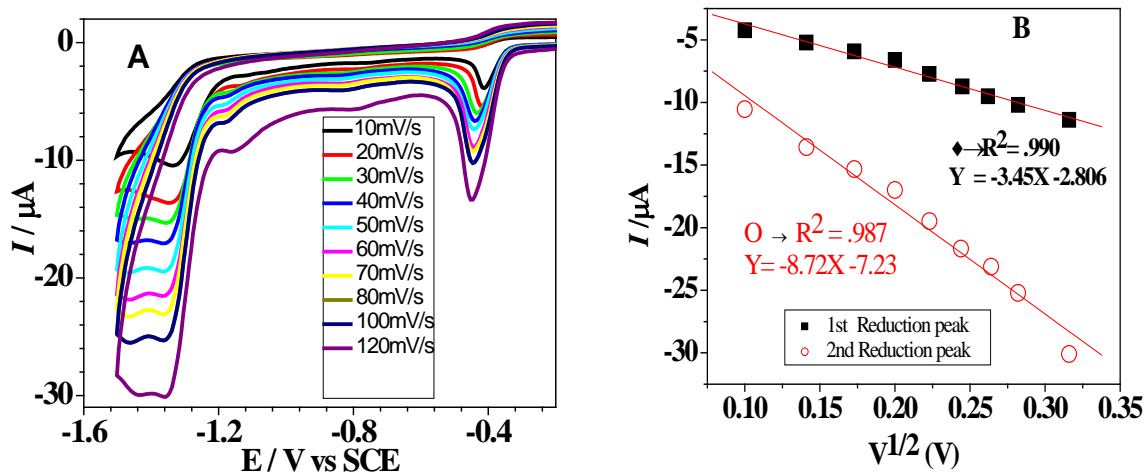


Fig. 4.11. (A) CVs obtained at a GCE in N_2 saturated solution of 0.4 mM IQN in buffer of pH 5 at different scan rates. (B) Plot of $I_{pc} / \mu A$ vs $v^{1/2}$ of 1st and 2nd reduction peaks.

The absence of peak in the reverse scan indicated the cathodic process to be irreversible. The current of all the peaks increased linearly with the square root of v as consistent with the diffusion controlled process. Such a process was further evidenced by the slope value (0.502) of the plot of $\log I_{pc}$ vs. \log of scan rate at pH 5 [5].

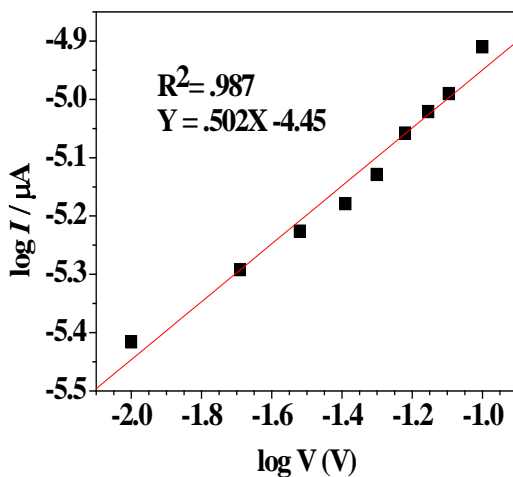


Fig.4.12. Plot of $\log I_{pc}$ (μA) vs. $\log v$ (V).

The value of diffusion coefficient was determined by plotting I_{pc1} vs $v^{1/2}$ using the following commonly used equation for an irreversible process:

$$I_{pc} = -2.99 \times 10^5 n (\alpha n)^{1/2} A C_0^* D_0^{1/2} V^{1/2} \quad (4.3)$$

Where I_{pc} is the peak current of the cathodic peak in amperes, n represent the number of electrons transferred in reduction process, D_0 the diffusion co-efficient in cm^2/s , C_0^* concentration of the solution in mol/cm^3 , v scan rate in V/s and A is the area of electrode in cm^2 . αn was calculated by

$$E_p - E_{p/2} = 47.7/\alpha n \quad (4.4)$$

From 56 mV value of $E_p - E_{p/2}$, $\alpha n = 0.424$ was calculated. Considering $n=2$ (from DPV) and from the measured slope of -3.45×10^{-5} the value of D_{IQN} was found to be $9.69 \times 10^{-6} \text{cm}^2/\text{s}$ with respect to first reduction peak.

A series of voltammograms at 100 mV/s were also recorded in medium of pH 5.0 using different concentration to obtain heterogeneous electron transfer rate constant for reduction of electrochemically active species. The electrode was polished before each scan to ensure the removal of electrochemically inactive adsorbed species on the surface of electrode. An increase in current was observed with increase in concentration. Current in μA was plotted against concentration (μM) and the K_{sh} was obtained using Reinmuth equation:

$$I_{pc} = nFA C_0 K_{sh} \quad (4.5)$$

$n=2$ (from DPV) and from the slope value of -14.4 the K_{sh} of IQN at pH 5.0 was calculated as $1.05 \times 10^{-3} \text{cm}/\text{s}$ with respect to 1st reduction peak.

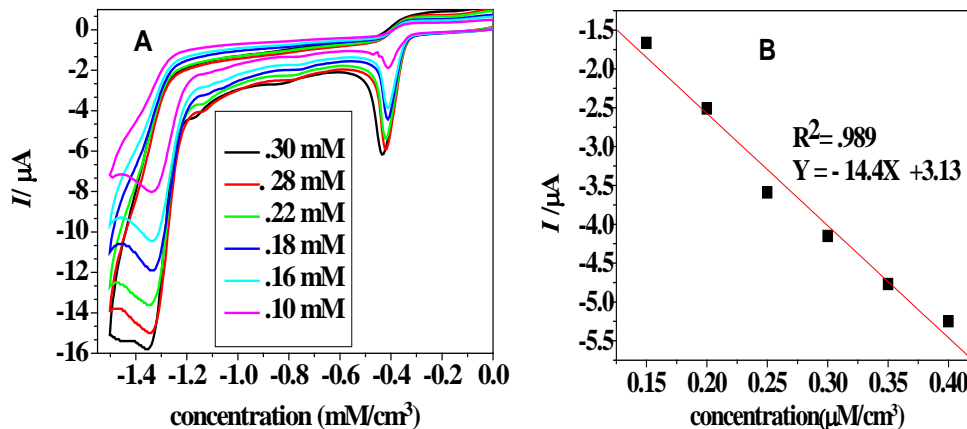


Fig. 4.13. (A) CVs recorded in pH 5.0 at 100 mV/s scan rate sing different concentrations of IQN (B) Plot of $I_{pc1}(\mu\text{A})$ vs concentration ($\mu\text{M}/\text{cm}^3$) using peak current data of 4.13A.

4.2.2.2. Electro-oxidation

As the oxidation peak was ensured to be independent of reduction process so for the detailed information it was studied separately. CVs were obtained in pH3.0-12.8 at 100 mV/s (Fig. 4.14A). Successive scans without cleaning the electrode surface showed a dramatic decrease in current intensity. Moreover, the peak disappeared in the 3rd scan due to very strong adsorption of nonelectroactive oxidation products of IQN on the electrode surface. In highly acidic media (pH 1.0-3.0) the oxidation could not appear thus suggesting the oxidizable moiety to be blocked under these conditions due to highly concentrated proton environment. But at pH higher then 3.0 upto pH12.8 the electrochemically active species exhibited oxidation in the positive going direction. Furthermore, a shift in peak position was also observed with a change in pH of the medium. In the pH regime 4.0 – 9.0 the peak showed a shift to less positive potentials exposing the fact that the oxidation becomes more and more facile in neutral and basic media. However, at pH higher than 9.0 the oxidation of the analyte lost its pH dependency and no shift in peak potential was observed above pH 9.0. The pKa value obtained from the plot of E_p versus pH (Fig. 4.14B) is 9.2 showing that protonation-deprotonation occurs at this pH. The slope value of 52 mV/pH of the plot of E_p versus pH obtained from CV results shows that the oxidation process of the electroactive species involves equal no of protons and electrons.

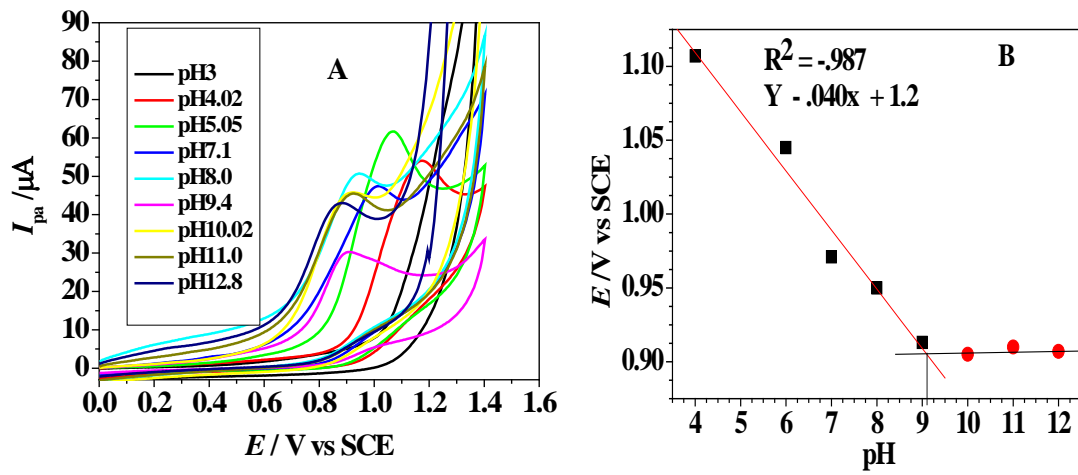


Fig.4.14.(A) CVs of 0.4mM solution of IQN recorded in a wide pH range at 100 mV/s scan rate (B) E_p vs pH plot for the oxidation peak of IQN.

To determine diffusion co-efficient a number of CVs were recorded at different scan rate in medium of pH 8.0 (Fig. 4.15A). A linear relationship consistent with diffusion controlled oxidation was found between peak current and square root of scan rate as shown in Fig. 4.15B. A very small shift in peak position was noticed towards the more positive potential with increase in scan rate. The peak current in amperes for an irreversible process is given by equation 4.3. αn with a value of 0.37 diffusion co-efficient was calculated from $E_p - E_{p/2}$ of 64 mV by using eq. 4.6 given as

$$I_{pa} = 2.99 \times 10^5 \alpha(\alpha n)^{1/2} A C_0^* D_0^{1/2} V^{1/2} \quad (4.6)$$

The slope value of the plot of peak current *versus* square root of v came out to be 5.78. Considering one electron oxidation (from DPV) and putting all other values the diffusion co-efficient of IQN in 0.1M phosphate buffer at pH 8 was quantified as $6.22 \times 10^{-5} \text{ cm}^2/\text{s}$.

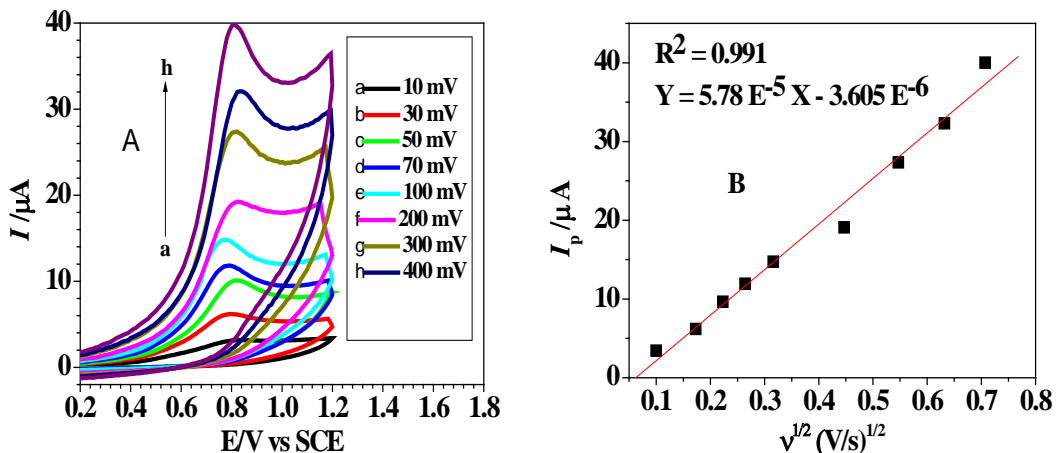


Fig.4.15.A. CVs of IQN recorded in 0.4mM solution at different scan rates at pH8. (B) Plot of I_{pa} vs $v^{1/2}$ using data obtained from Fig. 4.15A.

For the determination of heterogeneous electron transfer rate constant a number of CVs depicted in Fig.4.16A at 100 mV/s scan rate were recorded at pH 8.0 using different concentration of IQN. A linear relationship was found between peak current and concentration. Heterogeneous electron transfer rate constant was determined from the slope of current *versus* concentration by using Reinmuth equation for irreversible oxidation peak:

$$I_{pa} = nFACK_{sh} \quad (4.7)$$

Where n is the number of electron transfer involved in oxidation, F Faraday constant, C concentration in μM . By plotting peak current in μA *versus* concentration in μM the slope value came out as 40. By putting the values in the Rienmuth equation K_{sh} was evaluated as $5.839 \times 10^{-5} \text{cm/s}$.

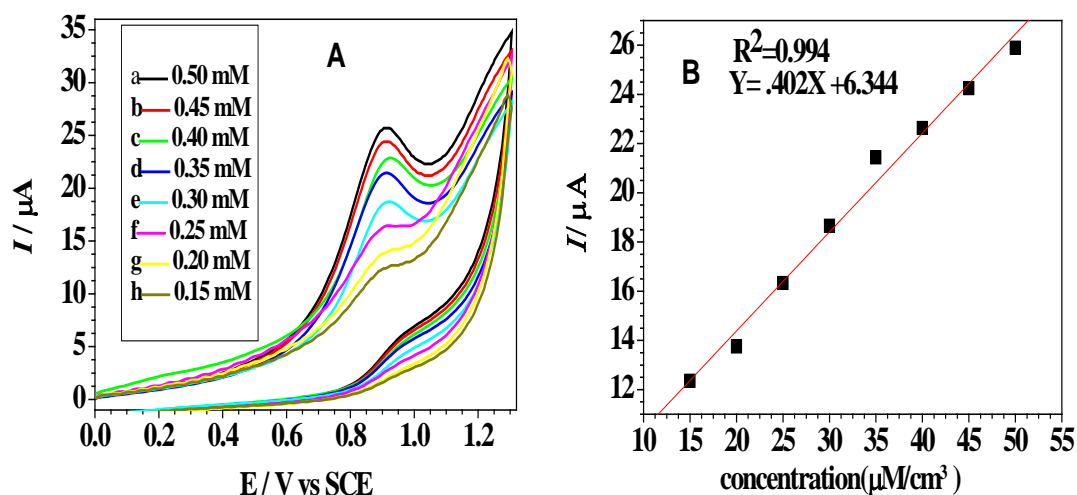


Fig.4.16. (A) CVs recorded in different concentration at pH8 and 100mV/s scan rate (B) Plot of I_{pa} vs concentration using data obtained from Fig. 4.16A.

4.2.3. CV of 1-hydroxy-2(hydroxymethyl)anthracene-9,10-dione (HAQ)

Cyclic voltammograms (Fig.4.17) of HAQ obtained in pH 7.1 using 0.1M phosphate buffers in the potential range of -1.5 V to +1.5 V were at 100mV/s. On scanning in positive direction from 0V one oxidation signal appeared at 1.17 V. On the reverse scan a cathodic peak registered at -0.606 V which was coupled by an anodic peak in the negative region at -0.409 V. During all the CV experiments the solution was continuously treated with a constant flux of nitrogen gas for 6 to 8 minutes to validate the complete

removal of oxygen. Furthermore, same flux of nitrogen was kept over the solution surface in cell to prevent the entrance of oxygen when the scan was recorded. Working electrode was polished with alumina powder before each scan and washed with ethanol and distilled water. Same number of peaks was observed in the second scan with a decrease in peak current for all peaks attributing to the adsorption of redox products on the surface of electrode. As for this compound oxidation and reduction peaks were separated by a wide difference of potential and both of these are independent of each other so for the detailed investigation further voltammetric assays were conducted separately in these two regions.

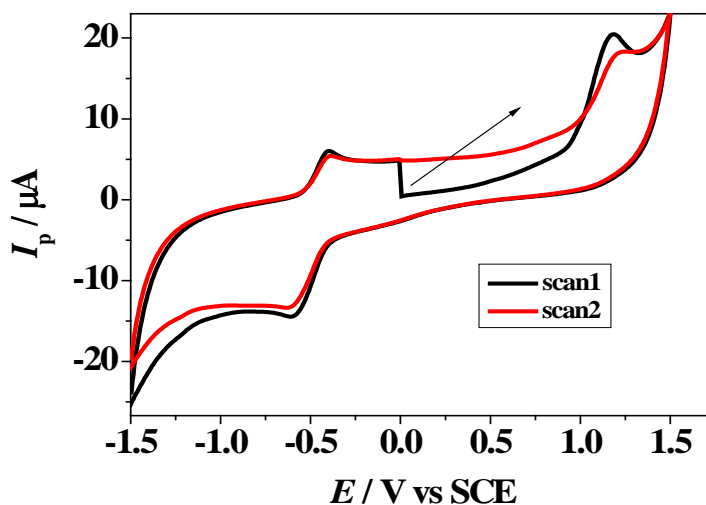


Fig.4.17. CVs of 0.2 mM solution of HAQ recorded with GCE in N₂ saturated solution of pH4 at 100mV/s scan rate.

4.2.3.1. Electro-reduction of HQA by CV

All the CVs corresponding to the reduction region of HAQ were recorded at a GCE in the potential range of -0.2 V to -1.1 V. To study the effect of pH on the reduction of HAQ CVs were obtained in different media of pH 1.2 to 12.8 (Fig. 4.18A). A regular shift in peak potential of reduction peak was observed with a change in pH of the medium which showed that the reduction involved the addition of both electron and proton. This effect of medium was used to propose the redox mechanism of HAQ. However, no further shift was observed above pH 10 for reduction peak indicating that above this pH reduction

only involves transfer of electrons. Peak potential of cathodic peak was plotted against pH as shown in Fig. 4.18B and pK_a with a value of value 9.8 was determined. The slope of 57 mV/pH showed that in reduction addition of electrons are accompanied by the same number of protons.

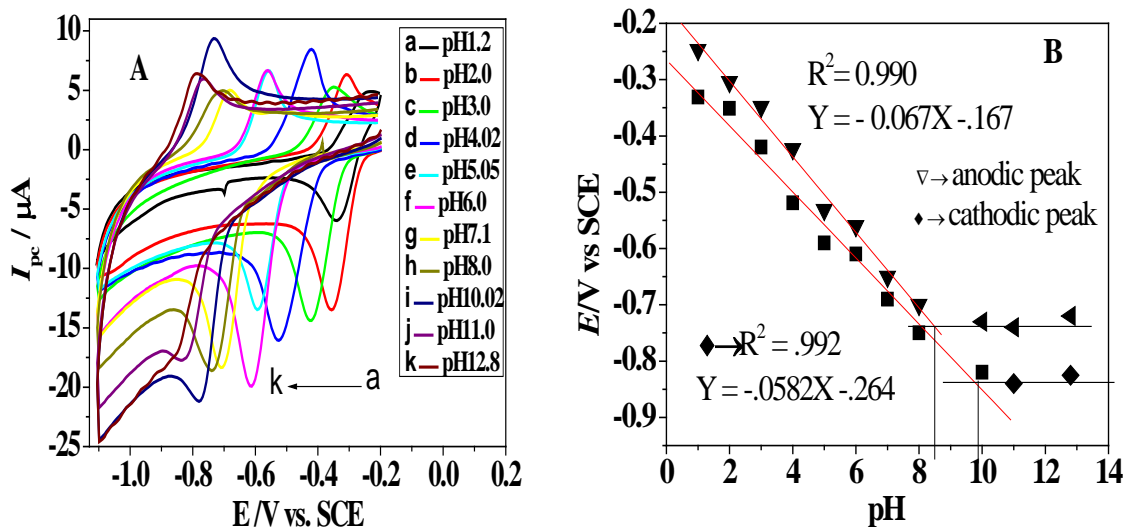


Fig.4.18.A. pH effect on the CVs of 0.2 mM HAQ obtained at 100mV/s scan rate (B) Plot of E_p vs pH of both anodic and cathodic peaks using data of Fig. 4.18A.

Similarly the oxidation of the corresponding reduction product is also pH dependent which becomes more and more difficult with increase in pH of the medium. The oxidation of the reduction product showed pK_a value of 8.4. By plotting E_p vs pH of the medium 67 mV/pH was obtained as the slope value which seems near to the theoretical value of 59 mV/pH value a criterion for the involvement of same number of electrons and protons. Hence, oxidation also involves the same number of electrons and protons.

To calculate diffusion constant and study the scan rate effect CVs of HAQ solution shown in Fig. 4.19 were recorded in pH 5.0 and 7.1 at different scan rates. A regular rise in peak current was observed with increase in scan rate with no significant shift in peak potential. At pH 7 the slope of the plot of I_{pc} vs square root of scan rate (Fig. 4.20B) came out as $-9.22 \times 10^{-5} \text{ A}/(\text{Vs}^{-1})^{1/2}$. In case of pH 5.0 two distinct segments appeared when I_{pc} was plotted against $v^{1/2}$ corresponding to scan rate below and above 100 mV/s (shown in Fig. 4.20A). However the scan rate lower than 100 was used for diffusion coefficient and $\alpha_a n$ calculations.

And from $E_{pc} - E_{p/2c}$ at pH 5 $\alpha n = 0.356$ and $n = 2$ (from DPV) diffusion co-efficient values came out as $3.63 \times 10^{-5} \text{ cm}^2/\text{s}$ and $6.06 \times 10^{-5} \text{ cm}^2/\text{s}$ at pH5.0 and 7.1. The lower D value in acidic conditions in comparison to neutral medium is suggestive of thick solvation sphere around HAQ that lowers its mobility towards electrode surface.

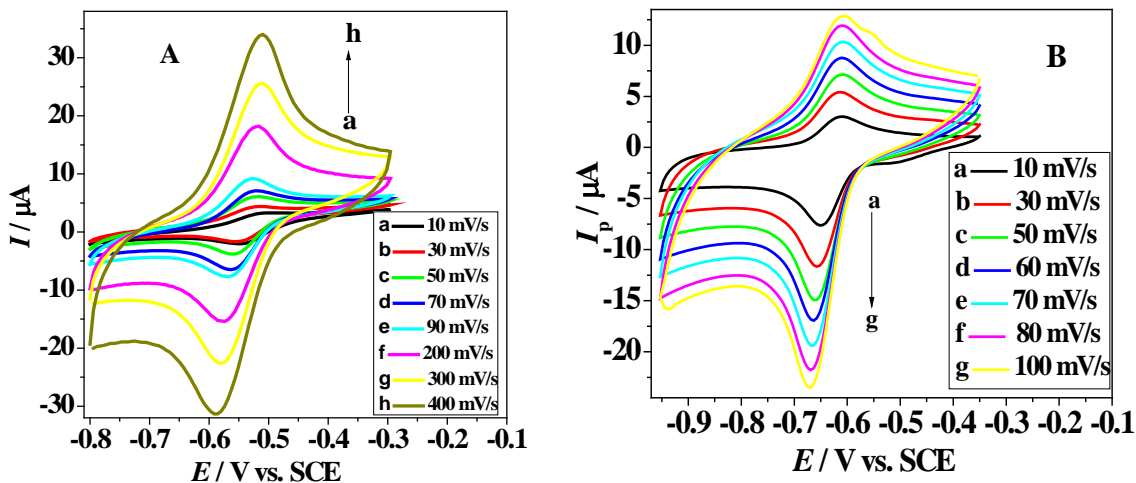


Fig. 4.19. CVs of 0.2 mM HAQ obtained with GCE obtained in (A) pH 5 and (B) 7.1 at different scan rates.

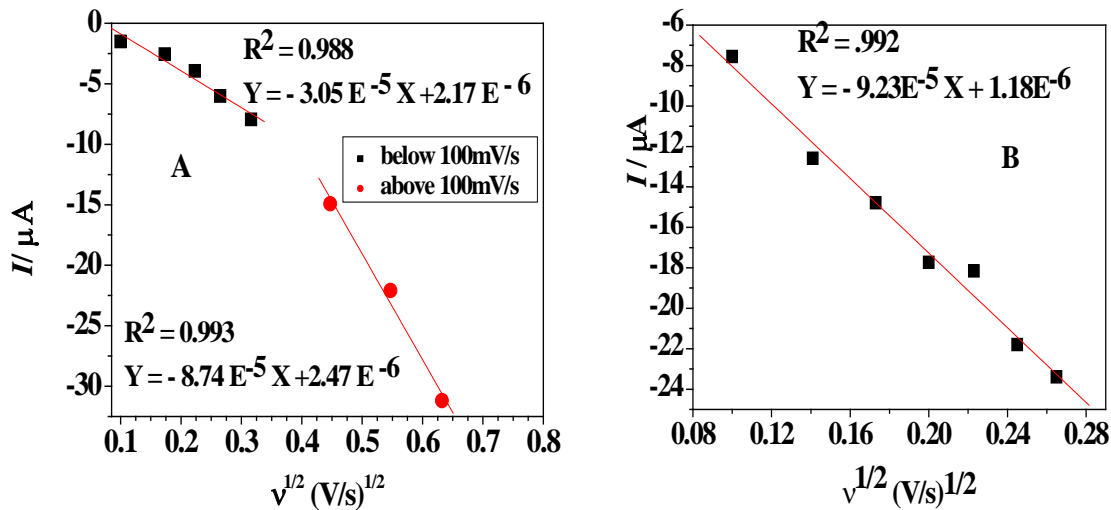


Fig.4.20. Plots of I_{pc} vs $v^{1/2}$ of cathodic peaks recorded in (A) pH 5 and (B)7.1.

The diffusion controlled nature of the reduction process was also confirmed by plotting $\log I_{pc}$ vs $\log v$ (Fig. 4.21). The slope values at pH 5 and pH 7.1 are -0.65 and - 0.58 respectively having a close agreement with the theoretical value of 0.5 [5,10]

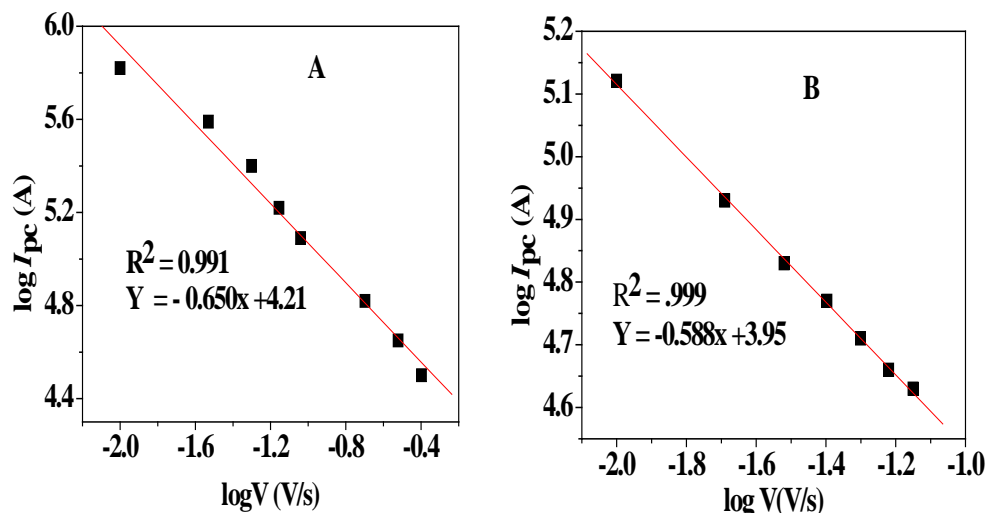


Fig.4.21. plot of $\log I_{pc}(A)$ vs $\log V(Vs^{-1})$ of cathodic peak of 0.2mM HAQ at (A) pH 5 and (B) pH 7.1.

Nicholson equation was used for the determination of heterogeneous electron transfer rate constant which is based on correlation between k_{sh} and peak separation by a dimensionless parameter Ψ and mathematically is given as

$$\Psi = (D_0/D_r)^{\alpha/2} k_{sh} / (\pi\alpha D_0)^{1/2} \quad (4.8)$$

Putting Ψ as 8.40 for peak separation of 65 mV at pH 7.1 and substituting the values of $\alpha = 0.71$ and $D_0/D_r = 0.36$, k_{sh} was calculated as $2.91 \times 10^{-3} \text{ cm s}^{-1}$. Thus the value of k_{sh} also supports the quasi-reversible nature of the redox process.

4.2.3.2. Electro-oxidation of HAQ by CV

For the separate study of oxidation region the potential range was fixed between the limits +0.3 V to +1.3 V and CVs were recorded on GCE at 100 mV/s scan rate in different pH conditions using 0.2 mM HAQ in the presence of 0.1M supporting electrolytes (Fig. 4.22A). No signal was appeared at and below pH 3 but above a permanent oxidation peak was noticed in the CVs of HAQ. However, this oxidation peak showed broadness at pH 10 and 11 indicating the merging of two oxidation peaks. This Peak shows change in its position with a change in pH of the medium which is an evidence of the involvement of protons. Owing to its shift in peak potential with pH, peak potential was plotted against pH (Fig.4.22B) and 55 mV/pH slope value which is in close

agreement with the theoretical value of 59 mV/pH was obtained. Thus this validates the fact that oxidation involves the loss of equal numbers of electrons and protons. Furthermore, peak current got highly decreased in the 2nd scan and disappeared in the 3rd scan that strongly supports the extreme adsorption of oxidation product on the electrode surface [11].

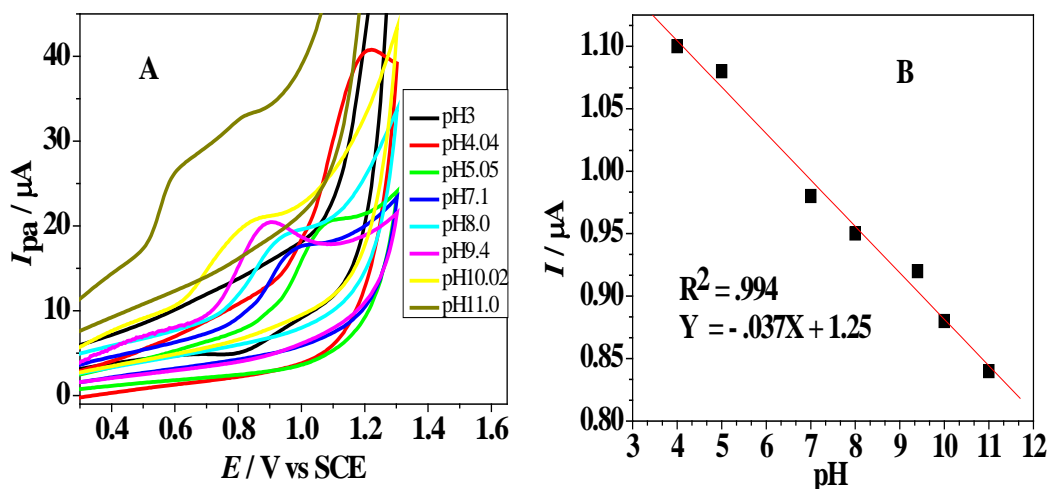


Fig. 4.22. (A) CVs of 0.2 mM HAQ obtained on GCE at different pH and 100 mV/s scan rate (B) Plot of E_{pa} vs pH.

Cyclic voltammetry was also performed at different scan rates in 0.2 mM HAQ, 0.1M phosphate buffer at pH 7.1. Peak current showed an increase with increase in scan rate (Fig. 4.23A). To monitor the dependency of peak current on scan rate I_{pa} was plotted against the square root of scan rate (Fig. 4.23B). A linear relationship was observed with the slope value of $1.86 \times 10^{-5} A / (Vs^{-1})^{1/2}$. αn with a value of 0.67 was calculated from the experimentally determined value of $E_{pa} - E_{pa/2} = 71$ mV. Putting $n = 1$ the diffusion co-efficient having value of $5.73 \times 10^{-5} cm^2/s$ was calculated by using equations 4.6.

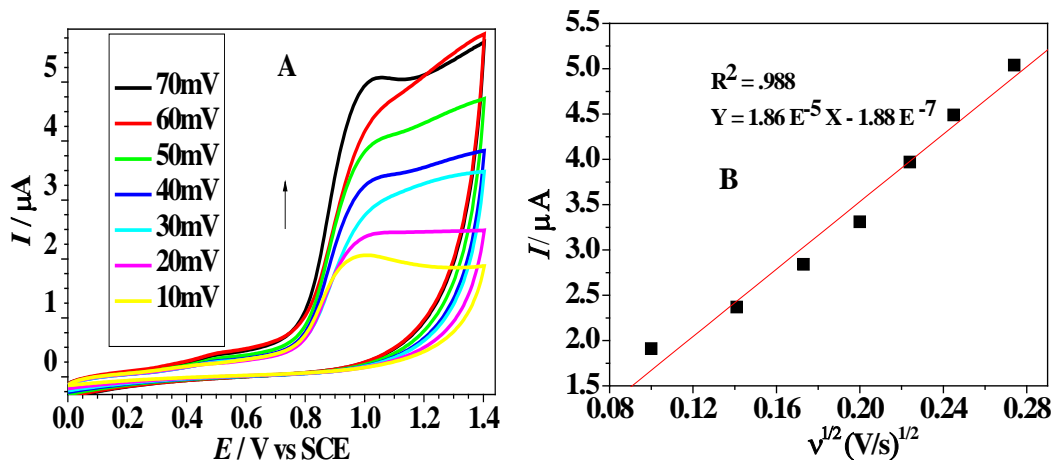


Fig. 4.23. (A) CVs of 0.2 mM HAQ obtained with GCE in pH 5 at different scan rates (B) Plot of I_{pa} vs $v^{1/2}$.

Similarly $\log I_{pa}$ was plotted against $\log v$ and a slope of $0.602 \text{ A}/(\text{Vs}^{-1})$ ensured the oxidation to be close to a diffusion controlled process.

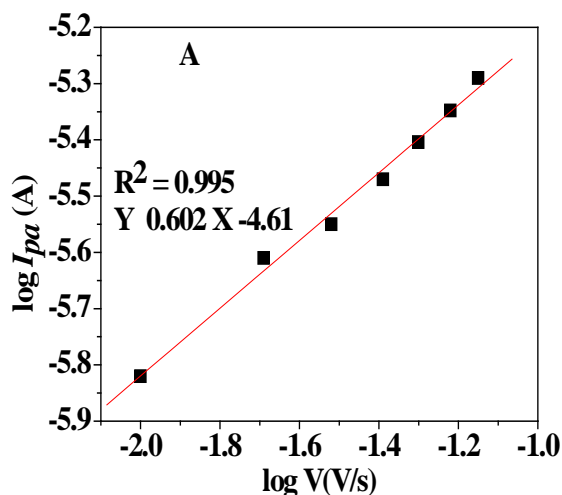


Fig. 4.24. Plot of $\log I_{pa}$ vs $\log v$ at pH 5.

Heterogeneous electron transfer rate constant was evaluated for the oxidation of HAQ at pH 5.0 by recording CVs in different concentrations at 100 mV/s scan rate. Effect of various concentration on peak current has been shown in Fig. 4.25A. A linear relationship was observed between peak current and concentration. The plot of I_{pa} vs concentration (4.25B) results in straight line with slope value of $0.46 \mu\text{A}/\mu\text{Mcm}^{-3}$. K_{sh} was determined by Reimuth expression $I_p = nFACK_{sh}$. The calculated value $5.72 \times 10^{-5} \text{ cm/s}$ recommends the irreversible nature of oxidation process.

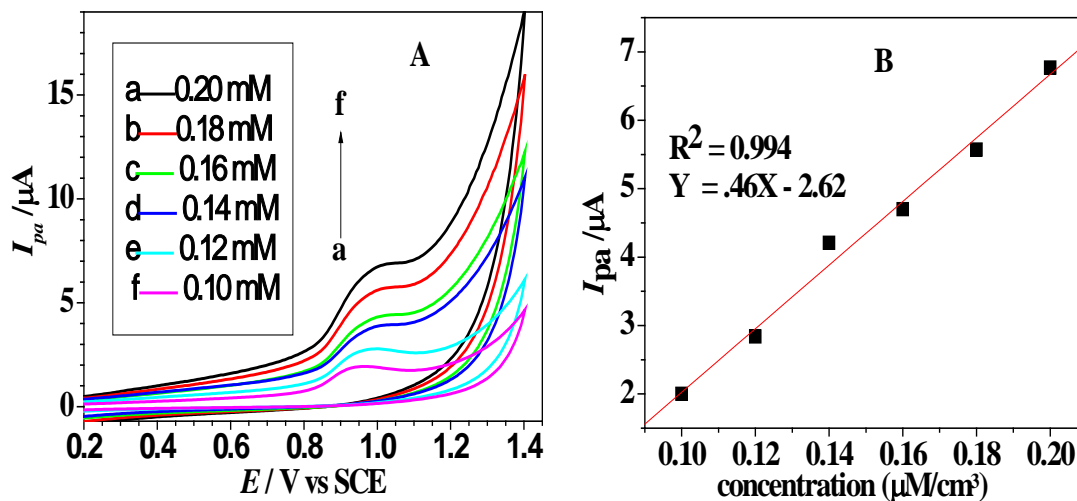


Fig. 4.25. A. CVs of different concentration of HAQ in pH 5 (B) Plot of I_{pa} (μA) vs concentration ($\mu\text{M}/\text{cm}^{-3}$).

4.3. Differential pulse voltammetry

In order to determine the number of electrons involved in reduction or oxidation process and to support the results obtained from CV; differential pulse voltammetry was carried out for all the three electroactive compounds. The number of electrons was determined from the width at half peak height ($W_{1/2}$) of DPVs.

4.3.1. Differential pulse voltammetry of 1-methoxyphenazine

Sensitivity of redox behavior of 1-methoxyphenazine was further confirmed via differential pulse voltammetry. It is evident from the voltammograms depicted in Fig. 4.26A that escalation in pH is accompanied with the shift of cathodic signal to more negative values ensuring difficulty of reduction phenomenon in basic media. Moreover, pKa value determined via differential pulse voltammetry (Fig. 4.26B) is complementing the CV and SWV results [12-14]. Variation in current is due to medium effect.

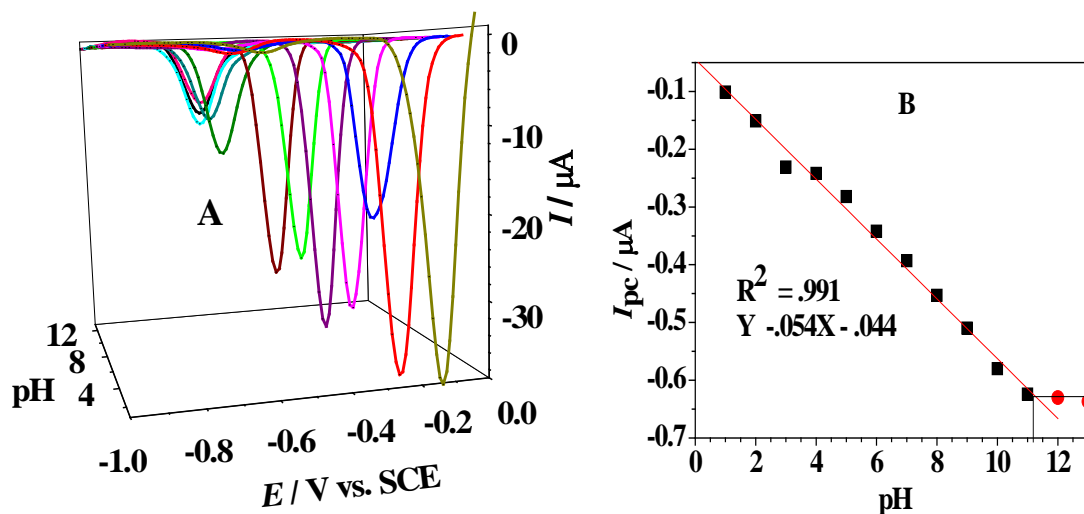


Fig. 4.26. (A) DPVs of 0.3 mM 1-methoxyphenazines in different media (B) Plot of E_p vs pH prom using data obtained from DPV results of Fig. 4.26A.

The average width at half peak height $W_{1/2}$ of all DPV scans is 92 mV close to the theoretical value of 90 mV corresponding to an electrochemical reaction involving the transfer of 1 electron.

4.3.2. (a) DP voltammetry of the reduction of IQN

The electrochemical reduction of IQN was studied using differential pulse voltammetry (DPV) in the presence of different supporting electrolytes over a pH range 1.2 to 8. The votammograms of IQN (Fig. 4.27A) obtained through DPV exhibited significant changes in peak positions on altering pH of the medium thus strongly supporting the CV results. Both of the reduction peaks were noticed under all these conditions. However, the peak current of the 1st reduction peak becomes very negligible at pH 7 and 8 and no peak was observable above pH 8. The peak width at half height of the first reduction peak was observed to be 48 mV which indicates that $2e^-$ are involved in this reduction process. Similarly the $W_{1/2}$ for second reduction peak was 54 mV which is also not far from the theoretical value of 45 mV so this reduction also shows the involvement of $2e^-$ [15]. Change in peak position of all the reduction peaks with variation in pH was found linear (Fig. 4.28B) and followed the relations

$$E_{pc1} / \text{V(vs SCE)} = - 0.200 - .052\text{pH} \quad (\text{pH}1 - 8) \quad (4.9)$$

$$E_{pc2} / \text{V(vs SCE)} = 1.023 - .054\text{pH} \quad (\text{pH}1 - 8) \quad (4.10)$$

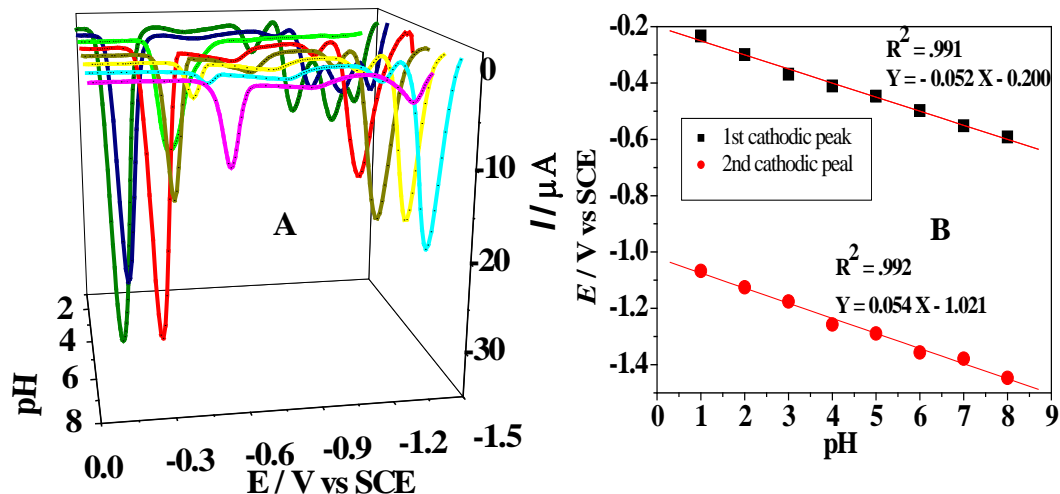


Fig. 4.27. (A) DPVs of 0.4 mM IQN in different media. (B) Plots of E_p vs pH for both reduction peaks.

4.3.2. (b) Differential pulse voltammetry of IQN oxidation

DPVs were also obtained for the characterization of anodic peak. All the DPVs of 0.4 mM IQN displayed in Fig. 4.29A were recorded at a cleaned GCE. Like the CV results a shift in peak position towards less positive potential was observed from pH 4 to 9 with a pK_a value of 9.1 at which chemical protonation-deprotonation occur. The average half peak width of 98 mV at all pH showed close agreement with the theoretical values revealing the involvement of one electron in the oxidation process. 53 mV/pH slope (Fig. 4.28B) shows that loss of electrons is coupled by equal number of protons. The linearity of pH versus peak potential is summarized in the following equation:

$$E_{pa} / \text{V (vs SCE)} = 1.2 - 0.053\text{pH} \quad (\text{pH } 4 \text{ to } 9) \quad (4.11)$$

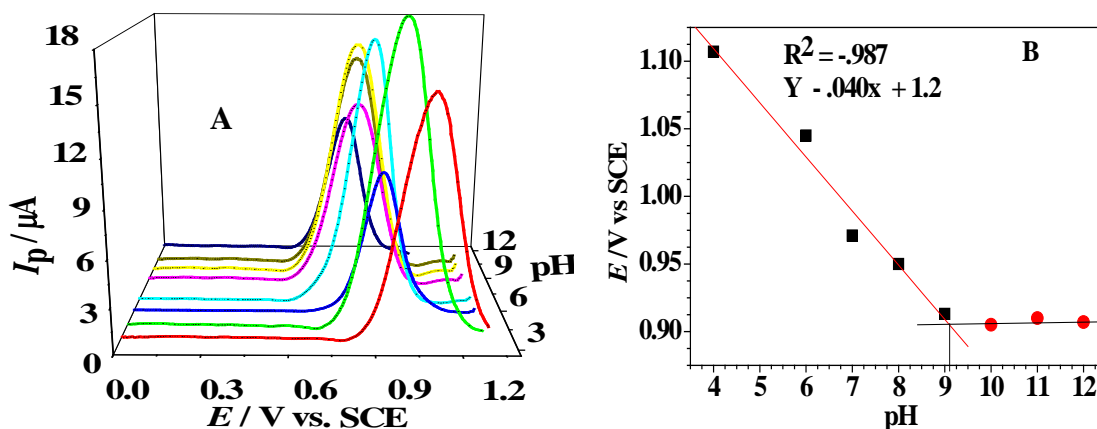


Fig. 4.28. (A) 3-D Representation of DPVs of the oxidation of 0.4 mM IQN in supporting electrolytes of different pH (B) Plot of E_p vs pH using data of Fig. 4.28A.

4.3.3. (a) Electro-reduction of HAQ by DPV

The redox behavior of HAQ was also studied by the most sensitive technique, differential pulse voltammetry to ensure the number of electrons that are involved in the redox reaction. DPVs were obtained with GCE in the pH range 1.2 to pH12.8 at 5 mV/s scan rate in nitrogen saturated solution of 0.2 mM HAQ (Fig. 4.29A). A shift in peak potential was noticed as a function of pH of the medium which supports the CV results. Moreover, pKa of HAQ was found as 9.66 (Fig. 4.29B). The average peak width at half height was found as 50 mV very close to the theoretical value of 45 mV criteria for the involvement of 2 electrons. The pH dependency of the reduction process is a proof of the involvement of protons. Similarly the slope (56 mV/pH) of the plot of E_p vs pH signifies that electrons are coupled by the same number of protons. Thus the reduction of HAQ involves the addition of 2 electron and 2 protons.

$$E_{pc} / \text{V(vs SCE)} = - 0.233 - 0.056\text{pH} \quad (4.12)$$

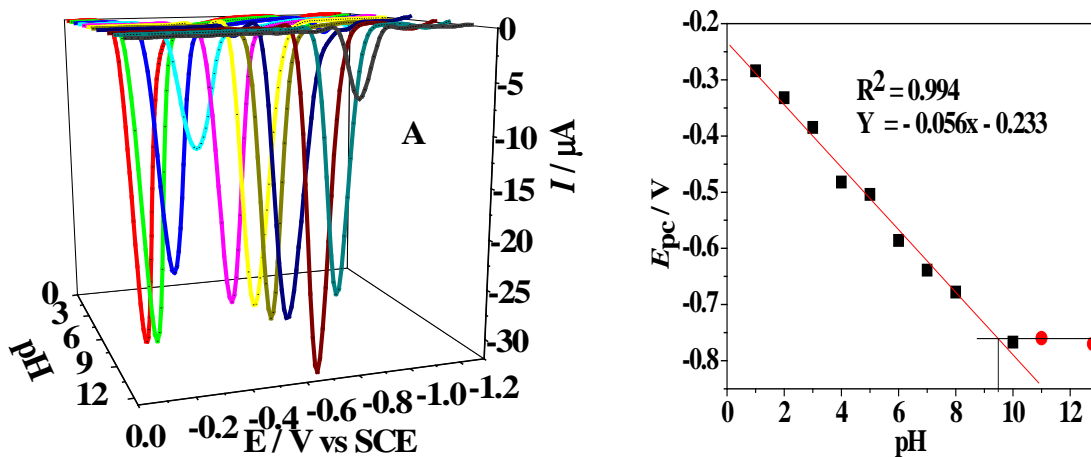


Fig. 4.29. (A) Representation of DPVs of 0.2 mM HAQ in various pH media (B) Plot of E_p vs pH of HAQ data obtained from Fig. 4.29A.

4.3.3. (b) Differential pulse voltammetry of HAQ oxidation:

The results of DPVs for 0.2 mM HAQ has shown 98 mV as the peak width at half height upto pH 9 somewhat close to the theoretical value of 90 mV, the maximum acceptable value for peak width providing a proof of the loss of one electron. However, above pH 9 this peak was splitted into two closely related peaks. The shifting of peak potential with change in pH of the medium strongly supports the CV results (Fig. 4.30A). Peak potential *versus* pH plot with a slope of 56 mV/pH (Fig. 4.30B) clearly indicates the loss of same number of electrons and protons through the following relation:

$$E_{pa} / \text{V (vs SCE)} = 1.25 - 0.055\text{pH} \quad (4.13)$$

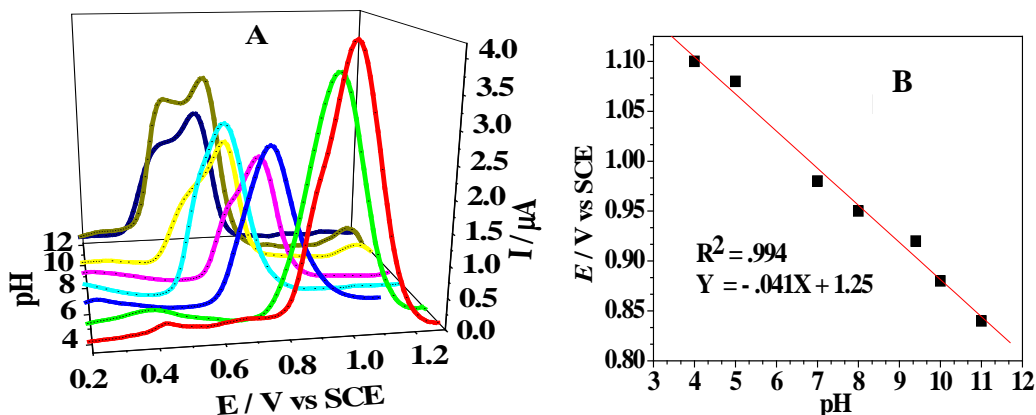


Fig. 4.30. (A) DPVs representing oxidation of 0.2 mM HAQ in different media (B) Plot of E_{pa} of HAQ vs pH

4.4. Square wave voltammetry

Square wave voltammetry was carried out for all the three compounds with the aim to determine the exact nature of the redox process, whether it is reversible, irreversible or quasi-reversible. Actually square wave voltammetry has some superiority over cyclic and differential pulse voltammetry due to low consumption of the analyte, fast speed of analysis, and less poisoning of the electrode surface. The most prominent edge of SWV over other voltammetric techniques is that one can check the reversibility of an electron transfer process in one scan because current is sampled in both forward and backward direction simultaneously in the same scan [2]. The details of SW voltammetric results of all the three compounds is presented here.

4.4.1. Square wave voltammetry of 1-methoxyphenazine.

Square wave voltammetry was employed to understand the redox behavior of this compound as it is a more sensitive technique. pH effect of 1-methoxy phenazine (Fig. 4.31) was also studied via this more sensitive tool. Here again reduction signal was observed to shift cathodically making reduction process less facile thus supporting CV results. Involvement of protons is also confirmed by the slope value of 0.054 volts for E_p vs pH plot.

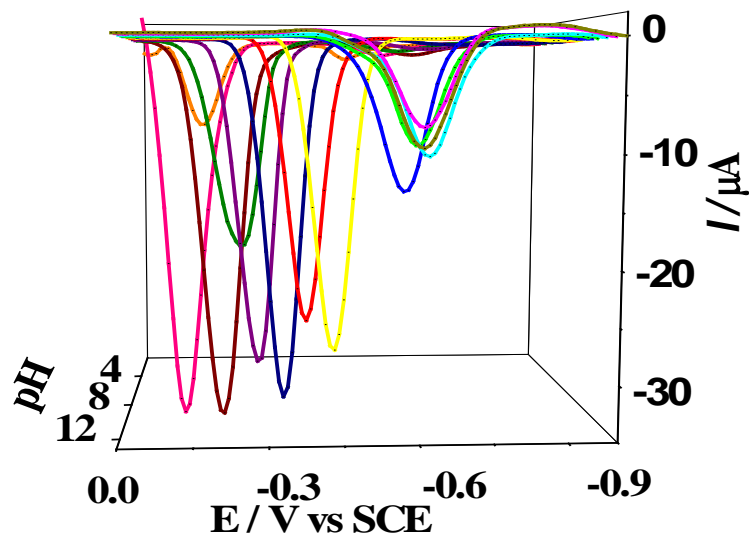


Fig. 4.31. SWVs of 0.3mM solution of 1- methoxyphenazine in different media at scan rate of 100 mV/s.

Redox activity of 1-methoxy phenazine was further examined via square wave voltammetry. It can be viewed from Fig. 4.32 that 1-methoxyphenazine registers two cathodic signals that correspond to its two step reduction. Moreover, inequality of reduction and its reverse anodic signal demonstrates the quasi-reversible nature of its redox mechanism at pH 7.1. Similarly the identical value of the potentials of peak 1_a and 1_c on the forward and backward current components is an indication of the adsorption of MPZ reduction products on the GCE surface .[16]

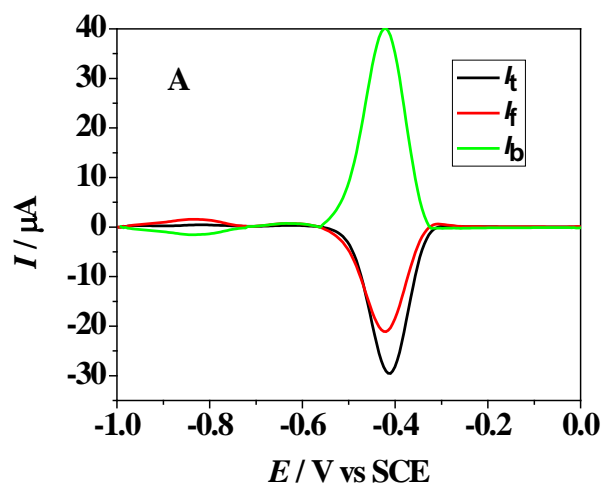


Fig. 4.32. Square wave voltammogram of 0.3 mM solution of 1-methoxyphenazine at pH 7.1 showing forward, backward and net currents at scan rate of 100mV/s.

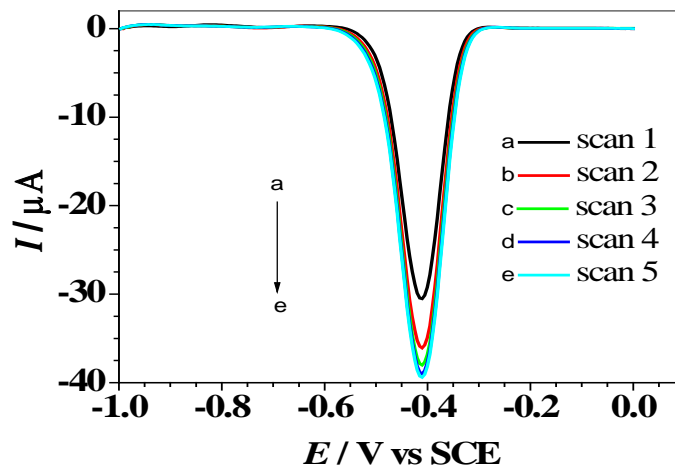


Fig. 4.33. Square wave voltammograms of 0.3 mM 1-methoxyphenazine at pH 7.1 without polishing the surface of glassy carbon electrode.

The voltammograms shown in Fig. 4.33 are displaying the effect of subsequent scans on the redox signature of the analyte. Increase in peak current with the successive scans without cleaning the electrode surface is indicating the adsorption of the reduced product (on the GCE surface) which acts as electron transfer mediator [17].

4.4.2. (a) IQN reduction by square wave voltammetry

The square wave voltammetric experiments were also performed for IQN to investigate the nature of its electrochemical processes. All the SWVs were recorded in the presence of constant flux of nitrogen up to pH 8 (Fig. 4.34A). Change in peak position towards more negative potential was observed for all the reduction peaks with an increase in pH of the medium. This behavior supported the CV and DPV results. SWV results show the reversibility of the 1st reduction peak and quasi-reversibility of the last peak. By plotting the forward and backward current components of the total current it appears that peak current of backward component is matching to forward component of 1st reduction peak thus confirms its reversibility while the 2nd reduction peak corresponds to a quasi-reversible process (see Fig. 4.34B).

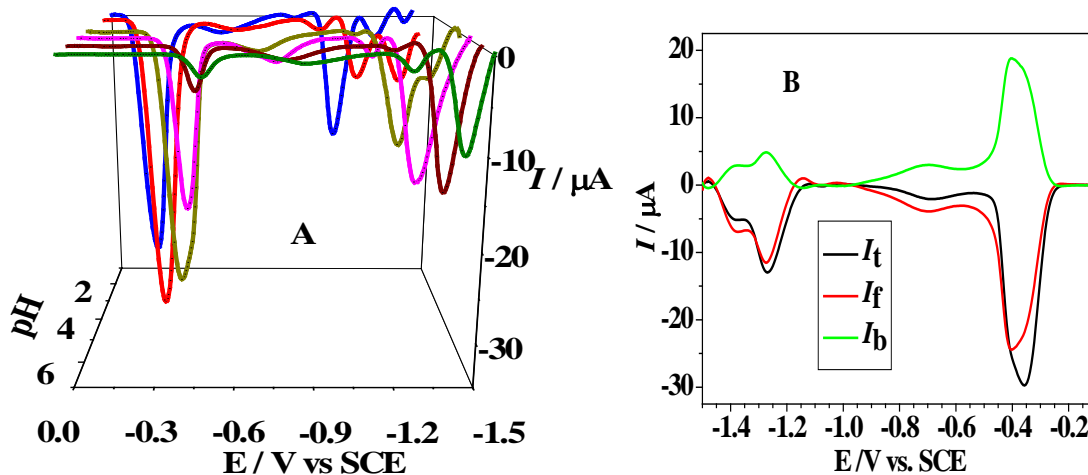


Fig. 4.34. (A) Representation of SWVs obtained in different pH (B) Square wave voltammogram of IQN showing forward and backward components of the total current at pH 4.

4.4.3. (b) Electro-oxidation of IQN by SWV

The oxidation of IQN was also studied via fast voltammetric technique, SWV to decide its nature. By plotting forward and backward components of the total current (see Fig. 4.35A) reversible nature of the oxidation was confirmed because the ratio of backward and forward current is 0.97 very close to 1. Moreover, a shift in peak position with change in pH of the medium was also observed from pH 4 to 9. This trend strongly supported the CV results.

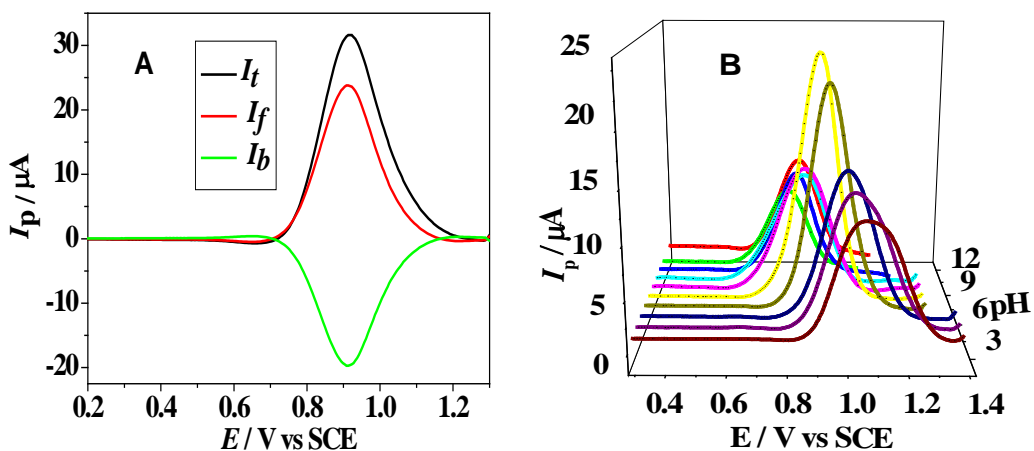


Fig. 4.35. (A) SWV of 0.4 mM IQN showing the nature of oxidation at pH 7.1 (B) SWVs representing IQN oxidation in different media.

4.4.4. (a) Electro-reduction of HAQ by SWV

The exact nature of the reversibility of HAQ reduction process was authenticated by square wave voltammetry. The SWVs depicted in Fig. 4.36A were recorded in 0.2 mM HAQ solution in the presence of different supporting electrolytes in the pH range 1.2 to 12.8. The same shift in peak potential as marked by CV and DPV results was observed with pH change. SWV response showed the quasi-reversible nature of this reduction process because the ratio of backward and forward current is less than 1 (Fig. 4.36A). Furthermore, successive voltammograms were also recorded in 0.2 mM HAQ solution for monitoring the outcome of number of scans. However, no significant effect on the peak current was noticed.

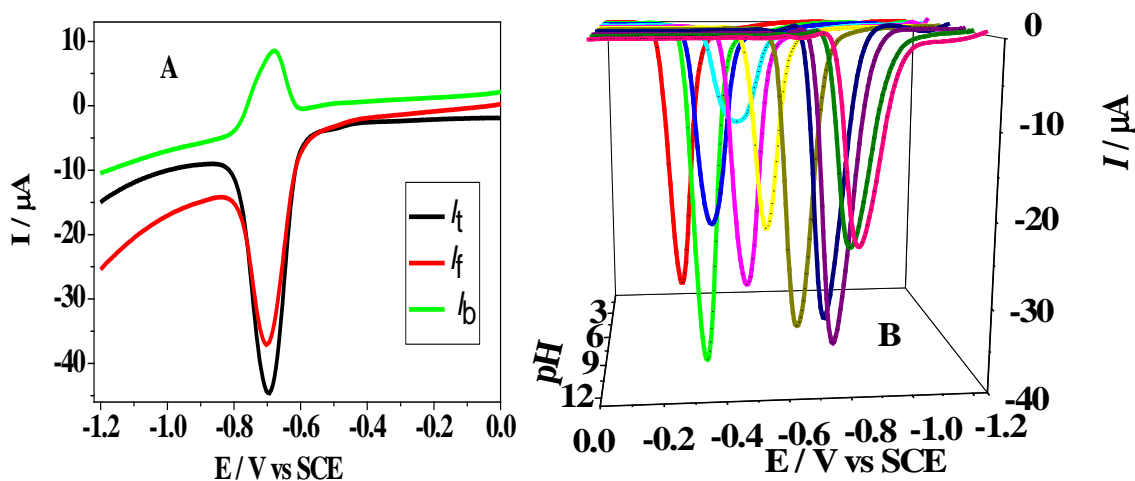


Fig.4.36. (A) SWV of 0.2 mM HAQ at pH 7.1 showing forward and backward components of the total current. (B) SWVs of 0.2 mM MAQ representing its reduction in different pH medium.

(b) SWV of oxidation of HAQ

The oxidation process appeared totally irreversible by plotting forward and backward components of the total current (Fig. 4.37). The forward current was found greater than the total current and the backward component showed the same sign as the forward. Such peculiar square wave characteristics signifying irreversible electrode reaction supported the CV and DPV results.

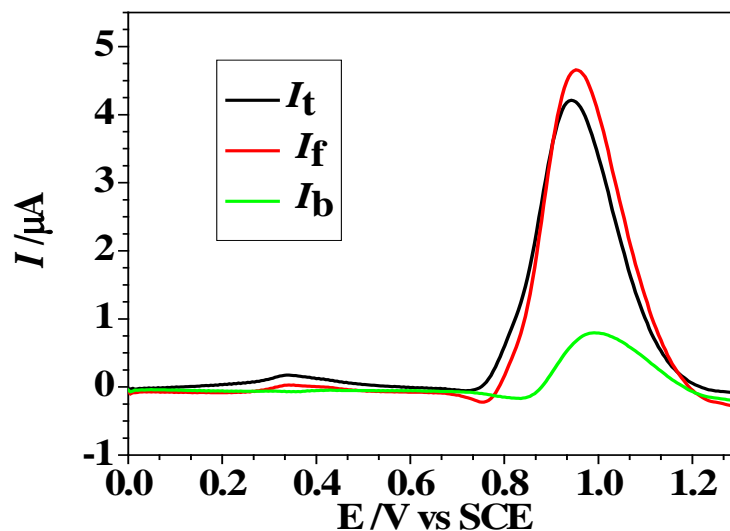


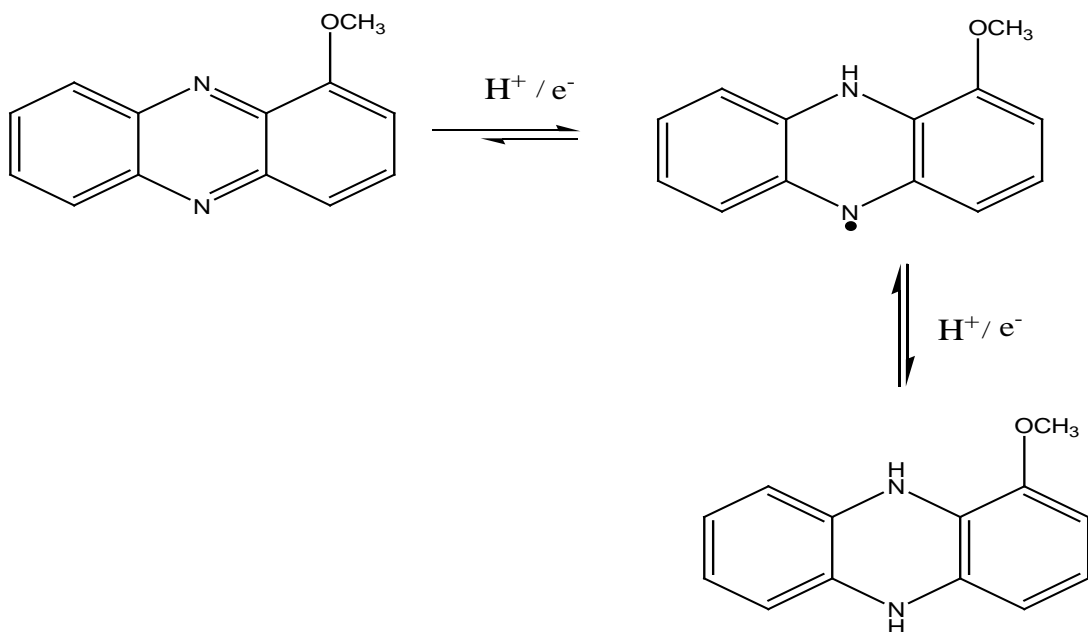
Fig. 4.37. SWV of 0.2 mM solution of HAQ showing irreversible oxidation in pH 7.1

4.4. Proposed Reduction / oxidation mechanism of electrode reactions

Redox mechanistic pathways of the studied compounds were proposed in the light of the results obtained via CV, DPV and SWV. The details are given below:

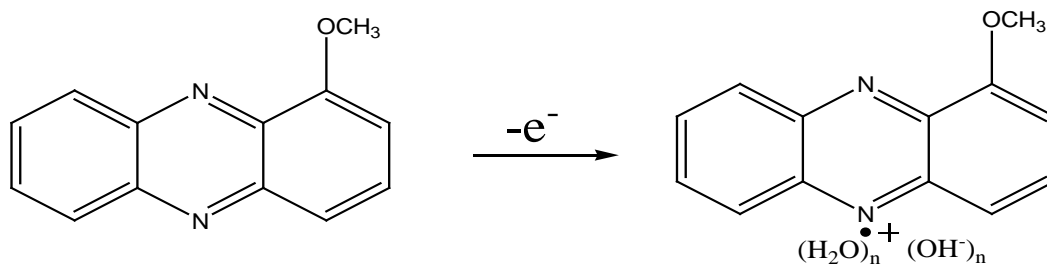
4.5.1. Redox mechanism of 1-methoxyphenazine

The appearance of two reduction peaks in the DPV and SQW indicates the stepwise addition of two electrons to 1-methoxyphenazine. The quasi-reversibility of first cathodic peak and reversible nature of the second cathodic peak were witnessed by SWVs. E_{pc} vs. pH plot provided the slope of 56 mV per pH unit justifying the involvement of $1e^-$ and $1H^+$ in the reduction step. The suggested mechanism of MPZ shown in Scheme 1 is also supported by the reported literature [18] regarding the reduction of phenazine.



Scheme 1. Proposed reduction mechanism of MPZ.

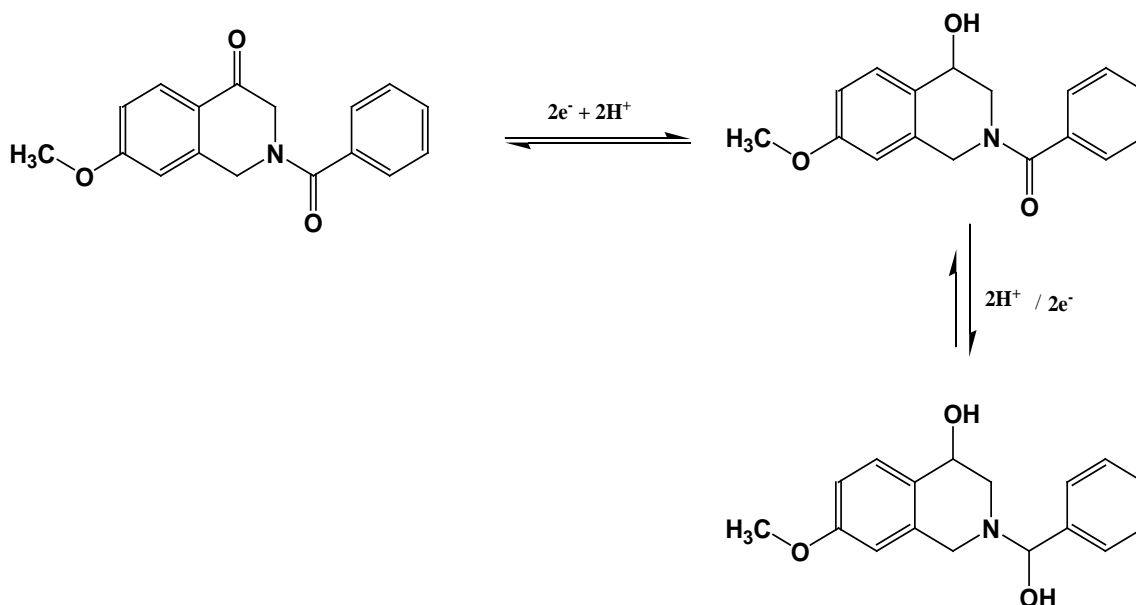
An oxidation peak was observed in neutral and highly basic media having $W_{1/2}$ close to 90 mV which displayed no shift in potential with pH indicating the removal of single electron only. Based upon the obtained electrochemical findings the mechanism illustrated in Scheme 2 was suggested.



Scheme 2. Proposed oxidation mechanism of MPZ.

4.5.2. (a) Proposed mechanism of IQN reduction

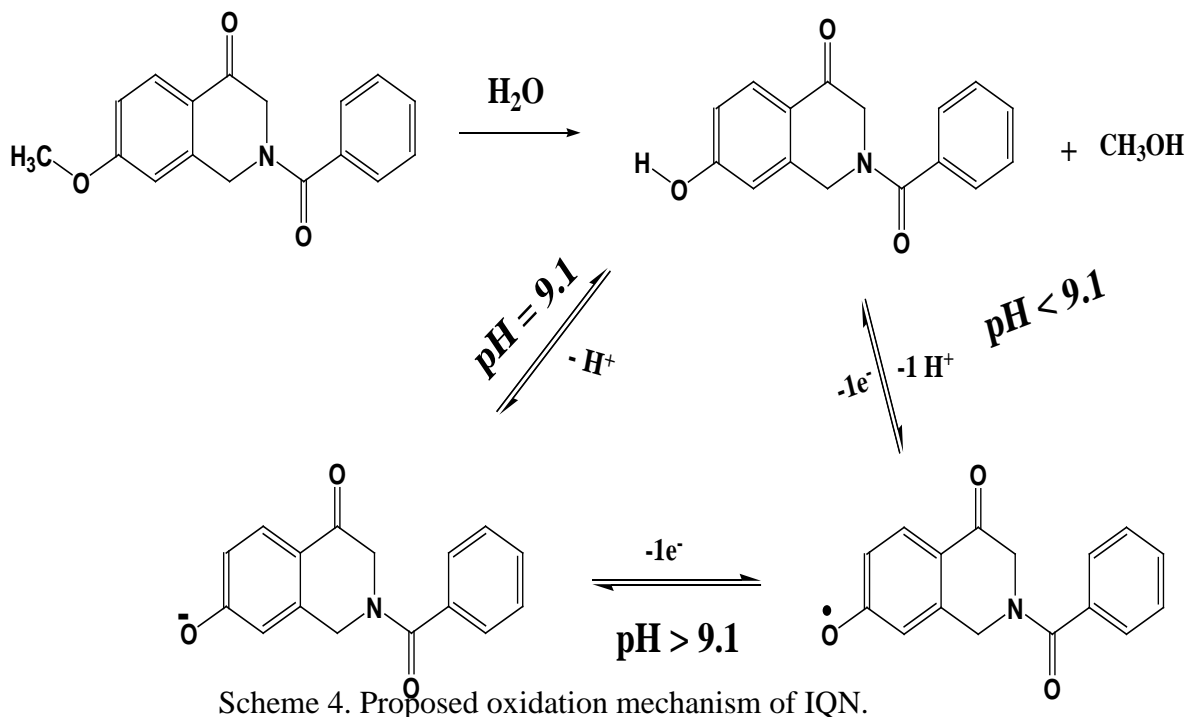
The 1st reduction peak was found to have $W_{1/2}$ of 48 mV and slope of E_{pc} vs. pH plot of 52 mV per pH unit. This suggests the conversion of the oxygen of the ring carbonyl into hydroxyl group by addition of 2 e⁻ and 2 H⁺. The current of this peak decreases with increase in pH of the medium which attributes to decrease in H⁺ concentration. Moreover, in highly acidic pH of 2 and 3 the voltammograms displayed multiple reduction peaks in addition to the main cathodic peaks. These are attributed to the reduction at carbon 10 and 20, due to the probable hydrolysis of the analyte under highly acidic conditions resulting in the formation of reducible products [19]. The second reduction peak appeared upto pH 8 having average $W_{1/2}$ of 54 mV and 54 as the slope of the plot of peak potential *versus* pH authenticating the addition of 2 e⁻ and 2 H⁺ as shown in Scheme 3.



Scheme 3. Proposed reduction mechanism of IQN.

4.5.3. (b) Proposed mechanism of IQN oxidation

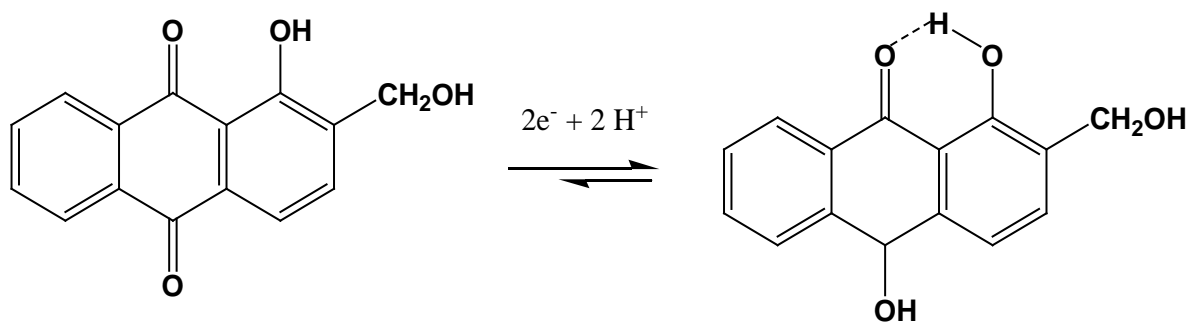
In the structure of IQN there is no moiety that can undergo oxidation. But the voltammetric assays have shown a well defined oxidation signal. The oxidation signal of this compound results from its hydrolysis [20]. From DPV findings $W_{1/2}$ of this anodic peak was 98 mV and 54 mV/pH was the slope of the plot of peak potential *versus* pH that validates the loss of 1 e^- and 1 H^+ in the pH range 4 to 9.1 (Scheme 4) but at pH higher than 9.1 the oxidation occurs due to the loss of one electron only.



4.5.4. (a) Proposed mechanism of HAQ reduction

The slope of E_{pc} vs. pH was found to be 58 mV per pH for the reduction step indicating the addition of same number of electrons and protons. The $W_{1/2}$ value of 50 mV suggests the transfer of 2 electrons. Thus, the reduction step involves the gain of $2e^-$ and $2H^+$ as shown Scheme 5. Literature survey showed that reduction of anthraquinones occur by two electrons and two protons which may take place in separate two steps or in a single

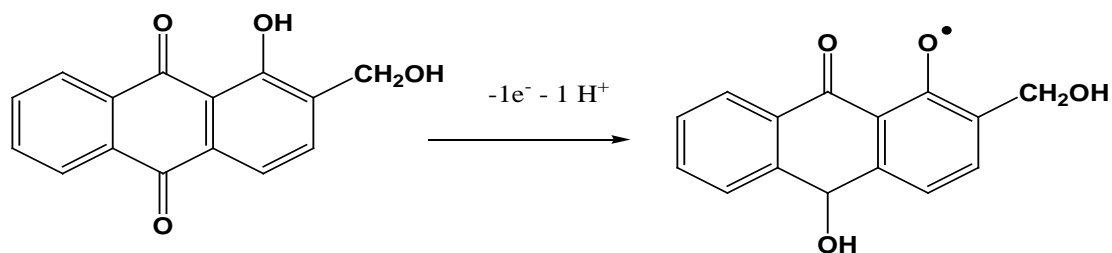
step depending upon the solvent system used. Two electrons and 2H^+ transferred was observed for well buffered system in acidic medium in the form of single reduction peak [21-23] but in alkaline medium only two electrons are involved in the reduction process [24,25]. However in aprotic solvents stepwise transfer of electrons takes place where the addition of 2nd electron takes place at more negative potential[26-28].



Scheme 5. Proposed reduction mechanism of HAQ.

4.5.4.(b) Proposed mechanism of HAQ oxidation

From the slope of E_{pa} vs. pH plot and $W_{1/2}$ of 98 mV it is suggested that the oxidation process occurs by the involvement of $1e^-$ and 1H^+ . The suggested oxidation mechanism on the basis of these results is shown in Scheme 6 where the removal of $1e^-$ and 1H^+ from the OH electrophore of the compound occurs resulting in the formation of cation radical which adsorb on electrode surface leading to the disappearance of oxidation signal in the 3rd scan. At pH 3 and below oxidation signal is not observed which can be explained by the fact that the acidic medium blocks the electrophore for oxidation due to high concentration of H^+ . The oxidation peak starts appearing at pH 4 indicating the OH moiety to be the oxidation site.



Scheme 6. Proposed oxidation mechanism of HAQ.

4.5. Electronic absorption spectroscopy

UV-visible spectroscopy was performed to investigate the electronic absorption behavior of the studied compounds in different media of pH range 1.2 to 12.8. All of the compounds showed a change in colour under some specific conditions. pKa values determination of these compounds was also made possible from this study at different pH.

4.6.1. Electronic absorption spectroscopy of 1-methoxyphenazine

The electronic absorption spectral response of 1-methoxyphenazine was studied in 50% ethanol water (1:1) solution. The yellowish green colour appeared at all pH conditions but in basic medium a slight change in colour was observed. Two peaks evident in Fig. 4.38 characterized the spectrum of 1-methoxyphenazine. A peak of high intensity came into sight at 261 nm; this corresponds to $\pi \rightarrow \pi^*$ transition of benzene ring [29]. The slight bathochromic shift was observed in this peak at higher pH which can be explained by the fact that in acidic medium a solvation sphere of solvent containing H^+ surround oxygen of methoxy group and block its electron donating ability to the ring. But in alkaline medium the non bonded electrons of methoxy oxygen is more easily available to increase charge density on the ring, making $\pi \rightarrow \pi^*$ more feasible and thus cause bathochromic shift.

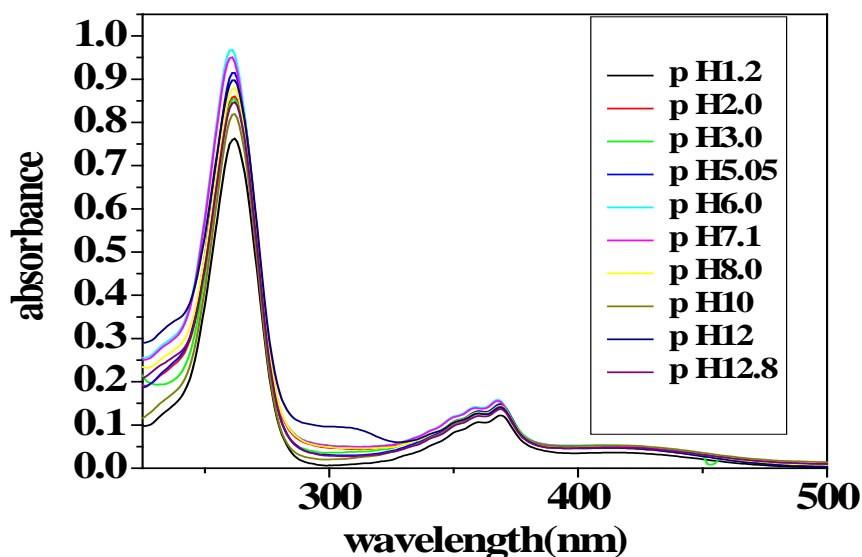


Fig. 4.38. UV-visible spectra of 16 μ M 1-methoxyphenazine in different media of pH range from 1.2 to 12.8.

The second broad and less intense peak became visible at 370 nm that arise from $n \rightarrow \pi^*$ transition of lone pair of electrons of nitrogen. The reported value of this broad peak (383 nm in ethanol) is 13 nm different from the experimental value of MPZ due to solvent effect. This transition exhibit mostly the same intensity at all pHs. However, the intense peak shows a regular increase in intensity from pH 1.2 to 7.1 and then somewhat irregular behavior was observed up to pH 12.8. The maintenance of both peaks at the same positions throughout the whole pH range shows its structure stability at all these pH conditions.

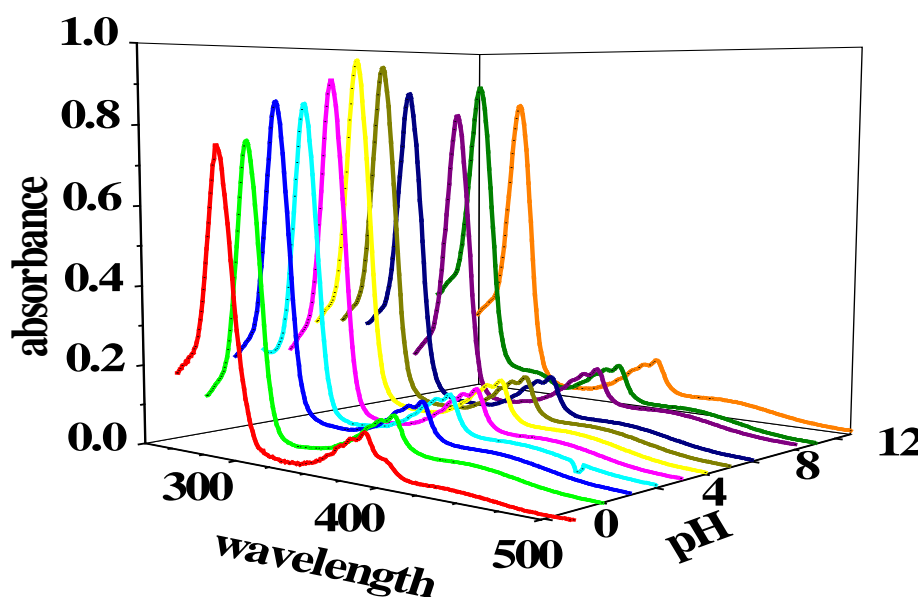


Fig.4.39. 3-D view UV-visible spectra of 16 μ M 1-methoxyphenazine showing absorbance in different media of pH range from 1.2 to 12.8.

Spectra at different pHs allow to determine pKa value. For 1-methoxyphenazine pKa was determined at 261 nm. By plotting absorbance *versus* pH at 261 nm (Fig. 4.40) the pKa of MPZ with a value of 2.4 was obtained which is slightly less than the reported value. This contradiction in pKa value arises due to the absence of ionizable proton and solvent effect.

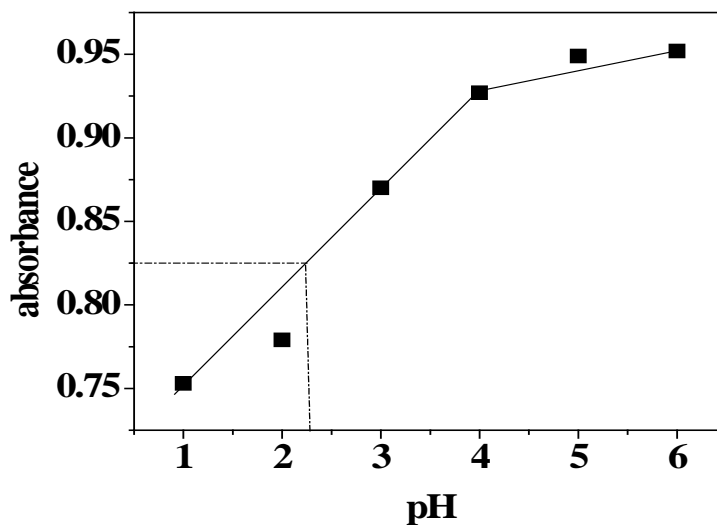


Fig.4.40. Plot of absorbance 1-methoxyphenazine vs pH at 261 nm for pKa determination.

4.6.2. Electronic absorption spectroscopy of IQN

To study the effect of pH on the absorption response of 20 μM solution of IQN its electronic absorption spectroscopy was carried out in the pH range 1.2 to 12.8. The spectra showed in Fig. 4.41 one broad peak at 368 nm having very low intensity, and another prominent peak appeared at 294 nm, third peak of highly variable nature came into sight at 230 nm. Owing to the structure of the compound and change in pH of the medium all of the three peaks put on display a change in intensity and position with a change in pH of the medium. Peak at 365 nm corresponds to a π^* transition of the carbonyl oxygen as it requires less energy for excitation and show a regular increase in intensity upto pH 3 without any shift in position but at pH higher than 3 a clear bathochromic shift is observed.

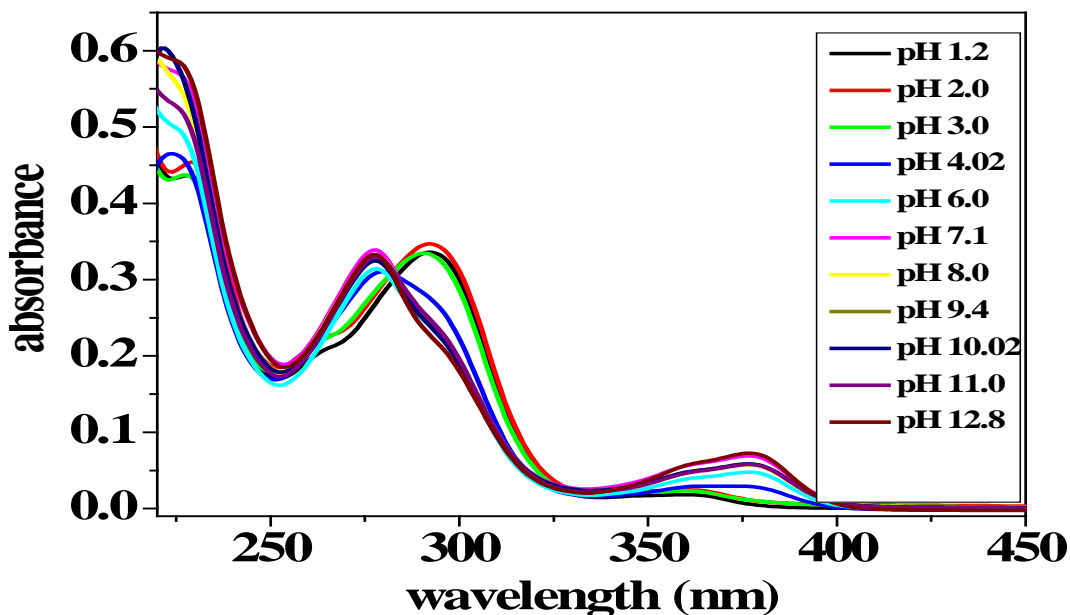


Fig.4.41. UV-visible spectra of 20 μM IQN in different media of pH range from 1.2 to 12.8.

From pH 4 to 12.8 this peak appeared at 378 nm with somewhat high intensity. This shift indicates that in high acidic medium the compound undergoes protonation decreasing the charge density on oxygen atom, increasing the energy gap for transition and thus shift absorption to lower wavelength. The second peak corresponds to $\pi \rightarrow \pi^*$ transition of the fused benzene ring. Below pH 4 this peak appears at 294 nm but at pH higher than 3 it shifts to 278 nm and intersect the peak of same transition at 283 nm. So 283 nm shows the isobestic point where both keto and enol forms of IQN absorb the same amount of radiations and thus witness their existence under these conditions. This 16 nm hypsochromic shift of the 2nd peak is due to the existence of the compound in the enolic form upto pH 3 which extend the conjugation upto N atom. The third peak which appear at 230 nm also corresponds to $\pi \rightarrow \pi^*$ transition of the bezoyl moiety of this compound. A slight increase in peak intensity was observed from pH 1 to 3 but on higher pH this peak disappeared in noise.

285 nm wavelength quite close to the isobestic point was used for the determination of pKa value of IQN. By plotting absorbance versus pH (Fig. 4.42) 4.66 was obtained as pKa value of IQN. However, literature survey has revealed 5.14 as pKa value of

isoquinoline. This small difference with the reported value arises due to the presence of substituents and solvent polarity.

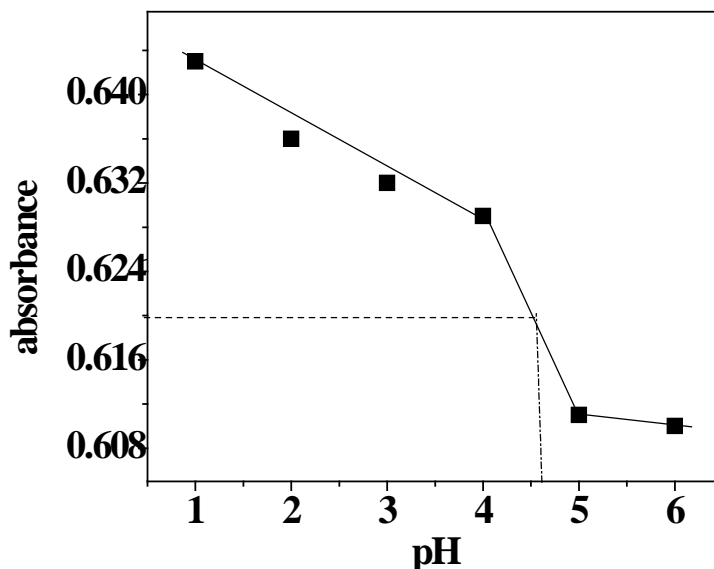


Fig. 4.42. Plot of absorbance of IQN *versus* pH at 285 nm for pKa determination.

4.6.3. Electronic absorption spectroscopy of HAQ

To investigate the effect of pH on HAQ electronic transitions, all the experiments were performed in 50% ethanol aqueous system. This compound shows a change in colour with varying pH of the medium. Spectrum of HAQ showed in Fig. 4.43 signaled three absorption bands typical of an anthraquinone. A broad and less intense peak at 408 nm, a shoulder at 279 nm, and an intense peak at 255 nm. The broad band of less intensity which corresponds to $n \rightarrow \pi^*$ transition of carbonyl group appeared at 408 nm in the pH range 1.2 to 9 with an increase in intensity. But from pH 10 to 12 this band shifted to 494 nm. Best reason for this bathochromic shift is that at lower pH both carbonyl oxygen atoms are surround by H^+ envelop that tightly holds non bonded electrons of oxygen and making $n \rightarrow \pi^*$ more difficult and hence shift the absorbance to shorter wavelength.

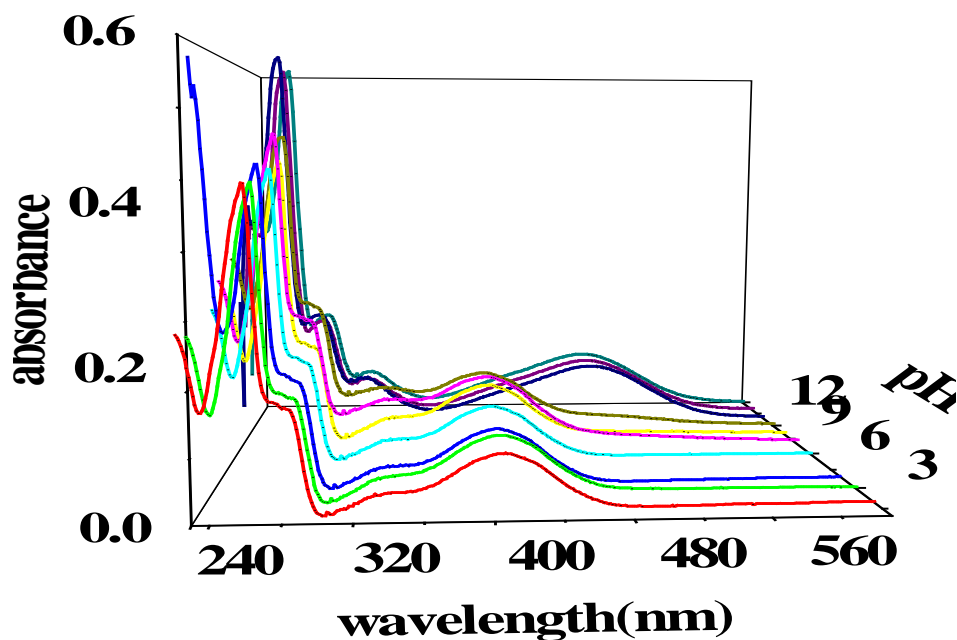


Fig. 4.43. UV-visible spectra of 15 μ M HAQ solution in the pH range of 1.2 to 12.

The shoulder that appears at 279 nm corresponds to $\pi \rightarrow \pi^*$ transition of the ring remains at the same wavelength throughout the whole pH range. It shows an increase in intensity with an increase in pH of the medium. The band of highest intensity in the ultraviolet region results from $\pi \rightarrow \pi^*$ transition of the rings having substituents exhibiting a slight hypsochromic shift in more basic medium. This increase in intensity and shift in wavelength to shorter wavelength occur due to the existence of keto form at higher pHs. Thus unavailability of hydroxyl group, having a strong electron donating ability and breaking of conjugation due to the formation of keto form cause a blue shift of the intense peak. These findings strongly support CV results where the oxidation peak became pH independent at higher pH values.

To determine pKa value of HAQ absorbance was plotted against pH at 280 nm (Fig. 4.44) as maximum change in absorbance occurred at this wavelength. Analysis of Fig. 4.43 shows an increase in absorbance at 280 nm upto pH9. Therefore, we selected this region for pKa determination. The value of pKa obtained from this plot of HAQ is 6.7.

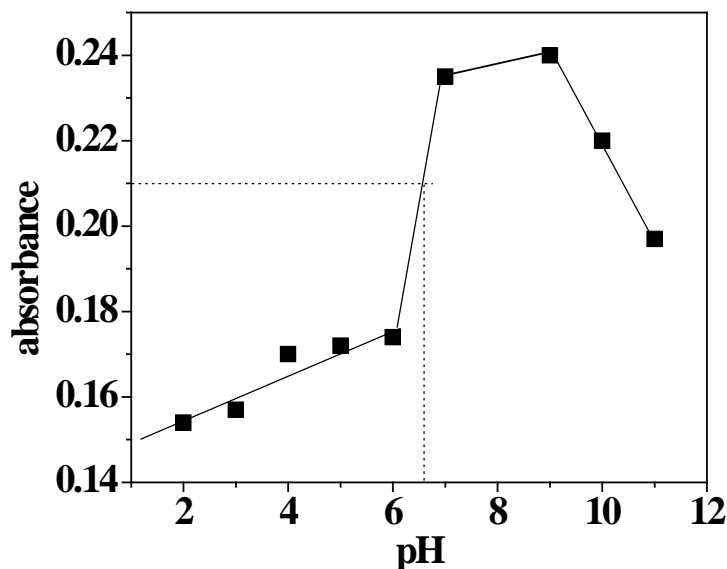


Fig. 4.44. Plot of absorbance of HAQ *versus* pH at 280 nm for pKa determination.

4.7. Computational study

4.8. In order to theoretically validate the voltammetric results of the studied compounds computational study was also performed. For this purpose PM3 ab initio method with 321G and 631G basis sets of density functional theory were used for the optimization of the molecular geometry followed by energy calculations and charge distribution on each atom. Energy of HOMO and LUMO were calculated for the optimized structures. Charge distribution on each atom and energies of HOMO and LUMO predict probable oxidation or reduction of the electro active species.

4.8.1. Mulliken charge distribution of MPZ

The two nitrogen atoms in MPZ have different charges (Fig. 4.45). More negative charge on a particular atom indicates its difficult reduction [30,31]. Nitrogen near to C₁ bears less negative charge as compared to 2nd nitrogen atom and hence shows an ease in its reduction. Furthermore, in this case methoxy group stabilize the resulting species through electron donating resonance effect. Thus nitrogen near to methoxy group is more prone to reduction and complements with CV results.

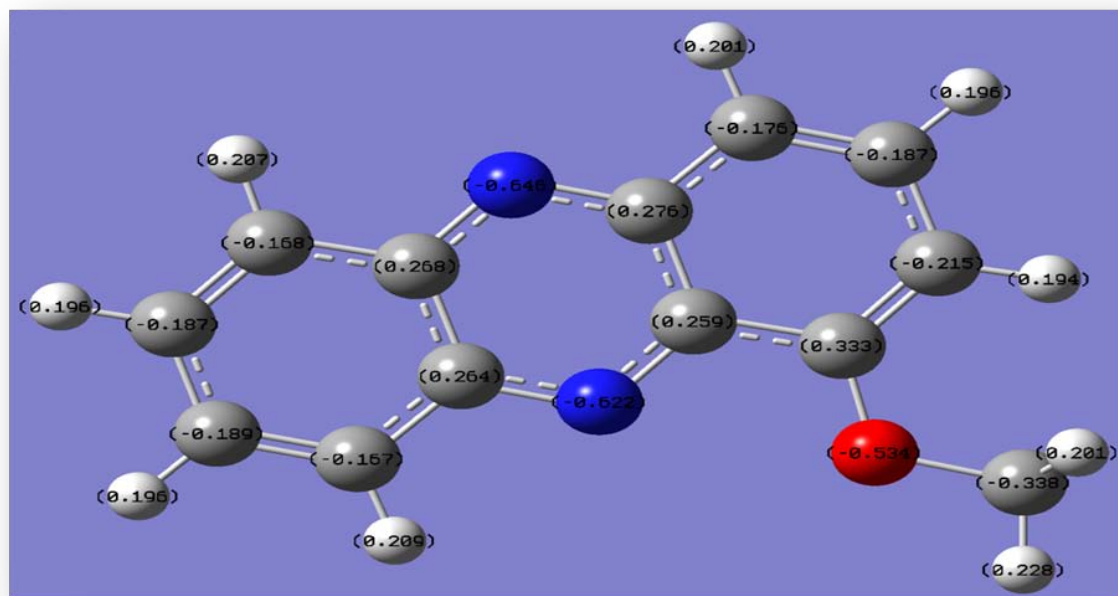


Fig.4.45. Mulliken Charge distribution on each atom of PM3 optimized MPZ structure using 631G basis set of ab initio method through gaussian 03 software.

4.8.2. Mulliken charge distribution of IQN

Charge distribution was also determined for IQN by running DFT calculations using 3-21G and 6-31G basis sets. The results shows (Fig. 4.46) that oxygen of the ring bears less negative charge (-0.427) as compared to the benzyl oxygen (-0.454). Less negative charge favors ease in reduction so oxygen of the ring will reduce at less negative potential as compared to the carbonyl oxygen of the benzyl group. In the light of these results in voltammetric experiments first reduction peak can be assigned to the reduction of ring carbonyl moiety while the 2nd cathodic peak for the reduction of benzyl carbonyl part. The calculated values for HOMO and LUMO are -0.23225 and -0.08495

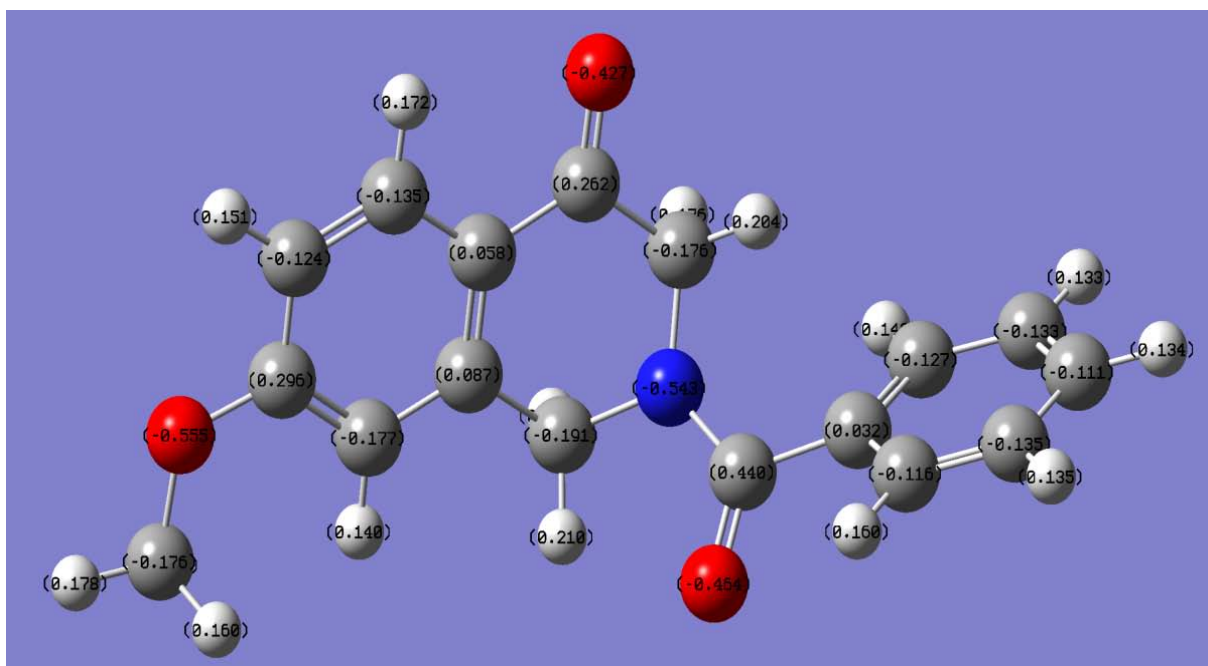


Fig .4.46. Mullikan Charge distribution on each atom of PM3 optimized IQN using 631G basis set of ab initio method through Gaussian 03 software.

4.7.3. Mulikan charge distribution of HAQ

Muliken charge distributions of HAQ was also calculated via DFT. It has shown by the lable optimized structure (Fig. 4.47) that oxygen atom attach to carbon 9 has less negative charge (- 0.406) as compared to oxygen present at carbon 10 (- 0.498) showing the high tendency of C=O moiety at C 9 for reduction rather than at C 10. Furthermore, oxygen of hydroxyl and methyl hydroxyl group bears - 0.646 and - 0.607 charges respectively indicating hydroxyl group suitable for oxidation. The optimized structure shows that hydrogen of hydroxyl group lies very close to oxygen of C 10 presenting a possibility for intramolecular hydrogen bonding.

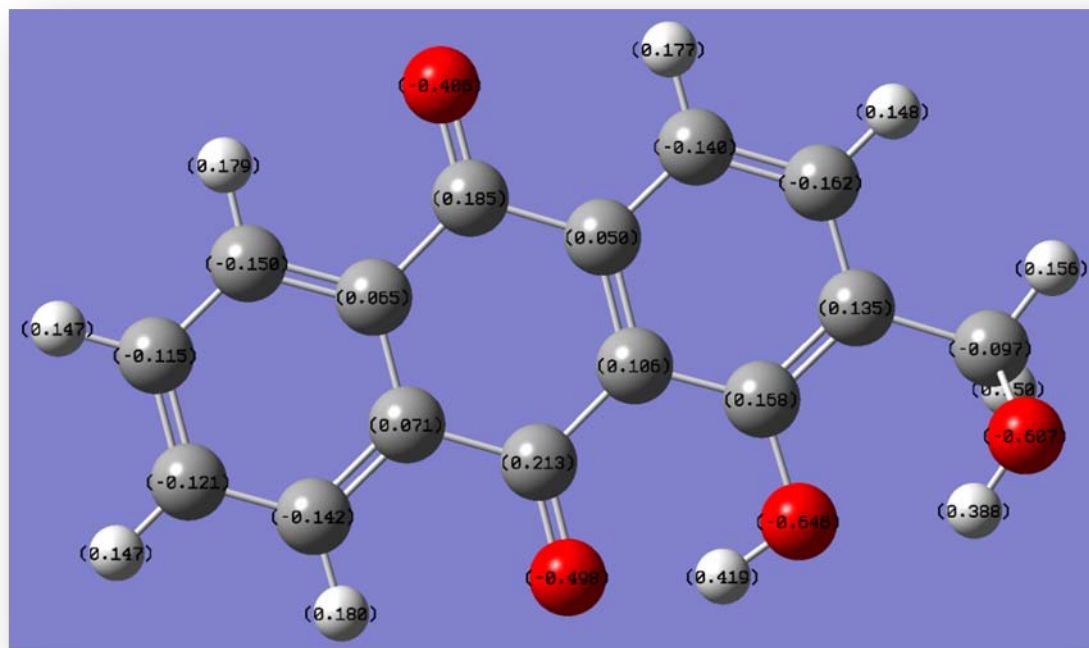


Fig 4.47. Mulliken Charge distribution on each atom of PM3 optimized HAQ using 631G basis set of ab initio method through gaussian 03 software.

6.7.4. E_{HOMO} and E_{LUMO} calculations of the studied compounds

For the comparison of redox behavior of all compounds energy values listed in Table 1 were calculated for both HOMO and LUMO using 3-21G and 6-31G basis sets. Pictorial representation of HOMO and LUMO of the investigated compounds can be seen in Fig. 4.48. The more negative value of LUMO shows the easier reduction. Energy values of LUMO showed the facile reduction of MPZ due to more negative value followed by IQN and HAQ. Energy of LUMO have shown the following order

$$E_{\text{MPZ}} > E_{\text{IQN}} > E_{\text{HAQ}} \quad (\text{LUMO values})$$

Energy of HOMO corresponds to oxidation potential [32,33]. The more negative value for HOMO represents the more difficult oxidation [34,35]. From DFT calculation the HOMO values varied in the following order

$$E_{\text{MPZ}} > E_{\text{IQN}} > E_{\text{HAQ}} \quad (\text{HOMO values})$$

HAQ shows the more facile oxidation as it has the least negative value of HOMO. These findings complement CV results.

Table 4.1. E_{HOMO} and E_{LUMO} values of compounds obtained through DFT

3-21G	Compound	E_{HOMO}	E_{LUMO}
	MPZ	-0.236	-0.112
	IQN	-0.232	-0.081
	HAQ	-0.209	-0.062
6-31G	MPZ	-0.251	-0.123
	IQN	-0.232	-0.085
	HAQ	-0.210	-0.063

Conclusion

All the studied compounds, 1-methoxyphenazine (MPZ), 2-benzoyl-7-methoxy-2,3-dihydroisoquinoline-4(H)-1one (IQN) and 1-hydroxy-2-(hydroxymethyl)anthracen-9,10-dione (HAQ) were found to be oxidized and reduced at the glassy carbon electrode. The redox behaviour showed strong dependence on the pH of the medium. The same value of pKa was obtained from the results of CV, SWV and DPV. On the basis of these voltammetric results the redox mechanistic pathways of all the three compounds were proposed. The appearance of one reduction peak of MPZ in CV and its shift to more negative potential with increase in pH of the medium enabled to conclude the quasi-reversible addition of 1 electron and 1 proton giving a free radical species. But in SWV results an other pH dependent reversible peak appeared at more negative potential showing the addition of 1 e⁻ and 1 H⁺. The Diffusion coefficient and heterogeneous electron transfer rate constant values of MPZ were successfully evaluated by the use of Randles Sevcik and Nicholson equations using CV data strongly supporting the quasi-reversible nature of the first reduction peak. The oxidation peak involved only the loss of 1 e⁻ by the negatively charge specie formed by the hydrolysis of methoxy group.

IQN was found to reduce by the appearance of two cathodic peaks in CV experiments upto pH 8 and both of these exhibited a regular shift to more negative potential with increase in pH of the medium. SWV results proved the reversible nature of the 1st reduction peak and quasi-reversible nature of the 2nd peak. Conclusively from shift in peak potential and DPV results each of these two steps involved the addition of 2 e⁻ and 2 H⁺ to the two carbonyl groups of the compound. The diffusion coefficient and heterogeneous electron transfer rate constant values of IQN were successfully evaluated from CV data. The oxidation of IQN was found to occur by the lose of 1 e⁻ and 1 H⁺ in a reversible manner in the pH range of 4 to 9.1 and above pH 9.1 the process involved only the loss of 1e⁻.

The last compound HAQ also showed pH dependent reduction through quasi-reversible mode of electron transfer. Medium effect and DPV results suggested the addition of 1 e⁻ and 1 H⁺. The diffusion coefficient and heterogeneous electron transfer rate constant values were evaluated by using CV data. The results strongly supported the quasi-reversible nature of the reduction process. HAQ also exhibited an irreversible oxidation

peak above pH 3 involving the loss of a single electron and proton. The mechanism proposed for the redox reactions of the studied compounds in the light of voltammetric results was complemented by computational results which were used for the prediction of redox properties of the studied compounds. All the studied compounds were found spectroscopically (UV-Vis) active as witnessed by the appearance of robust signals in a wide pH range. The pKa values were determined from absorbance versus pH plots. These investigations have the potential of providing valuable insights into the understanding of unknown mechanism by which phenazine, isoquinoline and anthraquinone exert their biochemical action.

References

- [1] Shankara, S.; Kalanur.; Seetharamappa, J.; Mamatha, G.P.; Hadagali, M.D.; Kandagal, P.B.; *int. J. Electrochem. Sci.* **2008**, 3, 756.
- [2] Brett, C.M.A.; Brett, A.M.O. *Electrochemistry principles, Methods and applications, oxford university press (1993)*. UK.
- [3] Sun, W.; Han, J.; Ren, Y.; Jiao, K. *J. Braz. Chem. Soc.* **2006**, 17, 510.
- [4] Nosheen, E.; shah, A.; Badshah, A.; Rehman, Z.U.; Hussain, H.; Qureshi, R.; Ali, S.; Khan,,A.M.; *Electrochem.Acta.* **2012**, 80, 108.
- [5] Ali, S.A.; Sami, M.A.; *Pak. J. pharm*, **2005**, 6, 18.
- [6] Wang, J. *analytical electrochemistry*, 3rd ed, (**2006**), john wiley& sons press.
- [7] Adrian, W.B. *curr, sep.* **1997**, 16, 61.
- [8] Alemu, H.; Khoabane, N.M.; Tsekibull, P.F. *Chem. Soc. Ethop*, **2003**,17, 95.
- [9] Goyal, R.N.; Bachheti, N.; Tyagi, A.; Pandey, A.K.*Anal. Chim. Acta.* **2007**, 605, 34.
- [10] Bard, A.J.; Faulkner, L.R.; *Electrochemical Methods, Fundamentals and Applications*,**1980**, John Wiley, New York.
- [11] Garrido, E.M.; Lima, J.L.C.; Matos, C.M.D.; Brett, A.M.O. *Talanta.* **1998**, 46, 1131.
- [12] Shah, A.; Nosheen, E.; Qureshi, R.; Yasinzai1, M.M.; Lunsford, S.K.; Dionysiou, D.D.; Rehman, Z.; Siddiq, M.; Badshah, A.; Ali, S. *Int. J Org Chem.* **2011**, 1, 183.
- [13] Brett, A.M.O.; Piedade, J.A.P.; Silva, L.A.; Diculescu V.C. *Analytical Biochemistry.* **2004**, 332, 321.
- [14] Diculescu, V.C.; Piedade, J.A.P.; Brett, A.M.O. *Biochemistry.* **2007**, 141.
- [15] Dey, J.; Warner, I.M. *J.Photochem.photobiol.A.chem.***1997**, 102, 105.
- [16] Marinov, M.; Minchev, S.; Stoyanov, N.; Ivanova, G.; Spassova, M. *Croat Chem Acta.* **2005**, 78, 9.
- [17] Catrănescu, R.; Bobirnac, I.; Crisan, M.; Cojocaru, A.; Maior, I. *U.P.B.Sci.Bull Series B.* **2012**, 74, 1.
- [18] Paduszek, B.; Kalinowski, M.K.; *Electrochim.Acta.* **1983**,28, 639.

- [19] Mumir, S.; *M.phil Thesis*, **2012**, department of chemistry, QAU.
- [20] Goyal, R.N.; Kumar, A.; Mittal, A. *J.Chem.Soc. Perkin trans.* **1991**, 2, 1369.
- [21] Rao, G.M.; Lown, J.W.; Plambeck, J.A. *Int. J. Electrochem.Sci.* **1978**,125, 534.
- [22] Wipf, D.O.; Wehmeyer, K.R.; Wightman, R.M. *J org.Chem.* **1986**, 51, 4760.
- [23] Guin, P.S.; Das, s.; Mandal, P.C.; *int. J. Electrochem.* **2010**, 2011, 1.
- [24] Guin, P.S.; Das, s.; Mandal, P.C. *Int. J. Electrochem.Sci.* **2008**, 3, 1016.
- [25] Anson, F.C.; Epstein, B. *J. Electrochem. Soc.* **1968**, 115, 1155.
- [26] Gomez, M.; Conzalez, I. *J. Electroanal Chem.* **2005**, 578, 193.
- [27] Goulart, M.O.f.; Lima, N.M.F.; Sant Anaetal, A.E.G. *J. Electroanal Chem.* **2004**, 566, 25.
- [28] Ferraz, P.A.L.; De Abreu, F,C.; Pinto, A.V.; Glezer, V.; Tonholo, J.; Goulart, M.O.F. *J. Electroanal. Chem.* **2001**, 507, 275.
- [29] Saosoong, K.; Wongphathanakul, W.; Poasiri, C. *KKU Sci. J.* **2009**, 37, 163.
- [30] Smith, S.J.; Sutcliffe, B.T. *Rev . comput. chem.* **1997**, 70: 271.
- [31] Levine, I. N. *Quantum chemistry*, **1991** , Englewood Cliffs, New jersey: Prentice Hall. 455.
- [32] Andrede, B.W.; Datta, S.; Forrest, R.S.; Jurovich, P.D.; Polykarpov, E.; Thompson, M.E. *organic electronics.* **2005**, 6, 11.
- [33] Riahi, S.; Eynollahi, S.; Ganjali, M.R. *Int. J. Electrochem. Sci.* **2009**, 4, 1128 .
- [34] Christopher J. Cramer.; *Essential of Computational chemistry, Theories and models*, **2003**, John Wiley &sons.
- [35] Frank Jensen.; *introduction to computational chemistry* , **2007**, John wiley & sons.